Mechanisms of Apoptosis Modulation and their Contribution to Genomic Instability in Tumor Cells

Dissertation zur Erlangung des naturwisseschaftlichen Doktorgrades der

Bayerischen Julius-Maximilans-Universität

Würzburg

vorgelegt von

Vladimir Vukicevic

aus

Prokuplje

Serbien und Montenegro

Würzburg 2004

Eingereicht am:……..

Mitglieder der Promotionskommission:

Vorsitzender:.....

Gutachter: …….....

Gutachter: …….....

Tag des Promotionskolloquiums:.....

Doktorurkunde ausgehändigt am:.....

1. Introduction

The concept of programmed cell death has been increasingly considered from various aspects since early 1970's. Primarily, knowledge of apoptosis referred to morphological changes in which chromatin is condensed and increasingly fragmented, revealed as small structure in the nucleus. The membrane shrinks and the cell becomes dense as can be seen by flow cytometry. Interestingly, similar modes of cell deletion were observed in nematodes indicating that apoptosis is a highly conserved machinery. Three Caeonorhabditis elegans gene products are found to have high homology with mammalian apoptotic genes: CED-9 inhibits apoptosis and is related to bcl-2; CED-3 and CED-4 promote apoptosis and are related to caspase 9 and APAF-1. Apoptosis is not accidental death, but a highly controlled and medically important molecular process. More general terms such as 'physiological' or 'regulated' cell death cover different morphologies and sequences. Programmed suicide of cells that were subjected to toxic exogenous and endogenous stimuli plays a key role in understanding cancer development and its treatment. Apoptosis involves sequences of events that may overlap and play contradictory or antagonistic roles in cell death. Generally, the ability to trigger apoptotic processes in cancer cells would benefit an organism by keeping homeostasis intact. Programmed cell death is a regularly present mechanism, for instance, in lymphocyte recruitment in the thymus where immature lymphocytes may recognize host antigens. Therefore, such lymphocytes become apoptotic and are removed by macrophages. Removal prevents possible autoimmune diseases. Unlike apoptosis, necrosis is a passive process of cell death recognizable by membrane morphological changes and accompanied by leakage of intracellular material into intercellular space that may cause inflammation in the organism.

Signals that may initiate apoptosis are generally classified into two groups: signals that launch extrinsic apoptotic pathways starting with aggregation of death receptors and intrinsic apoptotic pathways starting with disruption of intracellular homeostasis such as the release of mitochondrial factors or DNA degradation. Early in the process, apoptotic signals may lead to a broad range of signaling mechanisms such as DNA repair and assessment of DNA damage (check points). Thus, failure in any of these steps can cause a defective apoptotic response that plays a decisive role in both tumorigenesis and drug

resistance in tumor treatment. More distinctly, the capability of cancer cells to go into apoptosis prevents further neoplastic changes. Generally, the purpose of this study is to investigate the balance between formation of genomic damage and induction of apoptosis under genotoxic stress.

After genotoxic insult there are different possibilities for the fate of a cell (**Figure 1**). The genomic integrity is analyzed at cellular checkpoints, usually leading to a delay in cell cycle progression if DNA was damaged. Mutations in genes such as p53 and p21 change the cellular response to genotoxic stress and may alter the balance between apoptosis and genomic damage. However, p53 is usually mutated or not expressed in 70% of human tumors. Alterations in p53 states that reflect distinct apoptotic response upon induction of DNA damage were examined. In this study, three cell lines with distinct p53 states were used: TK6 harboring wild-type p53, WTK1 with mutated p53 and NH32 with knocked out p53.

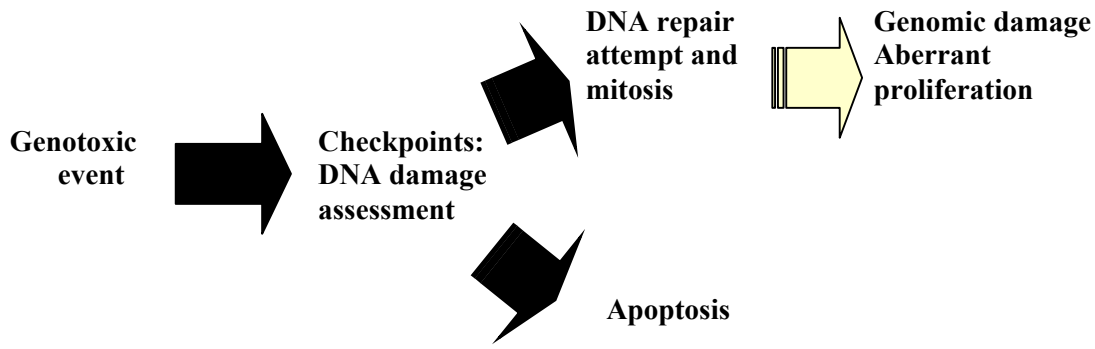

Figure 1: Distinct pathways that a cell may undergo upon genotoxic stimuli.

P53 responds to a variety of signals such as DNA damage surveillance and repair, cell cycle control and promotion of apoptosis. The P53 protein may be up regulated upon DNA insult, mainly because the normal cellular P53 protein becomes stabilized. P53 up regulation may lead to p53-dependent growth arrest in G_1 phases mediated by $p21^{WAF}$ up regulation. Induction of the $p21^{WAF}$ is controlled by p53 at the transcriptional level and inhibits cyclin-dependent kinases (cdk), thereby blocking cell proliferation. The cell goes through checkpoint signaling that may result in the activation of apoptotic pathways if cellular damage cannot be repaired properly. If DNA damage is repaired or apoptosis is induced, this cell does not pose a risk for tumor development for its host. However, if

DNA-repair is incorrect but the cell goes through mitosis, accumulation of DNA damage may lead the cell towards carcinogenesis. The efficiency of DNA repair system depends on the cell cycle stage and p53 states. Cells are most sensitive at mitosis when chromosomes are subject to strong torsions and when DNA breaks have less chance to be repaired. In contrast, the S phase is the most resistant phase, very likely due to the fact that the DNA replication machinery is coupled with DNA repair. P53 lack or temporary inhibition leads to engagement of low-fidelity DNA repair mechanisms (Lin et al. 2003). This may induce further genetic instability transforming surviving cells into genetically abnormal cells.

The decision whether an individual cell undergoes growth arrest or apoptosis following p53 activation appears to depend on a variety of factors, such as environmental conditions and cell type. Several models have been proposed to explain how cells might choose between death and growth arrest in response to activation of p53. The first model indicates that the decision depends on the amount of activated p53 and the duration of its activation: the stronger and longer the activation of p53, the higher are the chances for apoptosis. This mechanistic model considers p53 as evaluator of severity and reparability. In other words, stronger signals are induced by severe DNA damage. The second model indicates that the level of expression is predetermined by the spectrum of p53-responsive genes that modulate its function. Some cell types might have constitutively active sets of p53-responsive genes that predetermine a pattern of transactivation and transrepression. The response would depend on balance between active apoptotic and cell cycle genes. Cells expressing more apoptotic genes would be more likely predisposed to apoptosis than growth arrest (Gudkov et al, 2003). Moreover, it was found that a human tumor derived p53 mutant has lost apoptotic function but not cell cycle function (Zörnig et al., 2001). It is possible that certain point mutations reflect an altered p53 binding affinity for the binding sites in apoptotic promoters but leave binding to high-affinity sites in the cell cycle control promoters.

In the present work we applied different approaches to investigate the correlation between DNA damage and apoptotic responsiveness in cancer cell lines with different p53 states or in hormone responsive cell lines with over expressed bcl-2 gene. We were focused on effects caused by temporary down regulation of the p53 and Bcl-2 activity in

human lymphoblastoid cell lines. In addition, we investigated the impact of estradiol-induced proliferation on apoptosis and DNA damage in stably transfected cells with bcl-2 gene.

1-1 Inactivation of p53

In contrast to the notion that loss of p53 is an unfavorable event, some new opposite approaches emerged elucidating an interaction between apoptosis and DNA damage. Several years ago, the compound pifithrin-α (PFT-α, an abbreviation for 'p-fifty-three inhibitor') was isolated as possible selective protector from side effects during chemotherapy. It was reported that PFT-α is a reversible inhibitor of p53 and p53-dependent apoptosis in mice (Komarov et al., 1999), which successfully mimics p53 deficiency in a variety of cultured rodent and human cells. PFT-α also inhibits the induction of p21 and Bax, p53-responsive genes in CS-B cells (Proietti De Santis et al. 2003). PFT-α was thought to protect healthy cells from side effects during chemotherapy by temporary p53 inactivation, which is presumably functional in normal cells. PFT-α is not supposed to have any significant impact on tumor p53 that is mutated in most cancers. Thus chemotherapeutic agent would delete tumor cells by inducing apoptosis but leave normal cells unaffected. On the other side, it is generally accepted that a reduction of apoptotic capacity may lead to elevated genomic damage, since damaged cells cannot be eliminated any more (Bassi et al., 2002). In this work, the aim is to discuss the impact of such treatment on genomic integrity and apoptotic response after genotoxic stress considering the risk that surviving cells could be genetically modified.

1-2 Apoptosis induction by antisense oligonucleotide (AO)

Different strategies may be utilized for direct gene targeting. Most applied is the gene 'knock out' method achieved by homologous recombination. However, the use of specific nucleic acid sequences to act as 'decoys' for transcription factors turned out to efficient in cancer treatment. Since transcription factors recognize specific DNA sequences, it is possible to synthesize DNA segments that will efficiently compete with the native DNA sequences for available transcription factors.

The notion that gene expression could be modified through the use of exogenous nucleic acid derived from studies by Paterson et al., 1977 who first used single-stranded DNA to inhibit translation of a complementary RNA in cell-free system. Nowadays, the antisense approach has developed into an effective tool in cancer treatment if combined with chemotherapy. Antisense oligonucleotides (AO) are short stretches of nucleotides that are complementary to the region of targeted mRNA and can specifically suppress expression of that particular region. For the purpose of the present investigation, antisense bcl-2 oligonucleotide was used, designed to block the initiation codon and subsequent 15 bases of human bcl-2 mRNA. As a control, a scrambled bcl-2 oligonucleotide with two mismatched bases was introduced into the cell. Generally, AO blocks gene expression by hybridizing to the target mRNA, resulting in double-helix formation. Although the exact mechanism of AO action is not clear it is suggested that blocking may occur any time between transcription and initiation of translation. In addition, the long-half life of AO ensures modification in phospho-di-ester binding in which oxygen was substituted with sulphur forming phosphorothioate. Such a modification makes AO non-recognizable for RNase H extending its half-life in the RNA-AO hetero duplex. Prolonged AO half-life provides extended block of protein translation. Meanwhile, existing cellular protein that was synthesized before AO treatment will be degraded. AO introduction is very convenient in patient treatment due to existence of blood lipids that uptake AO and transport it into the cell. The capability of tumor cells (ex vivo) to uptake AO differs depending on tumor type (Duggan et al., 2001). Unlike in clinical practice, AO introduction into the cultured cells requires carriers such as cationic lipids, cationic porphyrins, fusogenic peptides and artificial virosomes. These compounds or structures share the same feature of forming complexes with oligonucleotides through electrostatic interaction between the negatively charged oligonucleotide phospate groups and positively charged vehicles themselves. In the form of such delivery vehicles, oligonucleotides are protected form nuclease degradation to some extend (Kuang-Yu et al., 2000).

In this work, we explored the role of over expressed anti-apoptotic Bcl-2 protein in human lymphoblastoid cell lines with different p53 states. Over expression of Bcl-2 occurs quite commonly in tumors, increasing cell's sensitivity for committing suicide. Bcl-2 was first identified in B cell lymphomas in which the genetic lesion was

translocation of the Bcl-2 gene to the control of the immunoglobulin promoter (t (14:18)). In higher eucaryotes the Bcl-2 family has at least 20 homologs, which are classified in three subgroups: Bcl-2 like survival factors (Bcl-2, Bcl-x_L, Bcl-w), Bax-like death factors (Bax, Bak, Bok/Mtd) and BH3-only death factors (Bid, Bad, Bik, Bik/Nbk, Puma) (Krammer, 2000). All of them are characterized by the presence or absence of four short Bcl-2 homology domains, BH1-BH4 which determines their role in apoptosis regulation. Anti-apoptotic Bcl-2 and its closest homologs contain four BH domains and a hydrophobic C-terminal tail which functions as a membrane anchor. The primary position of anti-apoptotic Bcl-2 protein is the mitochondrial membrane where it modulates opening of PTP pores. This leads to cytochrome c release and the formation of apoptosomes, the first stage in the launching apoptosis downstream of mitochondria. P53-dependent cytosol protein Bax modulates Bcl-2 activity. In the presence of fatal signals Bax is up regulated by p53 and is inserted into the mitochondria and form membrane anchors. Inserted Bax binds and antagonizes anti-apoptotic Bcl-2 proteins resulting in Bcl-2/Bax heterodimers. Over expression of Bcl-2 usually retards the cellular ability to launch programmed cell death. Expression of Bcl-2 usually predicts a bad prognosis in tumor development. Thus, we investigated the modulation of the apoptotic response by the appliance of bcl-2 antisense oligonucleotide and correlated it with induced DNA damage.

1-3 Novel function of Bcl-2 in cell cycle regulation

As the third approach to investigate the role of over expressed bcl-2, we stably introduced the gene into BG-1 human ovarian cancer cell line. This cancer cell line was selected because its proliferation rate can be increased by hormone treatment. This made it possible to study responsiveness of the cell to genotoxic stress from two aspects: exogenous proliferation induction and endogenous apoptosis modulation. Recent reports indicate a possible role of high-levels of Bcl-2 in G1 arrest resulting in replicative senescence instead of suppressed apoptosis, (Vairo et al., 2002). On the other hand, Rincheval et al., 2002 demonstrated that Bcl-2 was able to stop proliferation in G2 phase turning apoptosis-like phenotypes into replicative senescence phenotypes, whereas its capability to induce G1 arrest is not required. The latest Bcl-2 functional studies indicated ability of protein to control cell cycle retarding G1/S transition. It was proposed that Bcl-

2 consists of phosphorylating functional domains that can control cell cycle (Deng et al., 2004).

1.4 Micronuclei as endpoint in genotoxicity assessment

The micronuclei assay (MN assay) is applied as routine test in genotoxicity screening. It is considered at least as sensitive for the detection of structural genomic damage as the analysis of chromosomal aberrations (Miller et al., 1998). The appearance of apoptotic bodies, microscopically visible structures containing DNA, in apoptosis allows simultaneous detection of genomic damage and apoptosis on the same microscopic slides (**Figure 2**). Micronuclei are considered as subset of all chromosomal aberrations. Chromosome breakage leading to fragments as well as whole chromosomes that are not correctly distributed during mitosis give a rise to micronuclei in the next interphase (Stopper and Mülller, 1997). Other chromosomal aberrations such as translocations do not result in micronuclei formation. Other models of micronuclei formation have emerged over the last decade. It has been proposed that double-strand breaks generate in cells with gene amplification. It was shown that amplified DNA is localized at the periphery of the nucleus and eliminated via nuclear budding to form micronuclei during S phase (Shimizu, 2000; Fenech, 2002). It has been even proposed to consider nuclear buds as genotoxicity parameter (Fenech and Crott, 2002). The induction of the cytokinesis block with cytochalasin B further improved the micronucleus assay (Fenech and Crott, 2002). Cytochalasin B inhibits cell division by interfering with the formation of contractile microfilaments resulting in cells containing two, three or more nuclei. Increased number of nuclei within a cell indicates proliferation rate in analysis. Consequently, only proliferating cell can generate micronucleus formation. Hence, micronuclei scoring is limited to binucleated cells that have divided once. This prevents confounding effects caused by suboptimal cell division kinetics (Fenech et al., 2002).

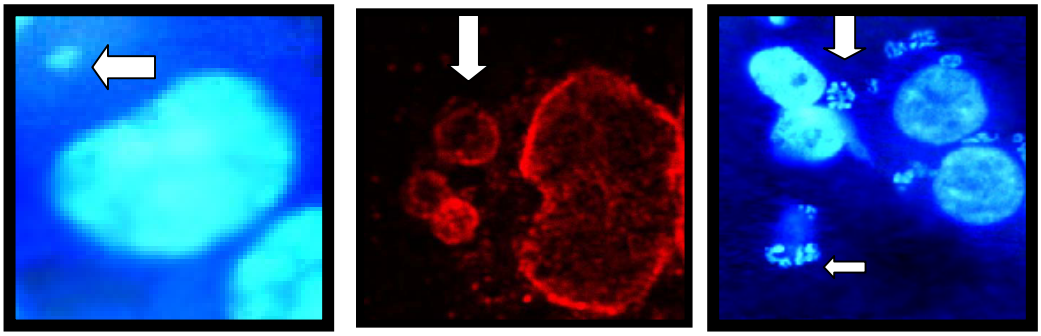

Figure 2: Microscopic analysis of cells containing micronuclei **(left, middle figure)** or apoptotic bodies **(right figure).** Micronucleus formation and apoptotic bodies **(left and right figure)** were visualized by bisbenzimid 33258 staining with affinity for DNA. The middle figure shows three micronuclei around the main nucleus of this cell, labeled with anti body specific for nucleus laminar related proteins, provided by Prof. Benavente. (figure in the middle kindly provided by M. Andrulis and A. Brink).

In the present work etoposide was used as genotoxic agent with 'multi hit' mechanism. Etoposide is characterized as topoisomerase II inhibitor inducing single- and double-strand breaks. Etoposide also induces apoptosis which makes this model compound suitable for investigating the balance between genomic damage and apoptosis (Hentze et al., 2004; Navakauskiene et al., 2004).

2. Materials and methods

2.1 Devices

Centrifuges	Universal K2S, Hettich, Germany
Coulter Counter	Coulter ElectronicsEngland
Cytocentrifuge	Cytospin 3, Shandon, England
Fluorescent microscope	Labophot 2A/2, Nikon, Germany
Incubator	Heraeus, Germany
LSR, flow cytometer	Becton Dickinson, Germany
Light microscope	Leitc, Labovert, Germany
Photometer	U-2000, Hitachi, Japan
Pipettes	Eppendorf, Sarstedt (1-10 µl, 1-100 µl, 1-200 µl, 1-1000 µl), Germany
BioRad Power Supply, Model 1000/500	BioRad, Germany
Mighty Small 245 Dual Gel Caster	Hoefer Scientific Instruments, USA
Semi-dry Transfer Cell	Transblot SD, BioRad, Germany
Software flow cytometry	CellQuest Pro, BD, USA; ModFit, Verity Software, USA
Mighty Small 2 SE 250/260	Serva, Germany

2.2 Special chemicals

Acridine Orange	Sigma, Germany
Acrylamide/Bisacrylamide	Roth, Germany
Amoniumpersulphate	Merck, Germany
Annexin-V-Fluos	Roche, Germany
Antisense bcl-2 oligonucleotide	BIOMOL, Germany
Antisense bcl-2 control oligonucleotide	BIOMOL, Germany
BD Cytofix/Cytoperm Kit	BD Biosciences, Germany
Bisbenzimid Hoechst 33258	Sigma, Germany
Blot Filter paper	Hartenstein, Germany
Dimethysulfoxide (DMSO)	Sigma, Germany
DMEM, Phenol free	Sigma, Germany
DMEM, Phenol red	Sigma, Germany
Electrophoresis Sample Buffer	Sigma, Germany
Etoposide, VP-16	Sigma, Germany
Fetal Bovine Serum	
Geneticin, G418-sulfate	Calbiochem, Germany
Horse serum	
L-Glutamine	Sigma, Germany
LipofectAMINE, 2 mg/ml	Life Tecnologies, Germany
Lipofectine, 1 mg/ml	Life Tecnologies, Germany
Modified Lowry Protein Assay Kit	Pierce, USA
Monoclonal Anti-α-Tubulin conjugate clone with FITC	Sigma, Germany
Nitrocellulose transfer membrane	Schleicher & Schuel, Dassel, Germany
$P21^{WAF}$ FITC (Ab-1), monoclonal antibody	Oncogene, Germany
P53 FITC (Ab-6), monoclonal antibody	Oncogene, Germany
Penicillin/Streptomycin- Solution	Sigma, Germany
Pifithrin-α	Calbiochem, Germany
Prestained Protein Molecular Weight Marker	Fermentas, Germany
Propidium iodide, 1 mg/ml	Molecular Probes, Germany
RPMI 1640, Phenol red	Sigma, Germany
Sodium Pyruvate- Solution	Sigma, Germany
TEMED	Sigma, Germany
Tween X-100	Sigma, Germany

2.3 Culture conditions

2.3.1. Human B-lymphoblastoid cell lines

Human B-lymphoblastoid cell lines TK6, WTK1 and NH32 originate from the same progenitor cell line WIL2 (Swartz et al., 2001). TK6 is wild type for p53, WTK1 cell line over expresses a mutant form of p53 (methionine-to-isoleucine substitution at codon 237) and NH32 is a double p53 knocked out (Swartz et al., 2001). TK6 and WTK1 cells were obtained from Dr. W.J. Caspary, NIEHS, RTP, USA. NH32 is a double p53 knockout cell line (kindly provided by H. Liber, University of Washington).

Growth medium:
RPMI 1640 medium
10% Horse serum (heat inactivated) (v/v)
107 μg/ml Natrium Pyruvat
0,25 mg/ml L-Glutamin
40 U/ml Penicillin
0,04 mg/ml Streptomycin
Cells were grown as a suspension at 37°C in 5% CO_2 in humidified atmosphere. Three times a week passaging was utilized.

2.3.2. Human ovarian cancer cell line- BG1

The BG1 human ovarian cancer cell lines (provided by Dr. S. Müller, NIEHS, RTP, USA) transfection with empty vector-pcDNA and vector containing bcl-2 has yielded two cell lines (vectors kindly provided by Dr. Jakob Troppmair, University of Salzburg, Austria).

Growth medium:
Dulbecco's modified Eagle's medium (DMEM)

10% fetal bovine serum (heat inactivated) (v/v)

107 μg/ml Natrium Pyruvat

0,25 mg/ml L-Glutamin

40 U/ml Penicillin

0,04 mg/ml Streptomycin

As needed, 500 µg/ml geneticin was added along with above specified supplements.

The BG1 human ovarian cancer cell lines were grown in DMEM medium under the same conditions, either parental or transfected (vector control and bcl-2 transfected). BG1 cell lines are adherent and were detached from the surface by adding 2ml 1x Trypsin /EDTA less then five minutes at 37°C. 3 ml DMEM medium was added and the cells were centrifuged at 1000 rpm for 5 minutes. The pellet was resuspended in 5 ml DMEM medium and 200 µl were taken to determine cell density. Cells were seeded in 10 ml complete DMEM medium at starting density of 100 000 cells/ml for seven days until approximately 70-80% confluence was reached. Confluence was microscopically assessed.

Transfected human ovarian cancer cell lines were cultured in complete DMEM medium with 500 µg/ml geneticin. Cells were given antibiotic for at least three days a week in order to maintain only cells that stably contained transfected vector. Cells were split once a week and grown in DMEM medium, at 37°C in 5% CO_2 humidified atmosphere.

2.3.4. Cells density adjustment

An automated cell counter was used to test cytotoxicity of applied compounds or to adjust cell numbers. Cytotoxicity was determined by adding 200 µl from a well-resuspended cell culture into 9,8 ml isotonic solution (Isotone II). This dilution was analyzed by the cell counter. For the purpose of cytotoxicity testing cell density was measured at the end of the experiments usually displaying decrease in cell number for treated compared to control cells.

2.4. Protein extraction

Cells were cultured in appropriate growth medium at a density of 10^6 cells/ml. Harvest was done by centrifuging for 5 minutes at 1000 rpm. The supernatant was discarded and samples were prepared by lysing cells in 200-1000 µl homogenization buffer, depending on the yield. The resulting crude cell lysate was additionally homogenized by pushing it through a syringe several times. Samples were stored at –20°C.

Homogenization buffer
10 mM HEPES,
0.2 M mannitol,
50 mM sucrose, pH 7.4

2.4.1. Determination of the sample protein concentration (Lowry Assay)

The Lowry assay was performed in two parts:

a) Creation of the standard curve

b) Determination of the sample protein concentration.

Standard curve preparation

In 1 ml vials following volumes were added:

1. Blank sample150 µL H2O. **0 µg / µL**;
2. 1µL BSA (bovine serum albumin) and 149 µL H_20; **2,05 µg/ µL**
3. 2 µL BSA and 148 µL H_20; **4,1µg/ µL**
4. 3 µL BSA and 147 µL H_20; **6,15 µg/ µ**L
5. 4 µL BSA and 146 µL H_20; **8,20 µg/ µL**
6. 8 µL BSA and 142 µL H_20; **16,41 µg/ µL**
7. 16 µL BSA and 134 µL H_20; **31,82 µg/ µL**

taken from1 mg/ml BSA standard stock solution.

Sample preparation:

1. Blank: 4 μL of homogenization buffer was added and filled up to 150 μL with H_2O. A crude protein sample was added in a volume of 4 μL into a vial and filled up to 150 μL final volume with demineralized H_2O.
2. 750 μL of MLPA (Modified Lowry Protein Assay) was added and incubated 10 minutes at room temperature.
3. 75 μL of color reagent (Follin Reagent) was added into a vial containing sample protein and MLPA and incubated at RT in at least 30 min.
4. Absorbance was measured at 750 nm wavelength at room temperature against a blank.

Determination of the value of the slope was obtained by entering values of the standard curve samples in a computer program vs. standard concentrations. The value of the slope is expressed as an equation, in which absorbance of sample protein is entered and its concentration was calculated.

Irrespective of protein volume, the mixture contained 50 μL of Electrophoresis Sample Buffer and then the mixture was filled up to 200 μL by homogenisation buffer. Samples were stored at –20°C.

2.5. SDS-PAGE: One dimension polyacrylamide gel electrophoresis

The standard electrophoretic technique used for the separation of proteins is polyacrylamide gel electrophoresis (PAGE). Polyacrylamide gels form chains and then networks after polymerization. The polyacrylamide chains are crosslinked by N,N'-methylenebisacrylamide forming a network of polyacrylamide chains that contain pores through which the proteins migrate. Initiation of polymerization is facilitated by addition of ammonium persulfate that dissociates to sulfate radicals, and tetramethylenediamine (TEMED), which catalyzes the formation of free radicals. We used a discontinuous system with a separating and a stacking polyacrylamide gel to separate proteins, described by Laemmli, 1970. Protein samples were heated (100°C for 5 minutes) to denaturate in the presence of SDS, which binds to the polypeptide chains giving a constant negative charge to mass ratio. Following the heating step, samples were

transferred on ice for several minutes. Chilled samples were loaded onto the 6% polyacrylamide stacking gel slots in final amounts of 50 µg per slot. Constant current was applied at 40 mA, 220 V. In an electric field proteins form a sphere with SDS molecules on the outer side and migrate towards the anode leaving the stacking gel and migrate along the separating gel. Depending on the protein size and polyacrylamide concentration separation occures on a certain distance from the starting line of the separating gel. Since protein migration in SDS-PAGE is proportional to protein size, it is possible to determine the molecular weight by comparing mobility with reference proteins. Thus, prestained molecular weight markers were also loaded on the gels (**Table 1**).

Table 1: Molecular weight marker contents and their separation on the gel.

Protein	Source	Specific MW kDa
β-galactosidase	E.coli	118,0
Bovine serum albumine	Bovine plasma	79,0
Ovalbumin	Chicken egg white	47,0
Carbonic anhydrase	Bovine erythrocytes	33,0
β-lactoglobulin	Bovine milk	25,0
Lysozyme	Chicken egg white	19,5

SDS polyacrylamide gel buffers:

Running buffer: TRIS 3,03 g, Glycin 14,42 g, SDS 1 g, Filled up to 1l in H_2O, pH 8,3

6% Stacking gel: Acrylamid/Bisacrylamid 0,789 ml; Buffer pH 6,1 0,125 ml; SDS 10% 0,05 ml; H_2O 3,98 ml; TEMED 5 µl; Ammoniumpersulfate 50 µl

Buffer pH 6,1:

Tris- HCl 26,16 g ; H_2O ad 100ml

10% Separating gel: Acrylamid/Bisacrylamid 2,34 ml; Buffer pH 9,18 1,8 ml; SDS 10% 0,1 ml; H_2O 4,6 ml; TEMED 5 µl; Ammoniumpersulfate 60 µl

Buffer pH 9,18: Tris-HCl 25,68 g, H_2O ad 100ml

2.5.1. Semi-dry western blot analysis

Western Blot analysis provides semi-quantitative analysis of protein expression in cells; protein transfer procedure consisted of several steps. In the Western Blot, proteins are transferred from a 10% SDS polyacrylamide gel to a nitrocellulose membrane after equilibration in blot buffer. Protein transfer can be done in buffer-tank-blotting apparatus or by semi-dry blotting. We used the semi-dry blotting method in which the gel and the membrane are sandwiched between two stacks of filter paper prewetted in blot buffer (15 pieces above and beneath). The gel was placed near the cathode (negatively charged) and the membrane was placed near the anode (positively charged). Transfer of the proteins lasted one hour on 20 V.

Blot buffer:
TRIS 5,814 g; Glycin 2,927 g dissolved in 800 ml H_2O and filled up to 1l with 100 % methanol

TBS-Tween buffer:
TRIS 0,121 g; NaCl 0,877 g; Tween 20 0,5 ml dissolved in 1l H_20

2.5.2. Immunobloting

The use of prestained molecular weight marker provided an information on proper protein transfer on the membrane. The blot membrane was blocked for 1 hour in 10% non-fat dried milk dissolved in TBS-Tween buffer. Milk leads to reduced antibody sensitivity preventing unspecific coupling.
The membrane was then washed out three times in TBS-Tween. Next, the membrane was soaked in an appropriate dilution of specific primary antibody dissolved in 10% non-fat dried milk TBS-Tween. Overnight incubation turned out to be optimal for each of the applied primary antibodies at +4°C (Table 2). After the membrane was rinsed, a visualization step was performed by incubation with secondary antibody conjugated with horseradish peroxidase (HRP) for 1 hour at room temperature.

Protein	Protein origin	Primary antibody	Secondary antibody
Bcl-2	**Mitochondral protein**	**Bcl-2 Ab Santa Cruz sc-783 Dilution 1:3000 in TBS-Tween in 10% Non-Fat Milk**	**Anti-rabbit HRP Ab 1:5000 in TBS-Tween in 10% Non-Fat Milk**
P53	**Cellular Protein**	**P53 monocolonal Ab, Calbiochem Dilution 1: 4000 in TBS-Tween in 10% Non-Fat Milk**	**Anti-mouse HRP Ab 1:5000 in TBS-Tween in 10% Non-Fat Milk**
α-tubulin	**Cellular Protein**	**α-tubulin Ab, Sigma Dilution 1:3000 in TBS-Tween in 10% Non-Fat Milk**	**Anti-mouse HRP Ab 1:5000 in TBS-Tween in 10% Non-Fat Milk**

Table 2: Primary and secondary antibodies used for Western Blot analysis.

The HRP enzyme reacts with chemiluminescent substrate and gives spontaneous light emission. In order to visualise bands, the membrane was washed and incubated for 1 minute in 2 ml Enhanced Chemiluminescence Kit that contains chemiluminescent substrate. Unlike the chromogenic substrates, chemiluminescent substrates are more sensitive with the advantage to enable multiple permanent records on photographic film. The film was exposed to the membrane chemiluminescent emission for 10 minutes under lowe light conditions.

2.5.3. Stripping of the primary-secondary Ab complex from the blot membrane

In order to confirm an equal loading of the protein, it was necessary to remove a complex of the antibodies that were previously coupled to the nitrocellulose membrane proceeding the so called membrane stripping. First, the membrane was submerged in stripping buffer and incubated at 50°C for 30 minutes in the water bath to denature and remove coupled antibodies. Next, the membrane was washed in TBS-Tween and blocked in TBS-Tween 10% Non-fat milk for 1 hour.

Immunodetection was then enabled with antibody against constitutively expressed α-tubulin with a 1-hour incubation at room temperature while shaking. The membrane was then rinsed three times with TBS-Tween for 5 minutes. The primary antibody was then detected with a secondary anti-mouse-antibody conjugated with horseradish peroxidase for 1 hour at room temperature. Bands were visualized by using The Enhanced Chemiluminiscence Kit.

2.6. Microscopic analysis

The micronucleus (MN) assay is an endpoint in the genotoxicity evaluation of a test compound. Moreover, the modified MN assay provides information on apoptotic effects and altered proliferation rate. Micronuclei formation occurs during mitotic division as a subset of all chromosomal alterations. Micronuclei are round shaped and surrounded with a nuclear membrane and sited in the cytoplasm. The size is approximately between 1/10 and 1/3 of the area of the main nucleus.

In order to reach mid-log phase of cell growth at the time of etoposide treatment, cells were washed with growth medium and adjusted to $1.0x10^5$ cells/ml the day before treatment. On the day of treatment, cells were pelleted and washed with appropriate medium. Cell density was adjusted to $1.5\text{-}2.0x10^5$ cells/ml. Etoposide was dissolved in DMSO (dimethyl-sulfoxide) and applied at the indicated concentrations. The solvent control contained 1% DMSO in each experiment. After 24 hours, the cell number (proliferation) was determined using a Coulter Counter and the remaining cells were harvested by cytospin-centrifugation. Slides were fixed in prechilled methanol for at least 2 hours and stained with bisbenzimide 33258 (5 µg/ml) and analyzed by fluorescence microscopy. Micronucleus induction was achieved by treatment with the indicated concentrations of etoposide for 24 hours (as indicated in the figure legends). The presented data represent 2 x 1000 cells from two slides from one sample that were analyzed for the presence of micronuclei. The numbers of independent repeat experiments are given in the figure legends.

2.6.1. Appliaction of cytochalasin B as modification of the MN assay

Another set of samples was prepared under identical conditions but treated with cytochalasin B along with the indicated etoposide concentrations for a 24 hours exposure

period. Cytochalasin B prevents division, resulting in a binucleated cell. At the 2 μg/ml concentration cytochalasin B induces minimal cytotoxic effects. Sample transfer and fixation were performed as described above. Slides were stained with acridine-orange and analyzed with fluorescence microscopy. Micronucleus scoring was performed on 2 x 1000 binucleated cells from two slides of one experiment. Scoring the number of binucleated cells per 2000 cells yielded an assessment of the proliferation. The numbers of independent repeat experiments are given in the figure legends.

2.6.2. Apoptosis analysis using the modified MN assay

The presence of apoptotic cells in which the DNA appears brightly stained and condensed as apoptotic bodies upon bisbenzimid 33258 or acridine-orange staining was registered and is shown only where analysis by flow cytometry was impossible (AO oligonucleotide-treatment). In that case, 2 x 1000 cells from two slides were analyzed for each sample. The numbers of independent repeat experiments are given in the figure legends.

2.6.3. Pifithrin-α (PFT-α) treatment and micronuclei evaluation

In experiments with pifithrin alpha (PFT-α), a pretreatment with 30 μM PFT was performed for 4 hours before etoposide was also added for 24 hours. For microscopic analysis, 2 X 1000 cells from two slides were evaluated for the presence of micronuclei.
Solutions:
200 μM etoposide (m/w) dissolved in DMSO, stored at RT
11,5 mM PFT-α (m/w) dissolved in DMSO, stored at –20°C

2.7. Bcl-2 anti-sense oligonucleotide transfection

Blocking of bcl-2 gene expression was performed by addition of antisense bcl-2 oligonucleotide (Biomol GmbH, Hamburg, Germany). Antisense bcl-2 oligonucleotide (5'-TCTCCCAGCGTGCGCCAT-3') is designed to block the initiation codon and subsequent 15 bases of human bcl-2 mRNA. As a control, we used a scrambled bcl-2 oligonucleotide (5'-TCTCCCAGCATGTGCCAT-3') with two mismatched bases (underlined). Cells were grown in complete RPMI 1640 medium supplemented with 10%

fetal calf serum and antibiotics. Before transfection, the cells were washed in serum-free RPMI 1640 at 1500 rpm and adjusted to 3-5x10^5 cells/ml cell density. For introduction of oligonucleotides we used Lipofectin, 1 mg/ml suspension of 1:1, DOTMA:DOPE liposomes from Life Technologies (Invitrogen, USA). Lipofectin and oligonucleotides were diluted in serum-free RPMI in concentrations of 0.8 and 0.3 µg/µl in separate vials. The dilutions were incubated for 45 minutes at room temperature and mixed. The final solutions were incubated for 15 minutes at room temperature to form efficient DNA-Lipofectin complexes. Then, the DNA/lipid complex was added to the cells in a final concentration of 7.5 µg oligonuleotide and 20µg lipid per culture flask. Four and eight hours later 3.75 µg oligonucleotide was added to counteract the long half-life of the Bcl-2 protein. Six hours after the beginning of the transfection, 250 nM etoposide was added for a 24 hours exposure. A part of the cell suspension was then transferred onto slides by cytospin centrifugation, fixed, stained and evaluated as described above. The remaining part of the cell suspension was used for Western Blot analysis of the expression of Bcl-2 as described above. Flow cytometric analysis of apoptosis (Annexin V Fluos) was not possible due to cationic lipid treatment that interferes with cellular membrane (which becomes permeabilized). Thus, Annexin V Fluos enters the cell coupling phosphatydil-serine on the inner side of the membrane, which results in non-apoptotic signal.

Solutions:
Lipofectin (1mg/ml stock) 1:1 DOTMA-DOPE cationic lipids, stored at +4°C,
bcl-2 Antisense oligo, lyophilised 25 nmols, stored at –80°C ,
bcl-2 Scrambled (control) oligo, lyophilised 25 nmols, stored at –80°C,
Sterile water

2.8. Flow Cytometry

Flow cytometric data was obtained by using a BD LSR flow cytometer. The BD LSR system is based on six colour analysis incorporating two lasers: HeCd UV laser (325 nm, 8mW) provides analysis of samples stained with UV excitable dyes. This feature provides an opportunity to perform dual and multiple staining while electronic compensation, necessary due to spectral overlaps, can be avoided. Such performances provide high resolution and accurate analysis owing to increased laser power. Stained cells are analyzed while they pass one at a time through a focus laser beam. A single cell

is analyzed by several parameters such as a size (forward scatter -FSC), inner granularity (side scatter-SSC), intensity of fluorescence (apoptosis, protein expression) or pulse processing (DNA analysis).

2.8.1. Apoptosis analysis- Annexin V staining

Annexin V is a small phospholipid-binding protein that has high affinity for the membrane phospholipid phosphatidylserine. Phosphatidylserine is translocated from the inner to the outer leaflet of the plasma membrane during apoptosis. Externalised phosphatidylserine binds Annexin V Fluos conjugated with fluorescent dye. Phosphatidylserine is translocated in the early stages of apoptosis. The Annexin V fluorescent population therefore represents early apoptotic cells, whereas double positive cells (Annexin V-Propidium Iodide positive) represent the late apoptotic stages. Propidium iodide (PI) enters cells with disrupted membrane and bindes to DNA. Membrane devastation is a feature of late apoptotic and necrotic cells. Thus, in the analysis of apoptosis a mixture of Annexin V and PI was used to achieve a clear distinction between apoptotic, necrosis and viable cells (non stained).

Solutions
10x Binding Buffer: 0.1 M HEPES, pH 7.4; 1.4 M NaCl; 25 mM $CaCl_2$; diluted to 1x before use)
Propidium iodide stock staining solution 1 mg/ml
20 µl Annexin V Fluos ready to use aliquot dissolved in 1 ml 1X PBS
10X PBS buffer: 1,4 M NaCl, 27 mM KCl, 100 mM KH_2PO_4/K_2HPO_4, PH 7,5 diluted to 1X in H_2O prior to use.

Cells were treated with etoposide for 24 hours before staining for flow cytometry analysis. After completion of treatment, samples were washed twice in complete RPMI medium by centrifugation at 1000 rpm for 5 minutes and cell density was adjusted to approximately to 1 x 10^6 cells/ml. Prior to staining, 20 µl Propidium Iodide (PI) and 20 µl Annexin V Fluos were prediluted in 1 ml binding buffer. The pellet was then dissolved in 100 µl of this staining buffer. Samples were incubated for 15 minutes at room temperature under low light conditions. Staining buffer (0.4 ml) was added, and samples were analyzed on a Becton-Dickinson (BD-LSR) flow cytometer using the 488 nm argon-ion laser as standard and the 530/28 nm bandpass filter for annexin V-fluorescence

and the 670 nm bandpass filter for PI fluorescence. Annexin V and PI signals were acquired using a log scale and analyzed with CellQuest-Pro software. Between 20000 and 50000 gated events were analyzed.

2.8.2. Flow cytometric analysis of p53 and p21 protein expression

Tracking down apoptotic intracellular signaling was undertaken by analyzing inducibility of p53 and p21. The current model of p53 function postulates that p53 up regulates p21WAF inhibitor of cdk-kinases which results in cell cycle arrest either in G1 or G2 phases. If the DNA is irreparable, the cell undergoes p53-dependent apoptosis. Analysis was performed on human lymphoblastoid cell lines with different p53 states: TK6 wild type p53, WTK1 harboring mutated p53 and NH32 p53 double knock out. BG1 ovarian cancer cell lines (vector control and bcl-2 transfected) were also analyzed for expression of both proteins. Monoclonal antibodies specific for respective proteins are conjugated with fluorescein isothiocynate (FITC) to be detected.

Solutions
Cytofix/Cytoperm Kit consisting of Cytofix/Cytoperm and Perm/Wash solutions
Monoclonal p53 and p21 antibodies conjugated with FITC
10X PBS buffer: 1,4 M NaCl, 27 mM KCl, 100 mM KH_2PO_4/K_2HPO_4, PH 7,5 diluted to 1X in H_2O prior to use.

Cells were exposed to a range of etoposide concentrations for 24 hours. Samples were pelleted and cell density was adjusted to 2 X 10^6 cells/ml and washed once in PBS at 1000 rpm for 5 minutes. After washing, pellet was dissolved in 200 µl Cytofix/Cytoperm solution, component of Cytofix/Cytoperm Kit and incubated for 30 minutes at + 4°C. This enables cells to be fixed and permeabilized for antibody incubation. Next, cells were washed twice in 1 ml Wash/Perm solution at 1000 rpm for 5 minutes. Cells were maintained permeabilized during washing steps due to the Perm component in both Cytofix/Cytoperm and Perm/Wash solutions. Pelleted samples were dissolved in 200 µL Wash/Perm and 2 µL of FITC conjugated antibody was added. Samples were incubated for 1 hour at +4°C in the absence of the light with periodic vortexing to prevent spontaneous cell aggregation. In the next step, cells were washed twice in 1 ml Wash/Perm solution in order to discard unbound antibodies. Finally, pellets were

dissolved in 1X binding buffer and samples were analyzed with the flow cytometer, using the 488 nm argon-ion laser as standard and the 530/28 nm bandpass filter for FITC emission. Acquisition was adjusted to 10000 events and the results were acquired in three steps. First, obtained two populations in the FSC-SSC plot were gated under logarithmic amplification mode. Second, the gated populations were analyzed in a FL1 (FITC 530/28 nm) vs. FL2 (575/26 nm) plot to check the distribution of nonstained and stained populations and to avoid any interference of spontaneous cell fluorescence detectable on FL2. In this step, the stained population (highly positive for FITC) was gated. Third, the gated population was analyzed by measuring the intensity of the FITC fluorescence in histogram plot. The obtained data are presented as histogram in which treated cells showed shift towards higher fluorescence intensity values compared to untreated controls. Such a shift can be interpreted as induction of p53 or p21 protein.

2.8.3. Cell cycle analysis

During the cell cycle a normal replicating diploid cell undergoes distinct phases: G_1, S, G_2, M. A nonreplicating diploid cell rests in the so-called G_0 phase of the cell cycle. When cellular reproduction is initiated, cells enter the G_1 phase. The amount of DNA is constant although RNA and protein synthesis occurred. The DNA content is indistinguishable and cells are recognized together as G_0/G_1 on the plot (Figure 3). The DNA synthesis occurs in S phase and the DNA content is doubled. Then, the cells progress into G_2/M where the cellular DNA content remains the same but the cell prepares for mitosis. During mitosis the cell undergoes a division retaining the DNA content until it splits into two daughter cells.

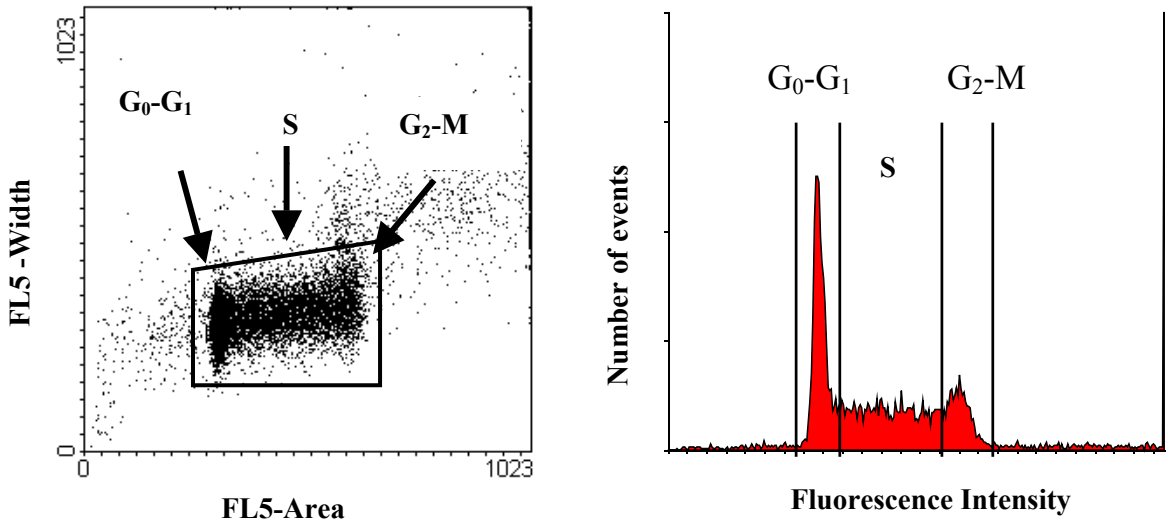

Figure 3: A typical DNA analysis in flow cytometry

Figure 4 shows the basic principle of pulse creation in flow cytometry measurements. A pulse begins with low fluorescence emitted from a cell that enters the laser beam. At this point, signal intensity is low (**Figure 4a**). The pulse reaches a maximum intensity or height when the whole cell is in the middle of the beam (**Figure 4b**). At this point, the **pulse height** is measured. As the cell leaves the beam, the pulse decreases (**Figure 4c**).

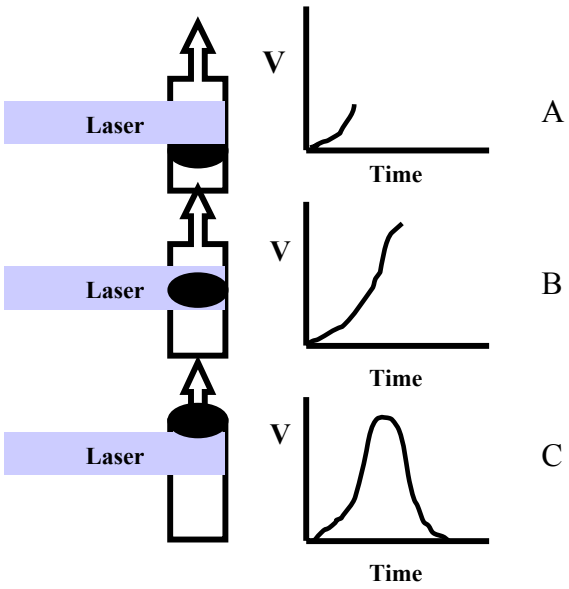

Figure 4: Basic principle of pulse creation while the fluorescent cell passes through the laser beam (Voltage vs. Time). The obtained electrical signal is the pulse.

Therefore, the pulse height indicates the highest signal intensity. **The pulse-area** measures cellular variation, in size and shape. **The pulse-width** is the amount of the time for which the cell was in the beam and it is proportional to the time the cell needs to transverse throughout the laser beam. This parameter is used to distinguish cell aggregates from single cells. In the cell cycle analysis the pulse area parameter was used for analysis (**Figure 5**).

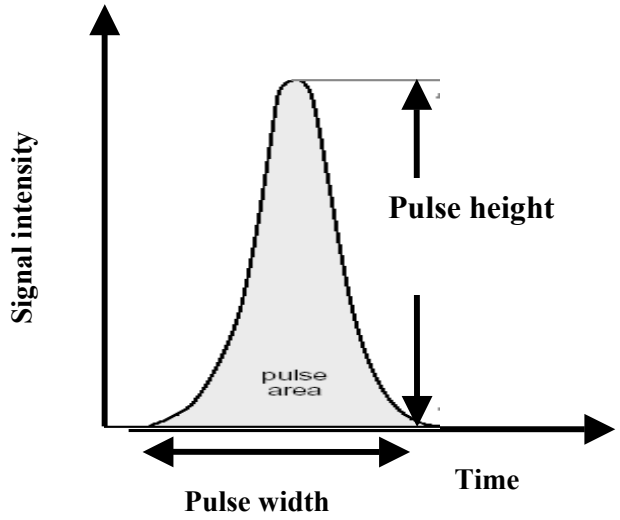

Figure 5: Parameter description in pulse measurement.

2.8.4. Preparation procedure for cell cycle analysis of the human lymphoblastoid cell lines

The suspension cell lines were harvested by centrifugation at 1000 rpm for 5 minutes. The pellet was resuspended in 2% paraformaldehyde, with vigorous vortexing and adding the buffer drop-wise. Samples were stored on +4° C for 1 hour fixation. Cells were washed twice in PBS and then dissolved in labeling buffer; 10 μM bisbenzimide was added for DNA labeling. Labeling was performed for at least 1 hour at 37°C. After that, washing was repeated twice and the pellet was dissolved in labeling buffer and transferred into conical flow cytometry tubes. Samples were analyzed by exciting bisbenzimide with the HeCd UV-laser (325 nm, 8mW) and using the FL5 band-pass filter for <510 nm emission spectra. Acquisition of 20000 single events was performed using CellQuest Pro software.

Solutions

500 µM bisbenzimide (stock solution) dissolved in PBS
10x Binding Buffer: 0.1 M HEPES, pH 7.4; 1.4 M NaCl; 25 mM $CaCl_2$; diluted to 1x before use)

2.9. Stable transfection with the bcl-2 gene

The human ovarian cancer cell line- BG1 was cultured in 6-well plates at a starting density of $2x10^5$ cells/ml, at 37°C in 5% CO_2/ humidified atmosphere until 60-70% confluence was reached. The vector constructs pcDNA3 (empty vector-control) and pc DNA bcl-2 were kindly provided by Prof. Jacob Troppmair, Institute of Radiation Medicine and Cell Biology, Würzburg. The vector constructs were dissolved in sterile water and stored at –20°C. For transfection 1,5 µg vector DNA was combined with 100 µl serum-free DMEM. In a separate tube, 100 µl serum-free DMEM medium was added to 6 µl Lipofectamine. These aliquots were combined, gently mixed and incubated at room temperature for 30 minutes; this allowed the components to form a complex able to transfer vectors into the cells. The complexes were diluted in 0,8 ml serum-free DMEM medium. The cultured cells were rinsed twice in 1xPBS and once in transfection medium to remove all traces of serum prior to addition of the complexes. Cells were covered with transfection solution and incubated for 10 hours at 37°C in 5% CO_2 humidified atmosphere. Antibiotics were not present during the lipid-mediated transfection. Following incubation, the transfection medium was replaced and 3 ml of growth medium was added containing serum and antibiotics for 24 hour incubation. Complete DMEM medium with 500 µg/ml Geneticin antibiotic was added in order to expose the cells to selection pressure for 24 hours. This eliminates nontransfected cells and those which might have lost the vector and therefore are sensitive to Geneticin exposure. The vector carries Neo-Gen sequence insert and only cells containing the pcDNA3 construct are resistant to Geneticin mediated selection (**Figure 6**).

Geneticin inactivates phosphorylation by binding aminoglycoside-3'-phosphotransferase. The cells were incubated in selection medium twice a week for 24 hours within the next

two weeks after transfection. Moreover, cells were cultured for three days in a selection medium after passaging.

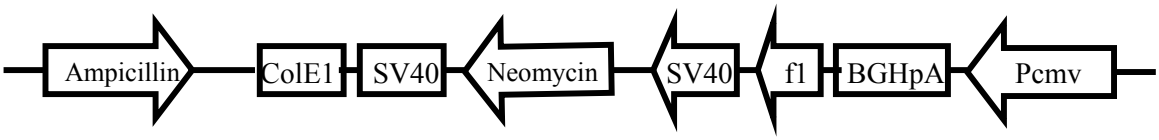

Figure 6: Linear scheme of the pcDNA3 transfection vector (5,4 kb).

2.10. Induction of genome instability by etoposide treatment in estradiol treated BG1 cell lines

Human ovarian cancer cells line-BG1 are hormone responsive because they carry an estrogen receptor. In order to investigate induced genotoxicity and apoptotic response in cells that are forced to proliferate, both cell lines (bcl-2 transfected and vector control) were subjected to induction of proliferation with estradiol. 1nM estradiol was added (**Table 3**) at a starting density of $5x10^5$ cells/ml in phenol red-free medium containing DCC serum to ensure absence of estrogens. The cells were grown at 37°C in 5% CO_2 humidified atmosphere for 72 hours. The cells were rinsed in 1x PBS and fresh medium was added plus 1 nM estradiol. Incubation was prolonged for another 24 hours at 37°C in 5% CO_2 humidified atmosphere.

Estradiol +/-	**Cytochalasin B**
BG1 pcDNA3 (vector control)-control	**+/-**
Vector control-1μM etoposide	**+/-**
BG1 pcDNA bcl2-control	**+/-**
BG1 pcDNA bcl2- 1μM etoposide	**+/-**

Table 3: Experimental set up for hormone induced proliferation in BG1 cells

Afterwards, the cells were subjected to 1 μM etoposide for 24 hours. Samples were rinsed in 1xPBS and harvested by trypsin-induced detachment. For micronuclei and apoptosis evaluation samples were prepared as previously described. Flow cytometric analysis of apoptosis (Annexin V staining) was not feasible due to transient membrane changes induced by trypsin. All samples were stained by acridine-orange and proliferation rate were assessed in samples treated with Cytochalasin B. The presence of

the MN and the proliferation rate was assessed by analysis of 2X1000 cells from two slides per sample. Numbers of independent repeat experiments are indicated in the figure legends.

Solutions and buffers

Growth medium:

500 ml Dulbecco's modified Eagle's medium (DMEM)-**phenol free**

5% DCC serum (v/v)

107 µg/ml Natrium Pyruvat

0,25 mg/ml L-Glutamin40 U/ml

Penicillin-Streptomycin0,04 mg/ml

Chemicals:

1 µM estradiol (m/w) stock solution dissolved in ethanol, stored at –20°C; 1X PBS buffer: 0,14 M NaCl; 2,7 mM KCl; 10 mM KH_2PO_4/K_2HPO_4, pH 7,5

3. Results

3.1. Effects induced by etoposide in human B lymphoblastoid cell lines

Cells from the three human lymphoblastoid cell lines TK6 (wild-type p53), WTK1 (mutated p53) and NH32 (knockout p53) were examined for p53 expression (**Fig.6**). The Western Blot analysis confirmed expression of p53 protein in TK6 cells (lane 1), abnormal expression of mutated p53 in WTK1 (lane 2) and absence of protein expression in NH32 cells (lane 3).

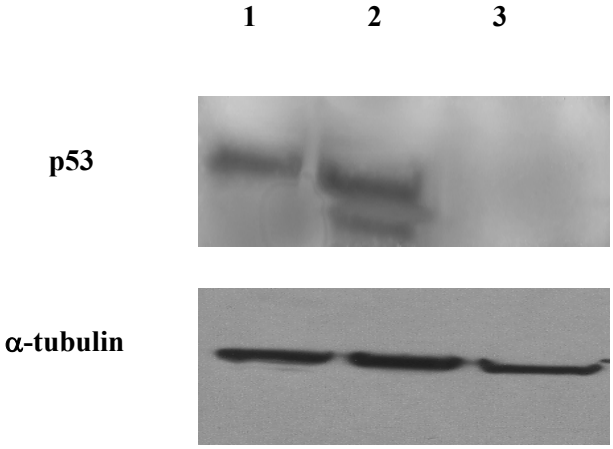

Figure 6:Western Blot analysis of p53 expression in human B lymphoblastoid cell lines (upper picture) and α-tubulin expression. Shown are (by lanes) TK6 (wild-type p53; 1), WTK1 (harbors mutated p53; 2), NH32 (no p53 expression; 3).

3.1.1. Micronucleus assay

Human B lymphoblastoid cell lines were treated with etoposide for 24 hours and micronucleus-induction was monitored microscopically (**Fig**.**7a, b and c**). Frequencies of micronuclei were scored by analysis of 2000 cells at each concentration of etoposide (**a**). Another set of samples was treated with the indicated etoposide concentrations along with 2 µg/ml cytochalasine B which results in binucleated cells (**b**). Since only cells that divide can form micronuclei, scoring was confined to 2000 binucleated cells (**Figures 7 b, d, f**). Micronucleus induction was more pronounced in WTK1 than in TK6 and NH32, which both do not harbor a mutated p53 gene.

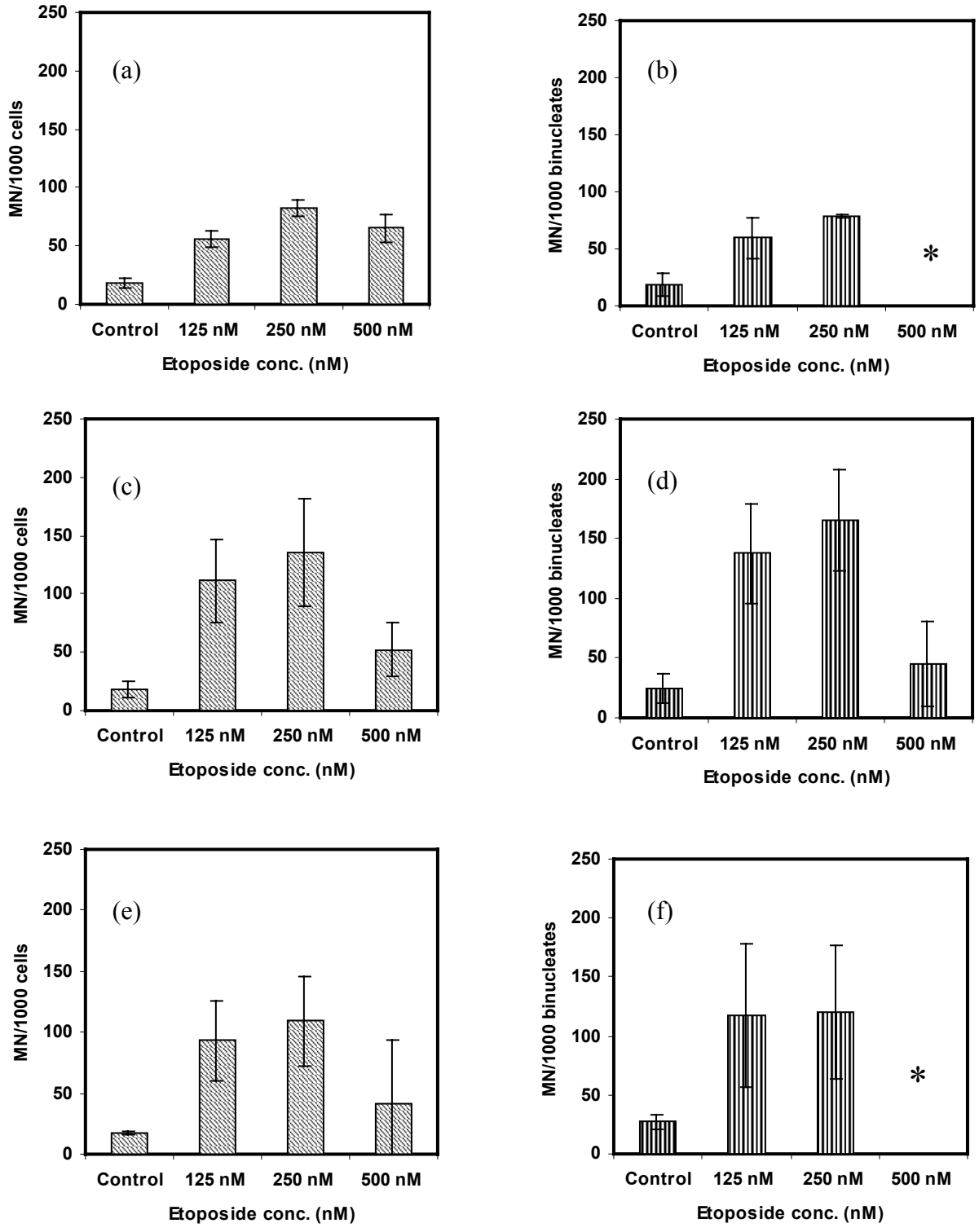

Figure 7: Analysis of micronuclei induction in TK6 (Fig.7 a,b) (wild type p53) cells, WTK1 cells (Fig.7c,d) (mutated p53) and NH32 (Fig.7e,f) (knock out p53 cells). For each cell line micronuclei test was performed without (**left charts**) and with addition of the cytokinesis inhibitor-cytochalasin B (**right charts**). Average values are from three independent experiments ± SD (**left charts)** or two independent experiments (**right charts**). The asterisk-cells do not proliferate due to toxicity at 500 nM etoposide concentrations.

3.1.2. Analysis of apoptosis induction

The induction of apoptosis was analyzed by scoring cells with altered nuclear morphology visible as fragmented DNA (so called apoptotic bodies). All three cell lines showed similar induction of apoptosis after treatment with etoposide (**Figure 8**).

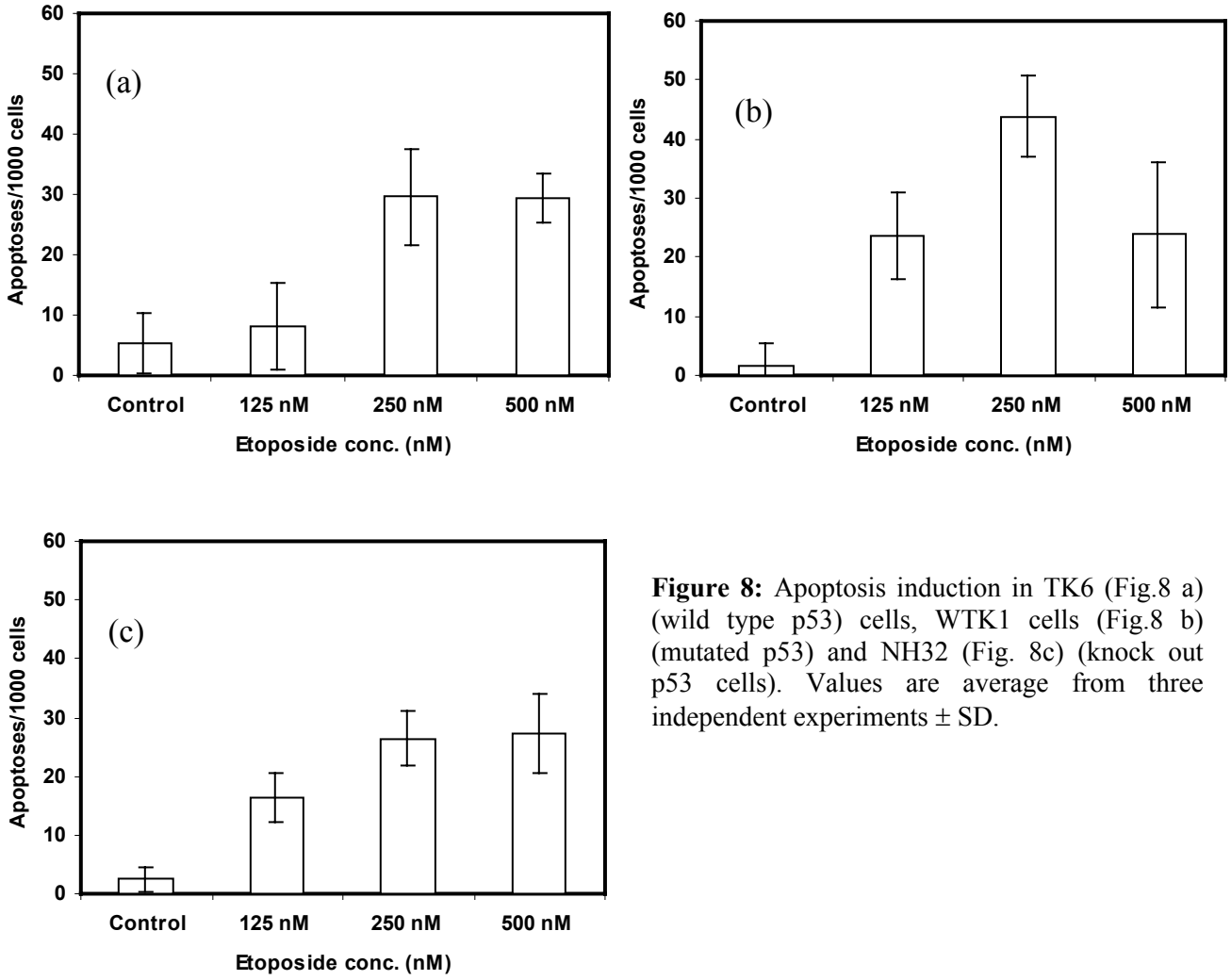

Figure 8: Apoptosis induction in TK6 (Fig.8 a) (wild type p53) cells, WTK1 cells (Fig.8 b) (mutated p53) and NH32 (Fig. 8c) (knock out p53 cells). Values are average from three independent experiments ± SD.

3.1.3. Proliferation and cytotoxicity analysis

An impaired proliferation pattern was revealed by cell counts (**Figure 9**) sensitivity for etoposide-induced cytotoxicity was similar in the explored cell lines.

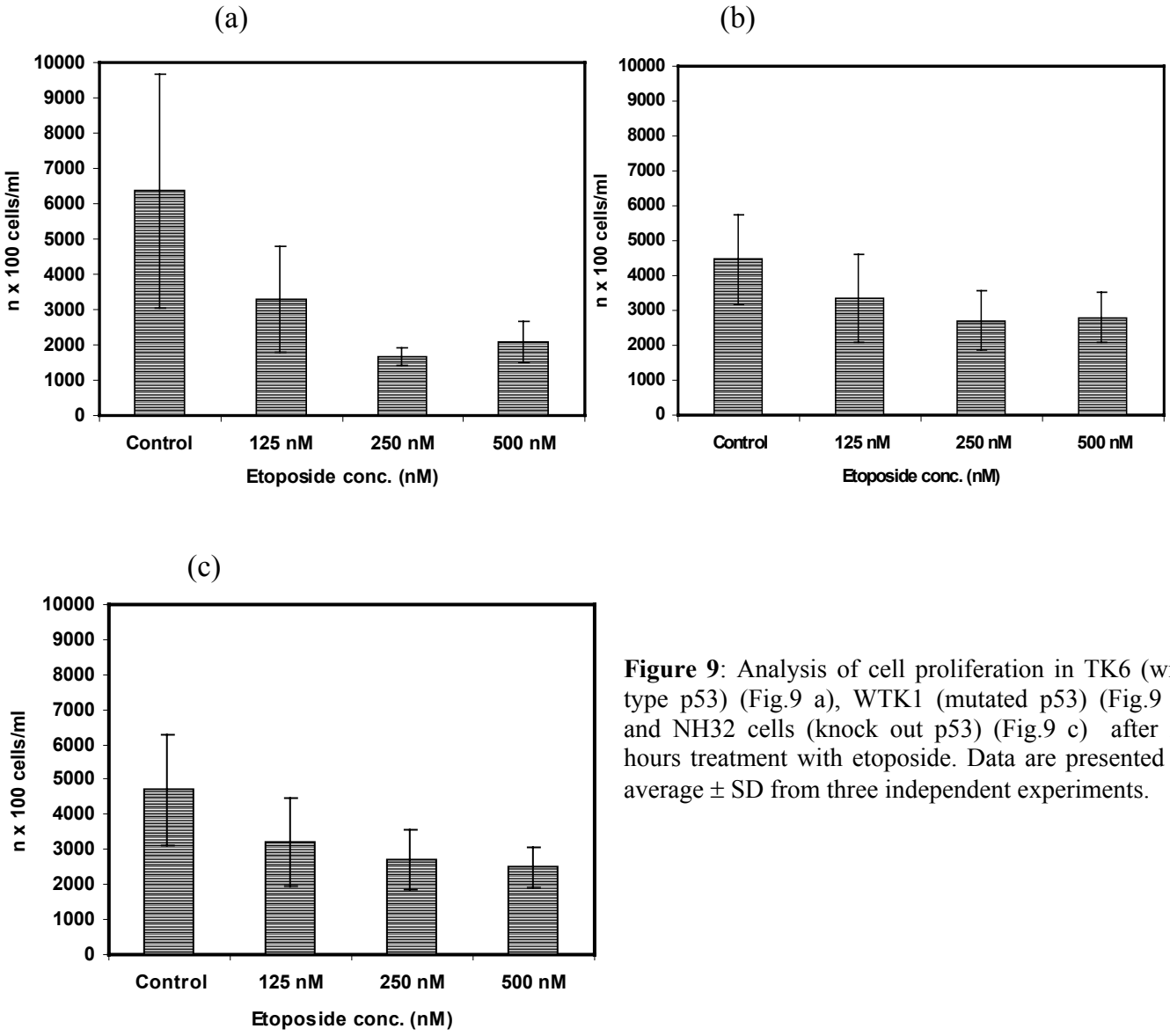

Figure 9: Analysis of cell proliferation in TK6 (wild type p53) (Fig.9 a), WTK1 (mutated p53) (Fig.9 b) and NH32 cells (knock out p53) (Fig.9 c) after 24 hours treatment with etoposide. Data are presented as average ± SD from three independent experiments.

The frequency of binucleated cells was analysed as proliferation marker (**Figure 10**). The reduction of proliferation induced by etoposide was similar in all three cell lines. In all three cell lines at a concentration of 500 nM etoposide, no binucleated cells were present

indicating arrest of proliferation. Although NH32 cells had the lowest proliferation rate in the control, a reduction of proliferation was found.

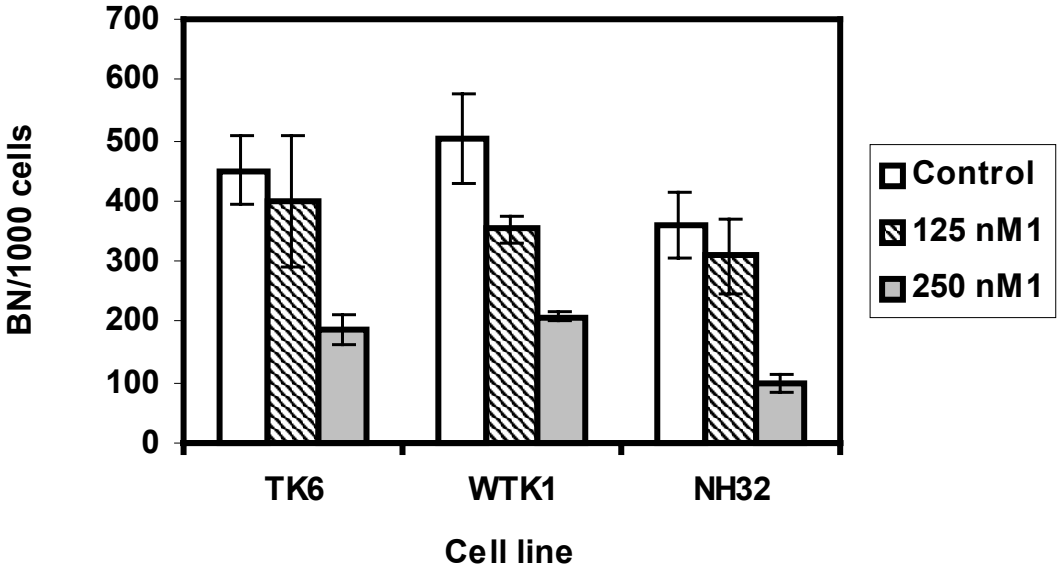

Figure 10: Frequencies of binucleated cells after etoposide treatment. Data are presented as average ± SD from three independent experiments.

3.1.4. Cell cycle analysis

Human lymphoblastoid cell lines showed altered cell cycle distribution patterns after etoposide treatment depending on the p53-status (**Figures 11-13; Tables 4-6**). TK6 (p53 wild-type) cells showed a dose-dependent accumulation in G2/M phase. G0/G1 phase was maintained, and a decrease in S-phase was observed. Subjection to 5 µM etoposide induced accumulation of 89,1% of the cells in G0/G1 phase.

In the literature, the apoptotic response is often described visible as 'subG$_1$ peak'. Although defined as a percentage of all modeled events minus debris, this kind of analysis is probably less selective and accurate than Annexin V-PI analysis. Analyzing the sub G1 peak we found induction of apoptosis by etoposide.

Etoposide concentration	%G0/G1	%S	G2/M	% Apoptosis (subG1 peak)
Control 1% DMSO	**32,6**	**55,66**	**11,74**	**0,43**
125 nM	**31,88**	**41,9**	**26,22**	**1,74**
250 nM	**30,41**	**39,02**	**30,57**	**2,49**
500 nM	**29,49**	**28,96**	**41,55**	**2,92**
5 µM	**89,10**	**10,86**	**0**	**3,21**

Table 4: Cell cycle analysis in TK6 wt p53 cells (using ModFit software).

WTK1 cells (mutated p53) showed a different response to a etoposide. The dose-dependent G2/M accumulation extended up to 5 µM etoposide, and G0/G1 as well as S-phase showed a decrease. A similar percentage of apoptosis as for TK6 cells was detected as sub G1-peak.

In NH32 (p53 knock out), an accumulation in G2/M was found for all tested concentrations. These cells also showed a decrease in S-phase and the highest sensitivity for decrease in G0/G1 and increase in G2/M of these three cell lines. No clear apoptotic response to etoposide treatment could be detected.

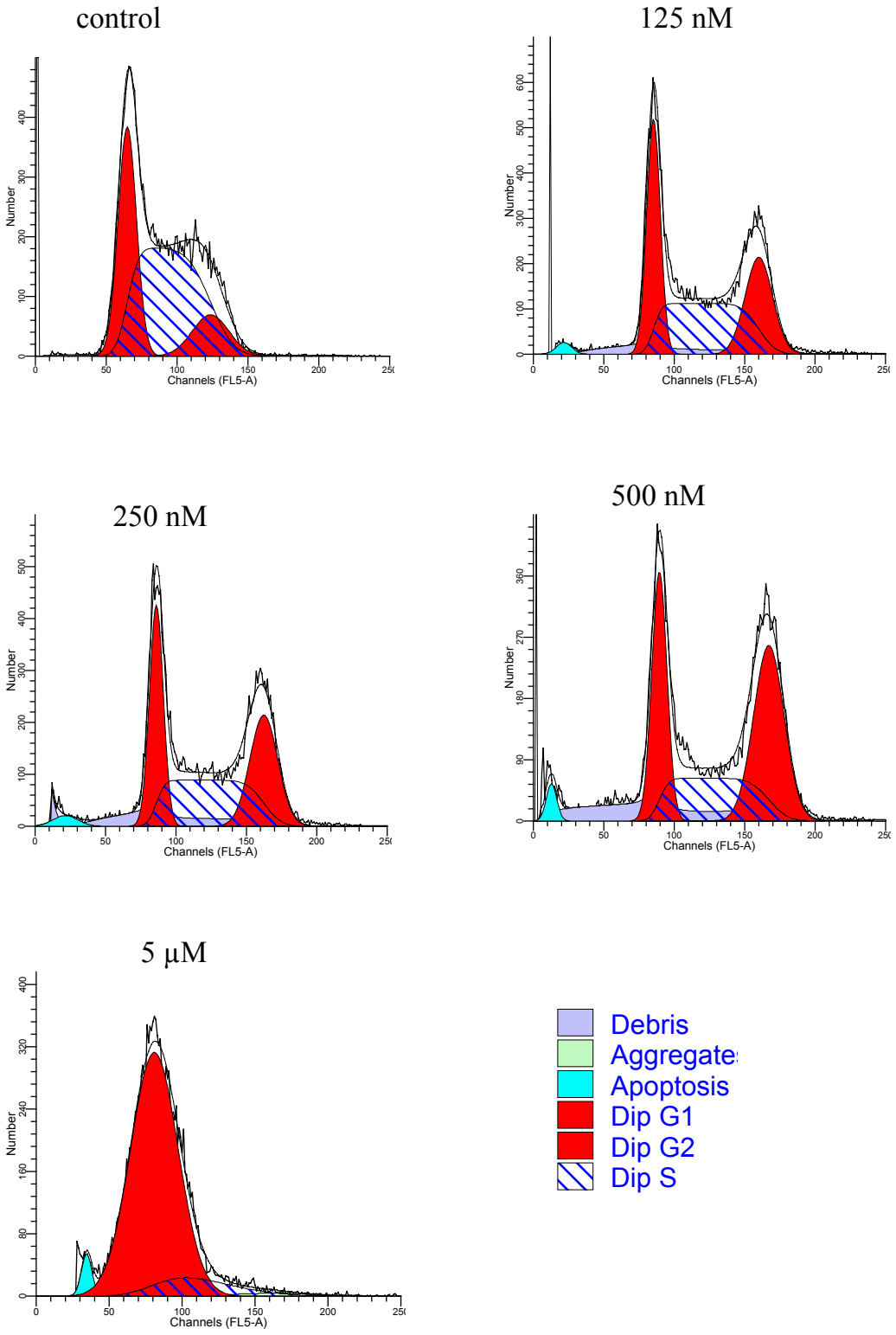

Figure 11: Cell cycle analysis in TK6 p53 wt cells. Plots show one representative out of three successful experiments. A quantitative analysis can be found in **Table 4.**

Etoposide concentration	%G0/G1	%S	G2/M	% Apoptosis (subG1 peak)
Control 1% DMSO	30,04	53,4	16,56	0,53
125 nM	22,98	50,64	26,37	0,94
250 nM	16,75	48,45	34,80	3,74
500 nM	9,66	25,92	64,38	2,16
5 µM	1,81	0	98,19	4,43

Table 5: Cell cycle analysis in WTK1 cells harboring mutated p53 (using ModFit software).

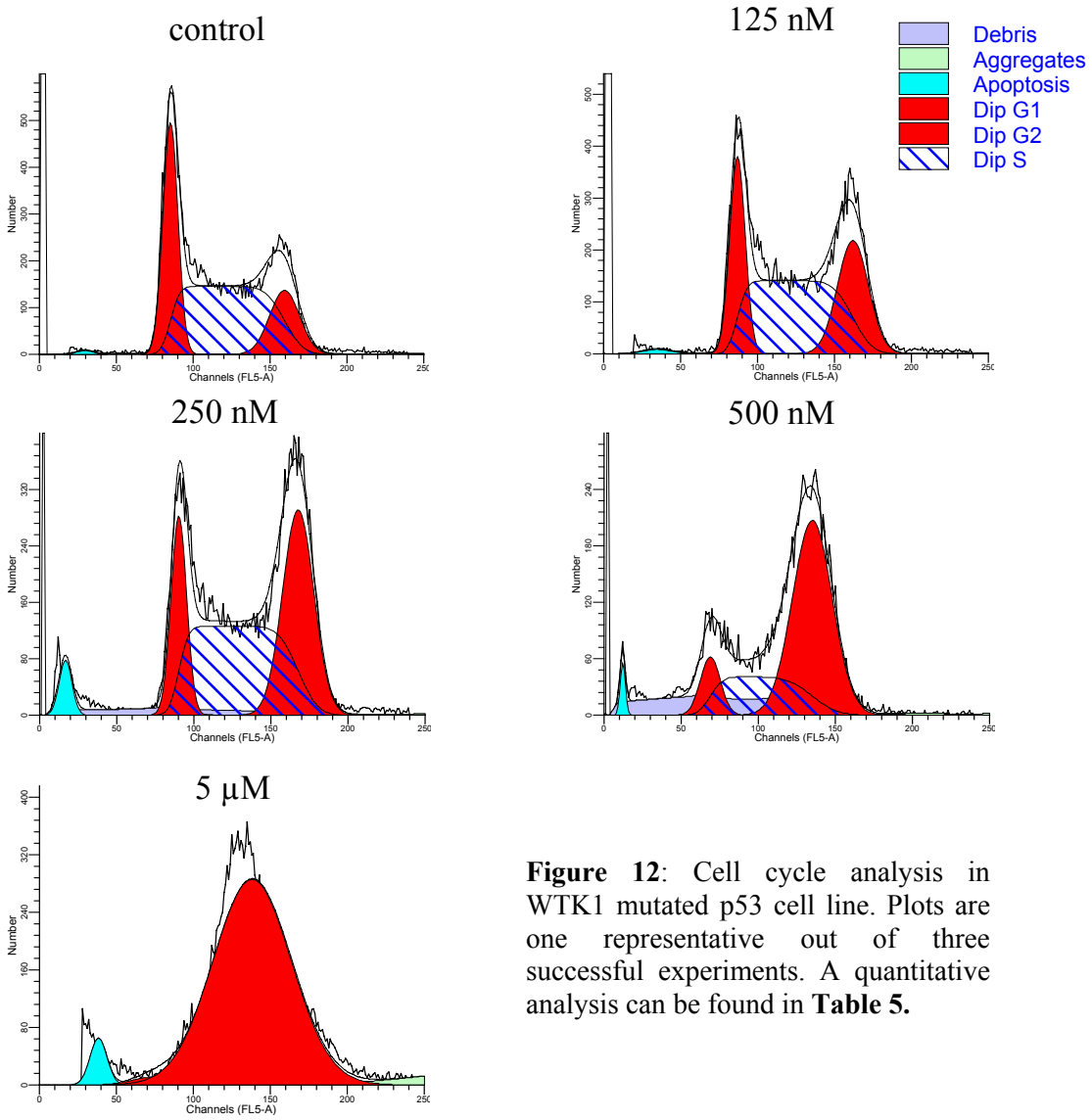

Figure 12: Cell cycle analysis in WTK1 mutated p53 cell line. Plots are one representative out of three successful experiments. A quantitative analysis can be found in **Table 5.**

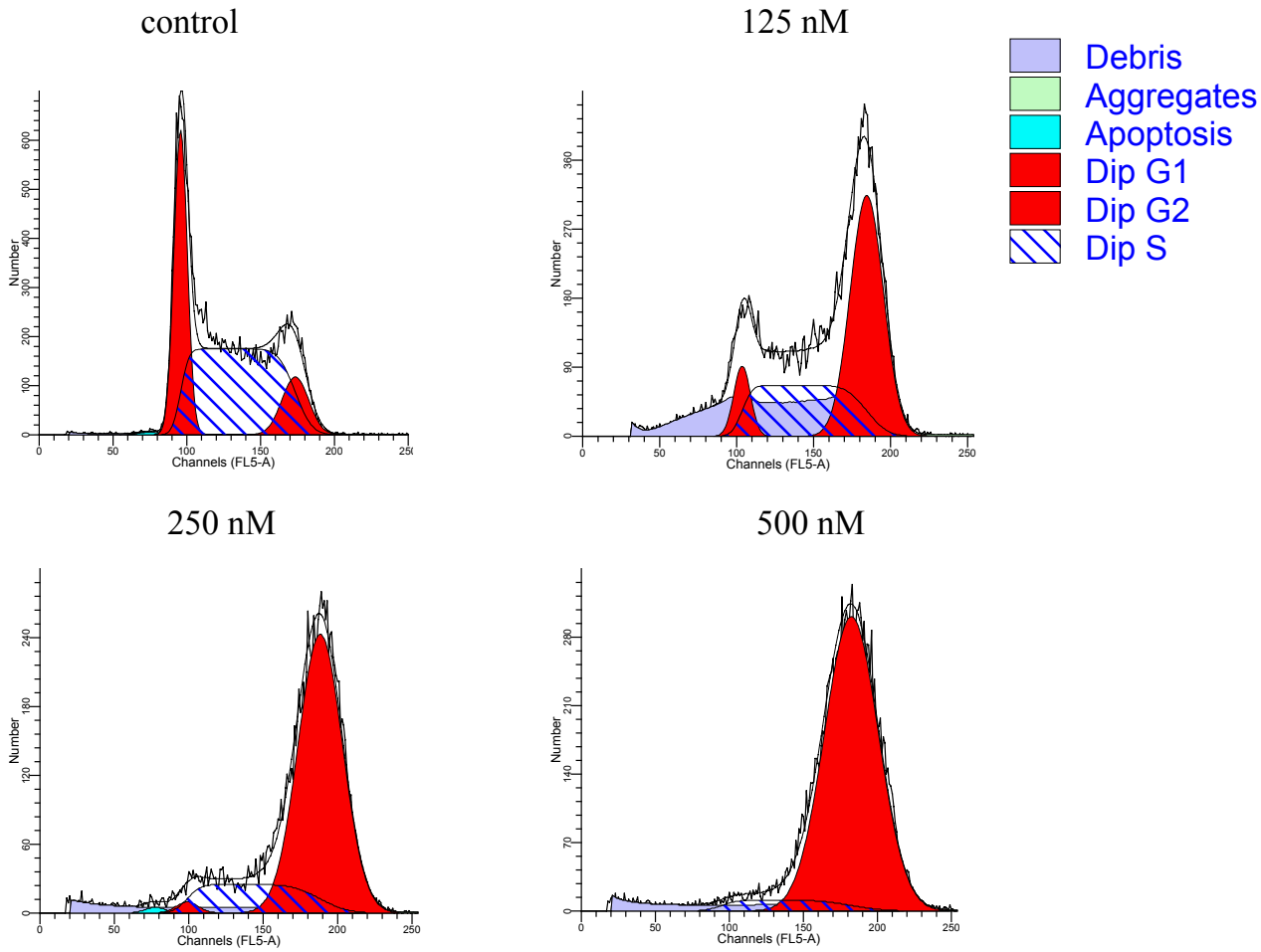

Figure 13: Cell cycle analysis in NH32 p53 null cell line. Plots are one representative out of three successful experiments. A quantitative analysis can be found in **Table 4.**

Etoposide concentration	%G0/G1	%S	G2/M	% Apoptosis (subG1 peak)
Control 1% DMSO	**30,23**	**58,30**	**11,47**	**0,36**
125 nM	**8,2**	**35,74**	**56,06**	**0**
250 nM	**1,58**	**19,46**	**78,97**	**0,74**
500 nM	**0**	**6,79**	**93,21**	**0**

Table 6: Cell cycle analysis in NH32 p53 null cells (using ModFit software).

3.1.5. Analysis of p21 induction

In order to investigate possible effects of the p53 states we performed flow cytometric analysis of p21 induction. Up regulation of p21 induces inhibition of cycline-dependent kinases (cdk) resulting in cell cycle arrest. Induction was detected in all three cell lines after treatment with etoposide concentrations for 24 hours, as reflected by the shift of the expression curve to the right (**Figure 14 a,b,c**). The p21 induction was more pronounced in TK 6 cells than in WTK1 and NH32 (**Figure 14a**).

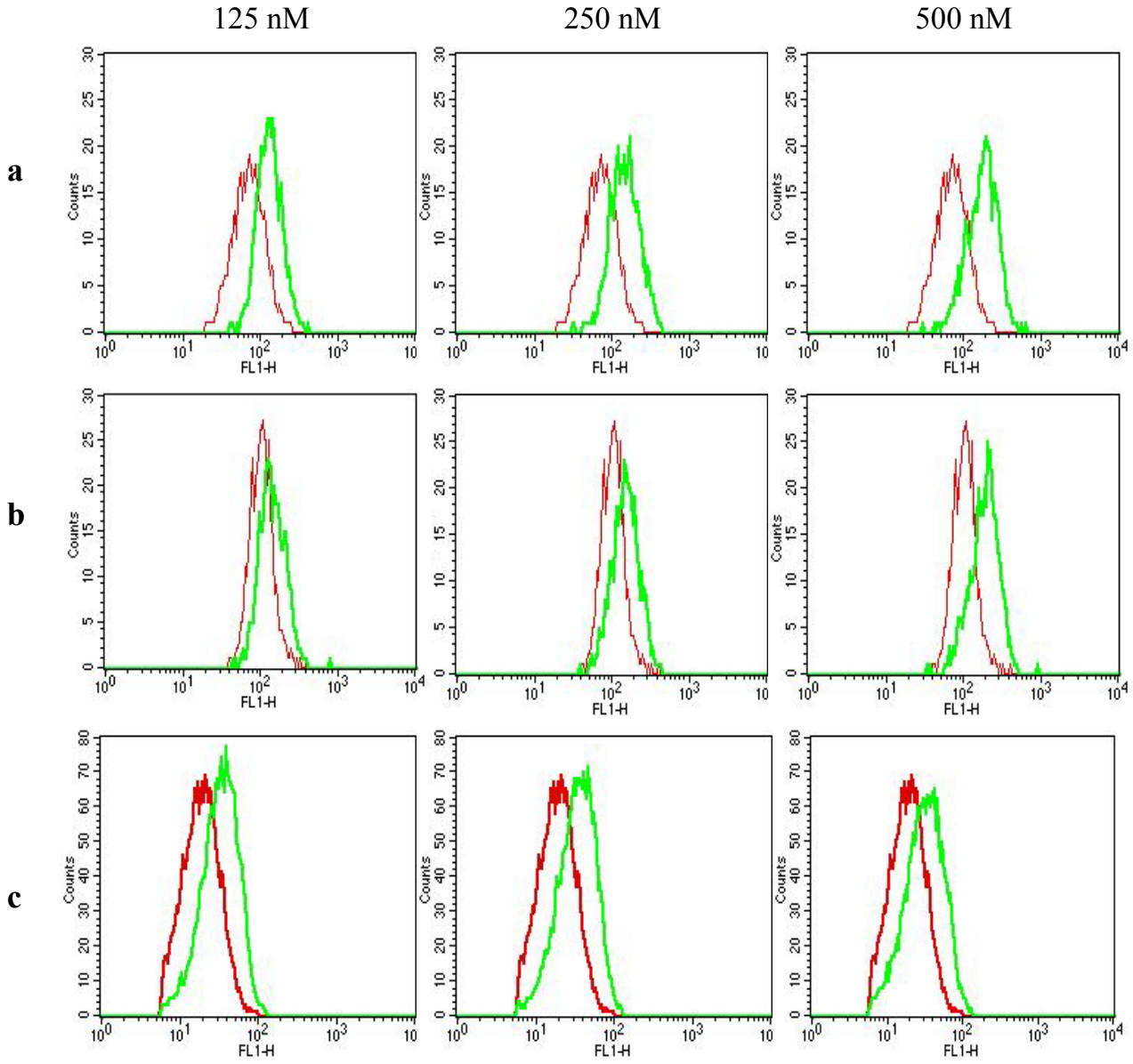

Figure 14: P21 induction in TK6 (wild type p53) (**Figure 14 a**), WTK1 (mutated p53) (**Figure 14b**), NH32 (p53 null cells) (**Figure 14 c**). Etoposide treated cells-**green line**. Control **-red line**. Shown histograms are representative samples from three independent experiments.

The induction was detected as shift to higher fluorescence intensity of the p21 protein within single cells compared to intensity in the control sample. Analysis was performed as p21-FITC intensity fluorescence versus cell count whereas unstained TK6 cell were used as negative control (Data not showed).

3.2. Temporary p53 inhibition induced by pifithrin-α (PFT-α)

Pifithrin-α application has been described to modulate apoptotic response in cancer treatment. While p53 mutated cancer cells undergo chemotherapy-induced apoptosis, healthy p53 wild type cells from normal tissue are protected by temporary disabling them to launch apoptosis. We observed an increase in p53 expression in TK6 and WTK1 cells (**Figure 15**), which was abolished by PFT-α addition.

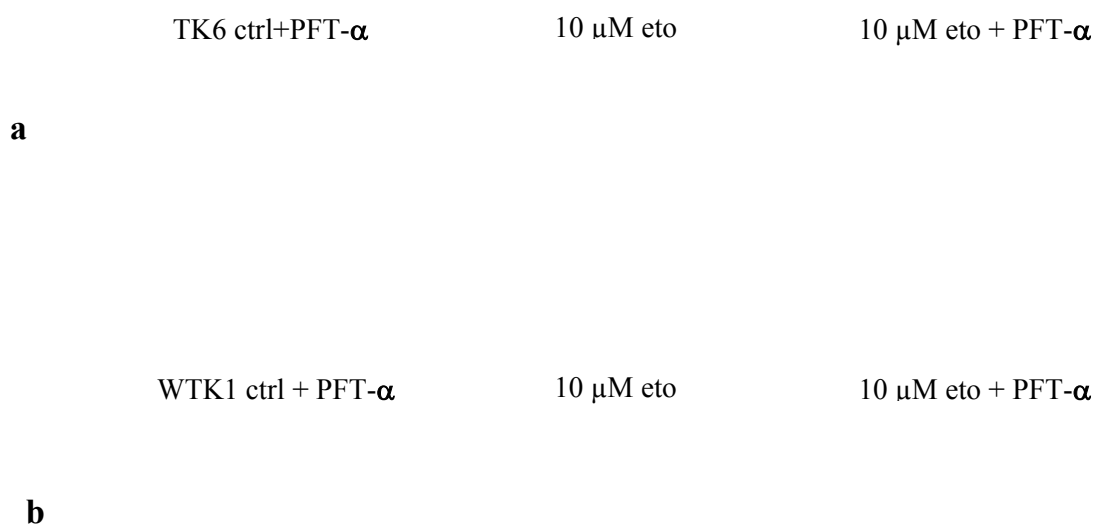

Figure 15: Flow cytometric analysis of p53 induction in TK6 **(a)** and WTK1 **(b)** cell line after combined treatment with pifithrin-α and etoposide. Etoposide treated cells-**green line**. Control -**red line**.

3.2.1. Analysis of micronuclei induction after PFT-α treatment

When we investigated the influence of PFT-α on etoposide-mediated micronuclei induction, we found a different response in the three cell lines depending on the p53 states. A significantly reduced induction of micronuclei formation in TK6 and WTK1 cells was observed upon co-treatment with 125 nM etoposide and 30 µM PFT-α compared to the solvent control (1%DMSO) and 125 nM etoposide treatment alone (**Figure 16a,b**). Since p53 is knocked out, in NH32 cells any similar effect could not be observed (**Figure 16c**).

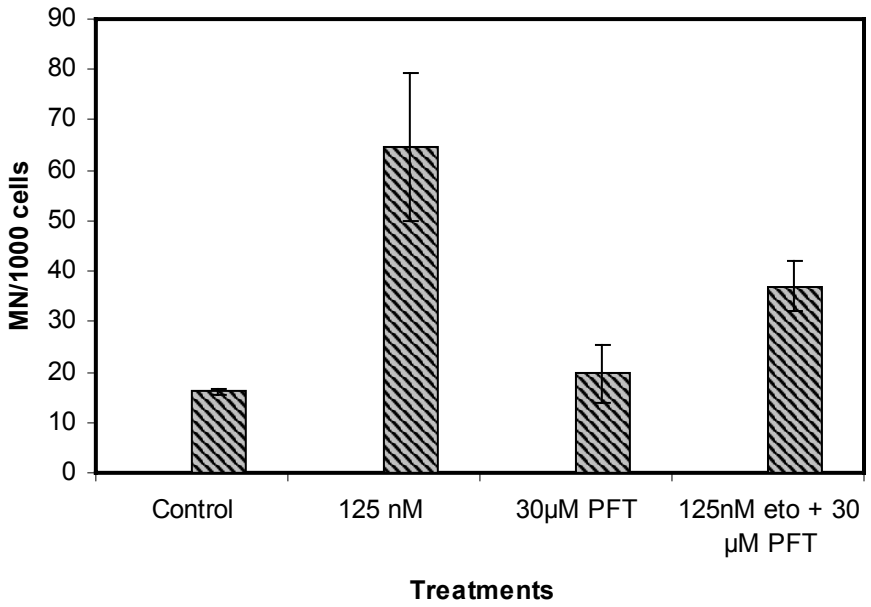

Figure 16a: The induction of micronuclei in TK6 cells treated with 125 nM etoposide for 24 hours in absence or presence of 30 µM pifithrin-α. Data are presented as an average ± SD from three independent experiments.

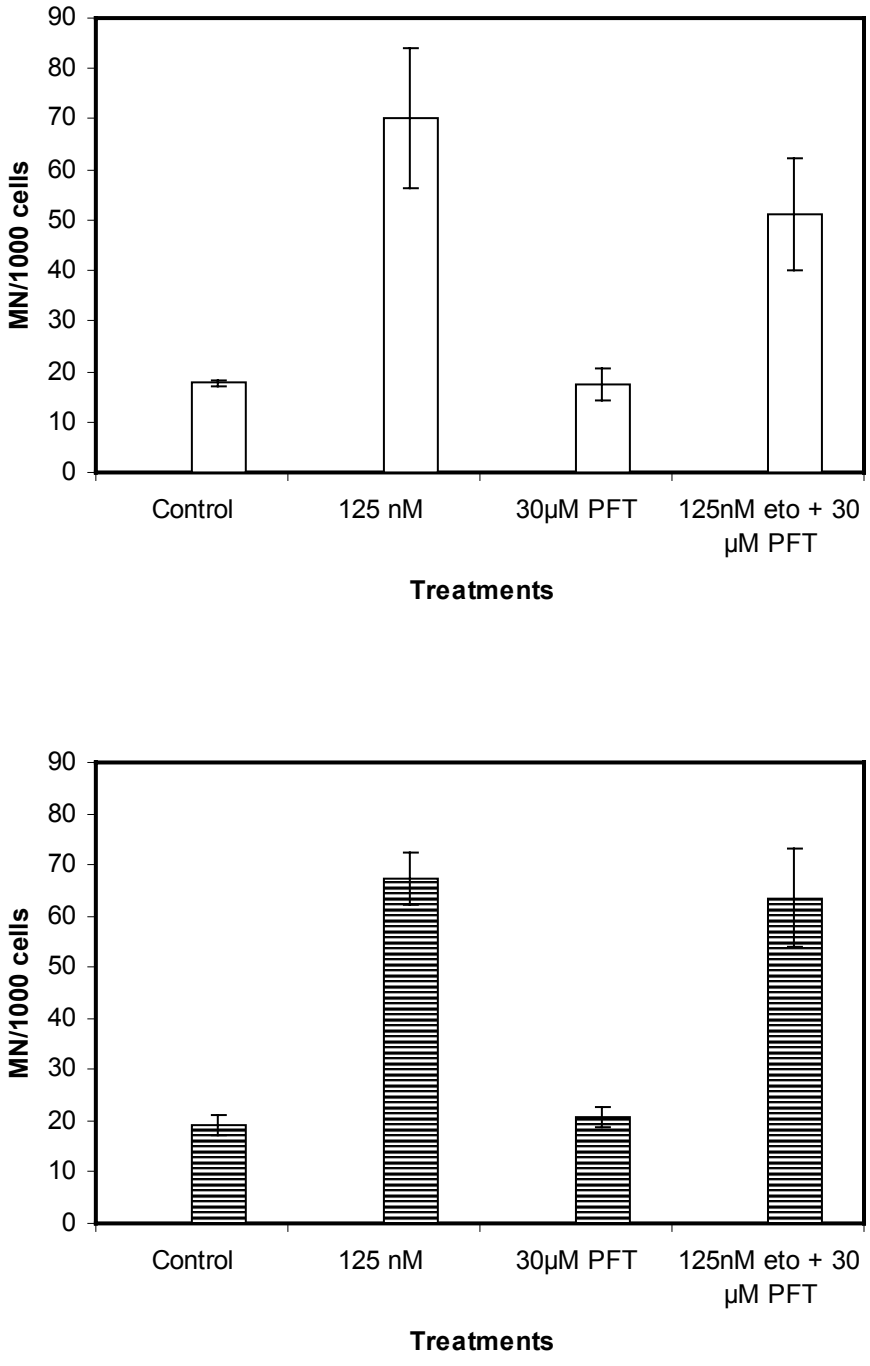

Figure 16c: The induction of micronuclei in WTK1 cell line (mutated p53) (**Figure 16b**) and in NH32 (p53 null cells) (**Figure 16c**) treated with 125 nM etoposide ± PFT-α. Data are presented as average value ± SD from three experiments.

3.2.2. Apoptosis suppression by Pifithrin-α

Application of Annexin V and PI provides a selective analysis of apoptosis. Initiation of apoptosis is accompanied by phospholipid phosphatidylserine (PS) migration from the inner to outer leaflet of the plasma membrane during apoptosis. PS remains on the outer side of the membrane in early and late stages acting as substrate for Annexin V (**Figure 17**). Necrotic cells are permeable for propidium-iodide that binds DNA and RNA (**Figure 18**).

After etoposide treatment all cell lines showed induction of apoptosis (**Figure 19 a, b, c and Tables 7-9**). In TK6 (p53 wild type) and WTK1 (p53 mutated) but not in NH32 (p53 knock out) apoptosis was reduced after the addition of PFT-α;

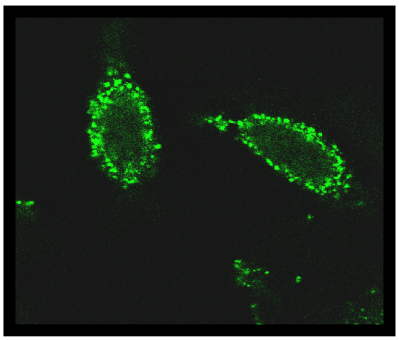

Figure 17: Confocal microscopy analysis of live apoptotic cells labelled with Annexin V bound at the edges of cell membrane.

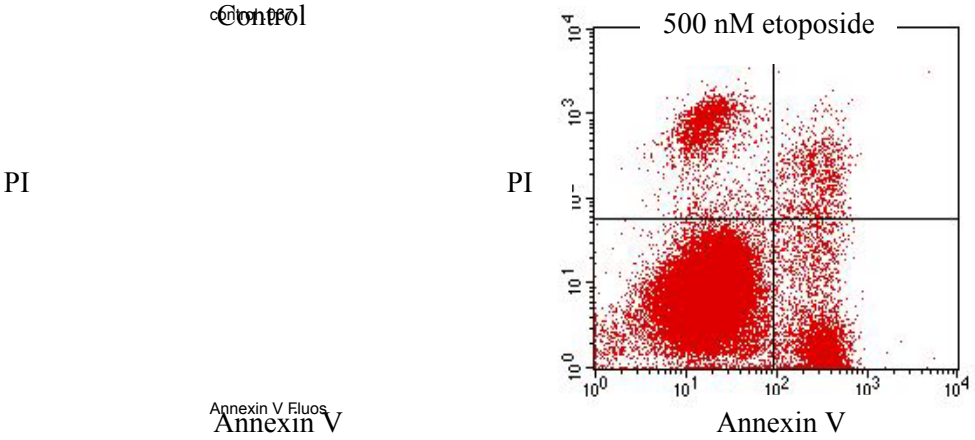

Figure 18: Flow cytometry analysis of apoptosis using Annexin V labelling. TK6 cells were treated for 24 hours with solvent (1% DMSO, left) or 500 nM etoposide (right panel). The lower left quadrant contains viable cells; the upper left quadrants contain propidium iodide positive cells (necrotic), and the two right quadrants Annexin V positive cells. The lower right quadrant contains early apoptotic stages and the upper right quadrant late apoptotic stages.

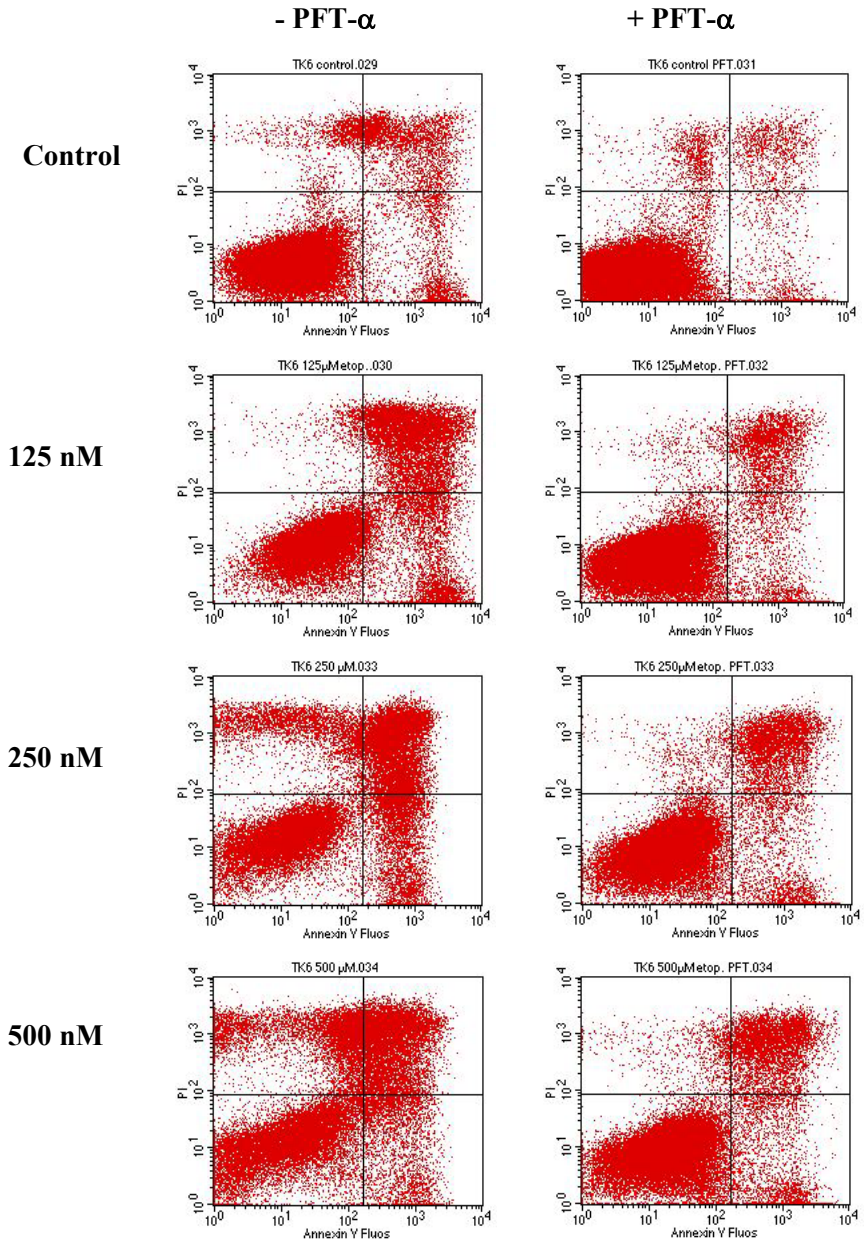

Figure 19a: Apoptotic response in TK6 cell treated with etoposide (left column) and treated with etoposide and pifithrin-α (right column).

Table7: Apoptosis induction in TK6 cells (% cells in quadrants)

Etoposide	control	125 nM	250 nM	500 nM
Annexin V positive	7.23	54	44.21	44.37
PI positive (A neg.)	4.83	13.14	14.11	18.82
Viable cells	87.95	41.09	30.44	37.75
TK6 cells; etoposide + pifithrin-α				
Annexin V positive	7.21	18.18	24.52	30.39
PI positive (A neg.)	2.01	1.07	1.9	1.49
Viable cells	90.73	80.75	73.58	68.11

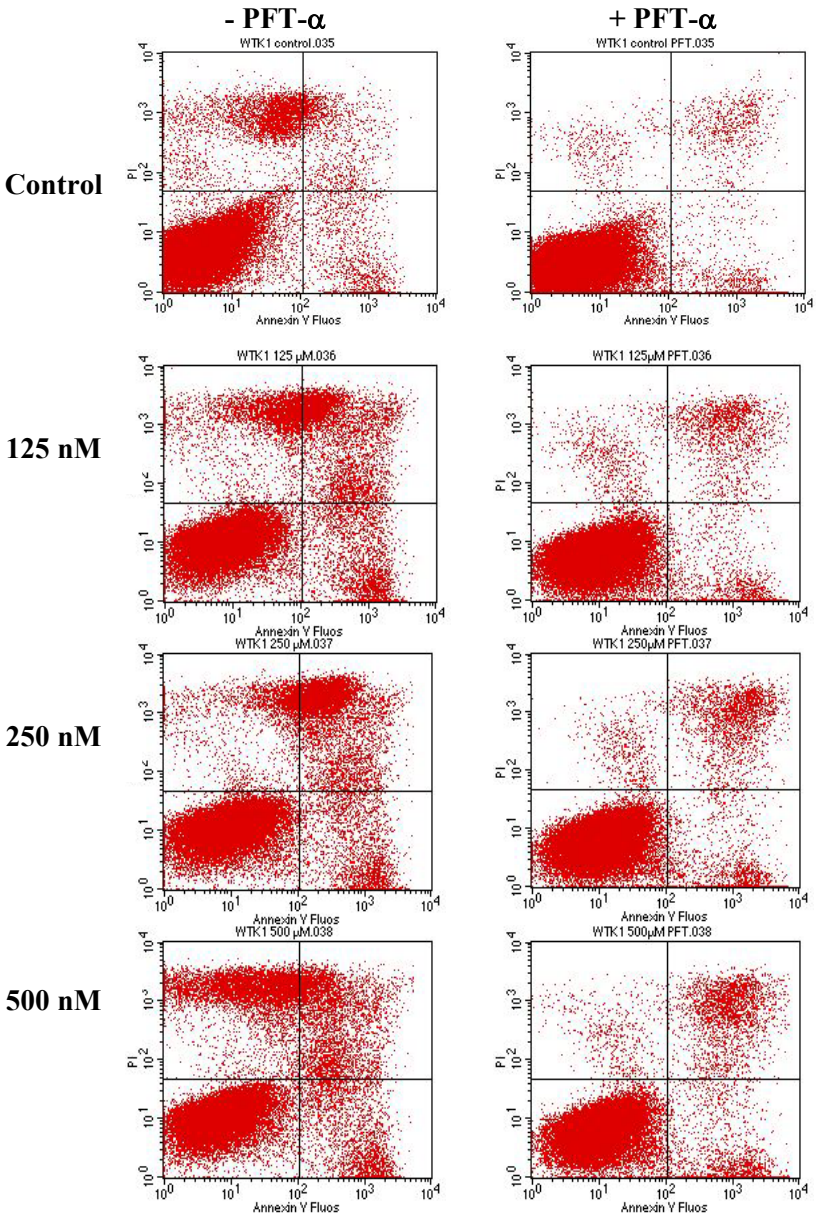

Figure 19b: Apoptotic response in WTK1 cell line treated only with etoposide (left column) and treated with etoposide and pifithrin-α (right column).

Table 8:Apoptosis induction in WTK1 cells (% cells in quadrants)

Etoposide	control	125 nM	250 nM	500 nM
Annexin V positive	4.38	19.46	22.9	17.78
PI positive (A neg.)	7.37	10.47	6.69	17.45
Viable cells	88.25	70.07	70.42	64.77
WTK1 cells; etoposide + pifithrin-α				
Annexin V positive	3.11	8.64	10.8	11.7
PI positive (A neg.)	0.66	1.58	1.24	1.18
Viable cells	96.23	89.77	87.96	87.12

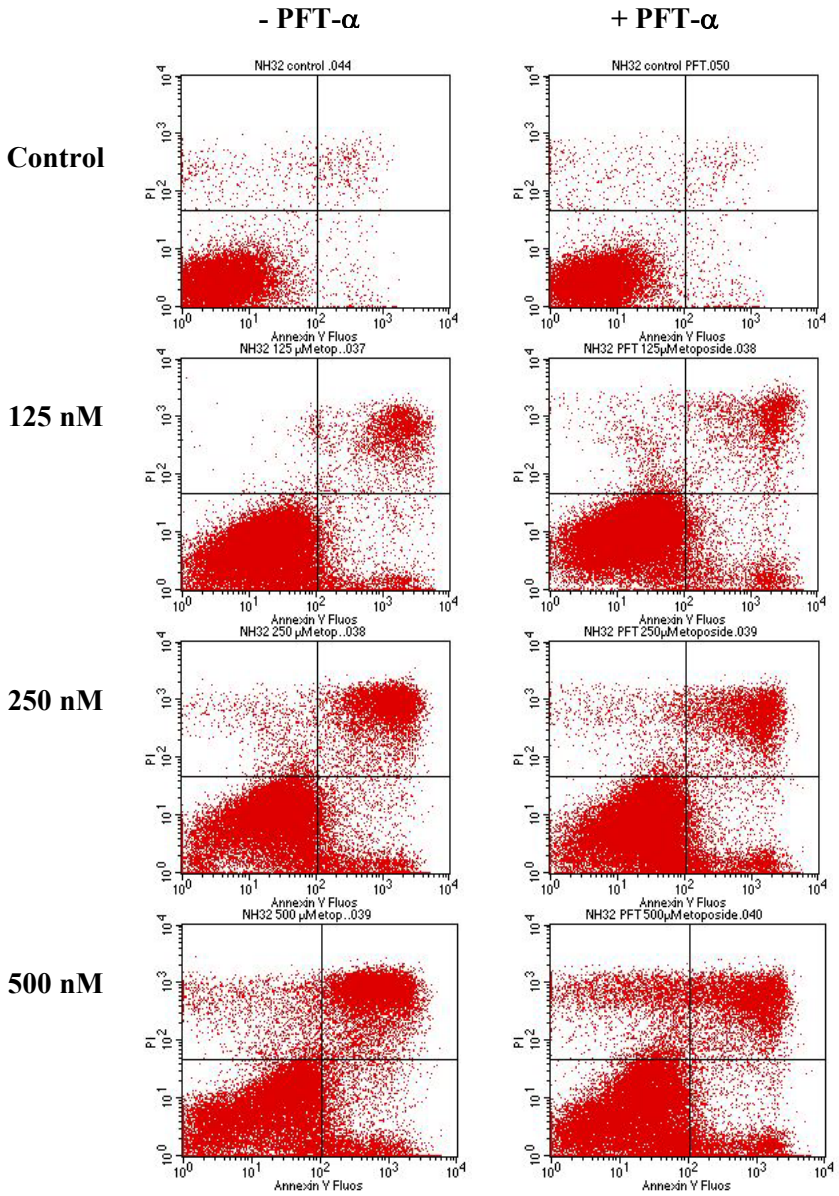

Figure 19c: Apoptotic response in NH32 cell line treated only with etoposide (left column) and treated with etoposide and pifithrin-α (right column).

Table 9: Apoptosis induction in NH32 cells (% cells in quadrants)

Etoposide	Control	125 nM	250 nM	500 nM
Annexin V positive	12.72	16.02	18.7	18.79
PI positive (A neg.)	6.76	5.40	6.47	7.77
Viable cells	80.53	78.58	74.83	73.44
NH32 cells; etoposide + pifithrin-α				
Annexin V positive	2.48	9.67	16.29	21.75
PI positive (A neg.)	1.11	3.85	5.28	13.8
Viable cells	96.41	86.46	78.43	64.45

.2.3. Impact of PFT-a on the cell cycle in human lymphoblastoid cell lines

We compared the cell cycle distribution of the three human lymphoblastoid cell lines with different p53 states after treatment with 125 and 250 nM etoposide concentrations and PFT-α. In TK6 cells the accumulation of cells in G2/M phase was enhanced with PFT-α at 125 nM etoposide, decreasing the percentage of TK6 cells in S phase. At 250 nM etoposide, percentages of cells in S phase were increased while those in G0/G1 and G2 were decreased (**Figure 20a; Table 10**). PFT-α alone did not induce clear alterations in cell cycle distribution.

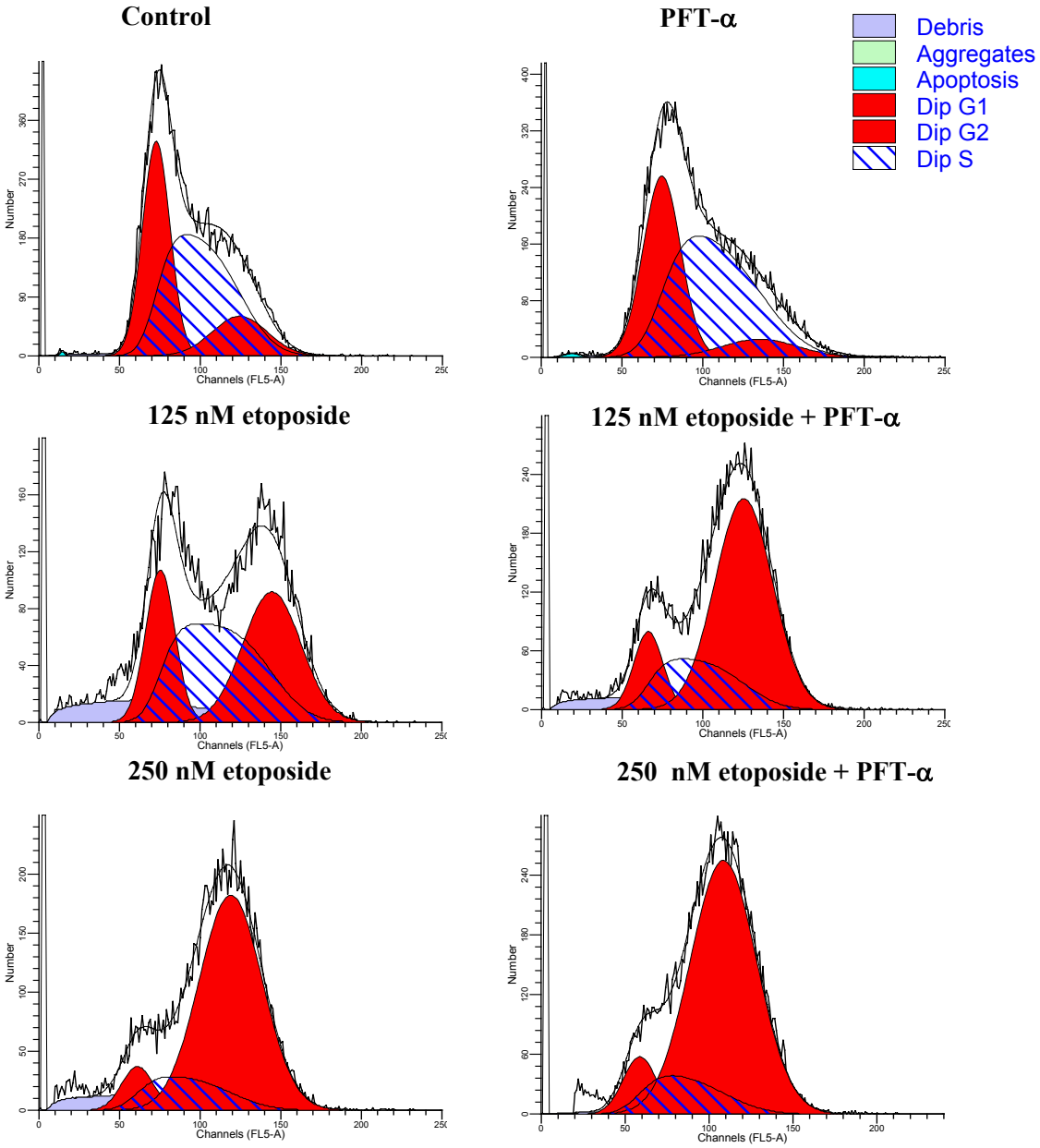

Figure 20a: Cell cycle analysis of TK6 cells (wild type p53) after treatment with pifithrin-α and etoposide.

Table 10: Distribution of TK6 cells to cell cycle phases after treatmentwith etoposide and PFT-α (analysis utilized using ModFit software).

Treatment	%G0/G1	%S	G2/M
Control (1% DMSO)	35,8	51	13,2
30 μM PFT-α	36,92	55,79	7,29
125 nM etoposide	24,36	37,66	37,98
125 nM etop. + PFT-α	14,54	19,55	65,91
250 nM etoposide	14,06	0,07	85,86
250 nM etop. + PFT-α	7,01	27,51	65,48

In WTK1 cells (**Figure 20b, Table 11**), PFT-α enhanced the etoposide induced G2/M accumulation, leading to decrease in S and G0/G1 phase cells. In NH32 cells (**Figure 20c, Table 12**) no clear effect of PFT-α on etoposide induced G2 accumulation was observed, but a reduction of the percentage of cells in S phase and G0/G1 phase. PFT-α alone did not induce a clear effect on the cell cycle distribution in WTK1 and NH32 cells.

Table 11: Distribution of WTK1 cells to cell cycle phases after treatment with etoposide and PFT-α (analysis utilized using ModFit software).

Treatment	%G0/G1	%S	G2/M
Control (1% DMSO)	31,05	62,13	6,83
30 μM PFT-α	34,49	59,62	5,89
125 nM etoposide	6,5	52,43	41,07
125 nM etop. + PFT-α	0,23	23,24	76,53
250 nM etoposide	5,71	39,27	55,02
250 nM etop. + PFT-α	1,94	0	98,06

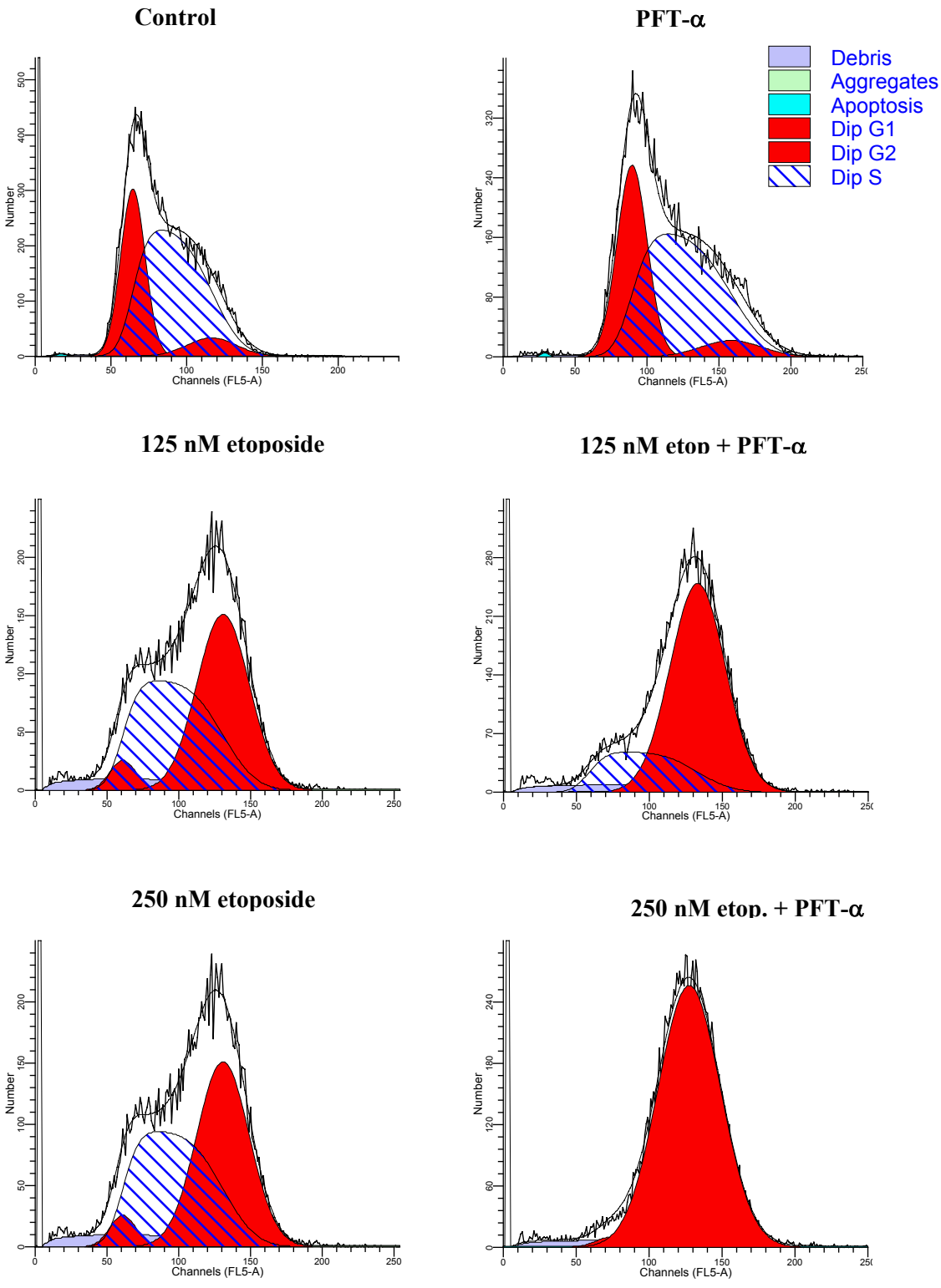

Figure 20b: Cell cycle analysis of WTK1 cells (mutated p53) after treatment with pifithrin-α and etoposide.

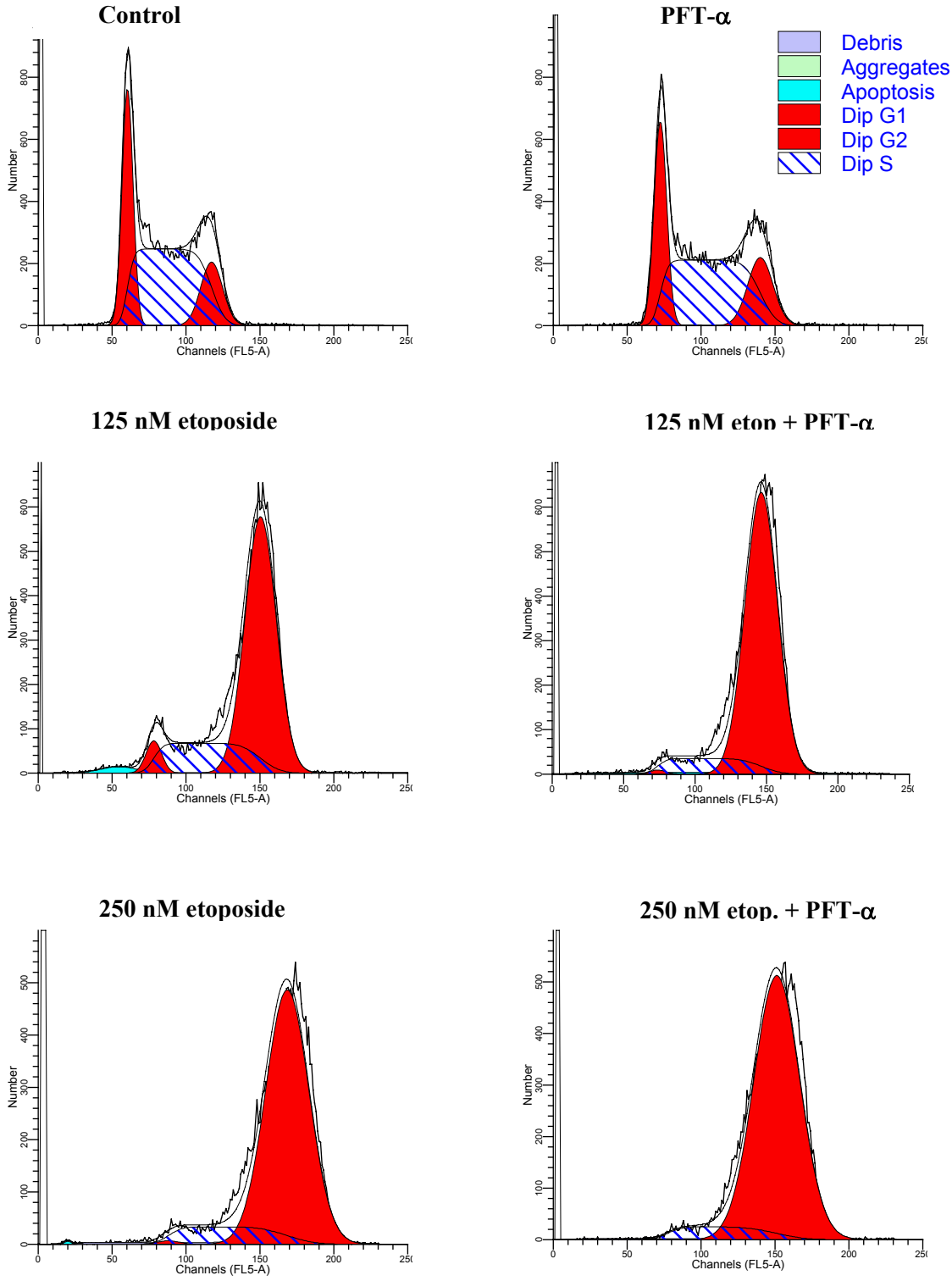

Figure 20c: Cell cycle analysis of NH32 (p53 null cells) after treatment with etoposide and pifithrin-α.

Table 12: Distribution of NH32 cells to cell cycle phases after treatment with etoposide and PFT-α (analysis utilized using ModFit software).

Treatment	%G0/G1	%S	G2/M
Control (1% DMSO)	28,46	56,33	15,21
30 µM PFT-α	27,1	54,86	18,05
125 nM etoposide	4,57	23	72,43
125 nM etop. + PFT-α	0,62	12,34	87,03
250 nM etoposide	0,61	12,98	86,41
250 nM etop. + PFT-α	0	8,44	91,56

3.2.4. Flow cytometric analysis of the influence of PFT-α on p21^{WAF} expression

Flow cytometric analysis showed an elevated p21^{WAF} expression which did not reveal the expected decrease after PFT-α treatment. Particularly, a decrease was expected in p21^{WAF} expression after etoposide treatment, which was not reduced by the addition of PFT-α; PFT-α alone did not induce p21^{WAF} expression (**Figure 21**).

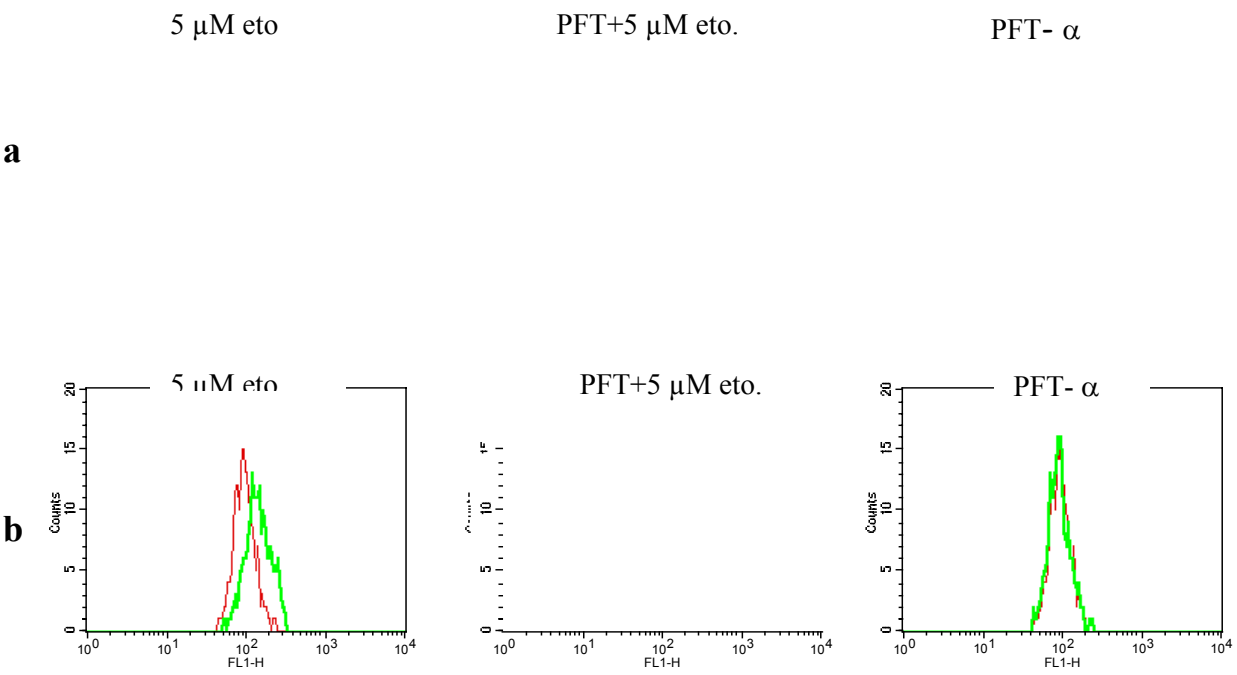

Figure 21: Flow cytometric analysis of p21 ^{WAF} expression in TK6 (**a**) and (**b**) WTK1 cells after etoposide and PFT-α treatment. The induction was detected as shift to higher fluorescence intensity of the p21 protein within single cells compared to intensity in the control sample.

3.3.Transient transfection with antisense bcl-2 oligonucleotide

p53 has indirect control over mitochondrial integrity via up regulation of the pro-apoptotic Bax protein that inserts in the mitochondrial membrane. Opening of the PTP pores and launch of apoptosis may be reached by Bax overexpression when it exceeds Bcl-2 activity. As described in previous experiments, human lymphoblastoid cell lines show different apoptotic response depending on their p53 states. When we investigated the status of the anti-apoptotic gene bcl-2 in the three human lymphoblastoid cell lines, a clear signal for Bcl-2 on Western Blot analysis was found under conditions where a control cell line (BG1) did not show any visible expression (**Figure 22**).

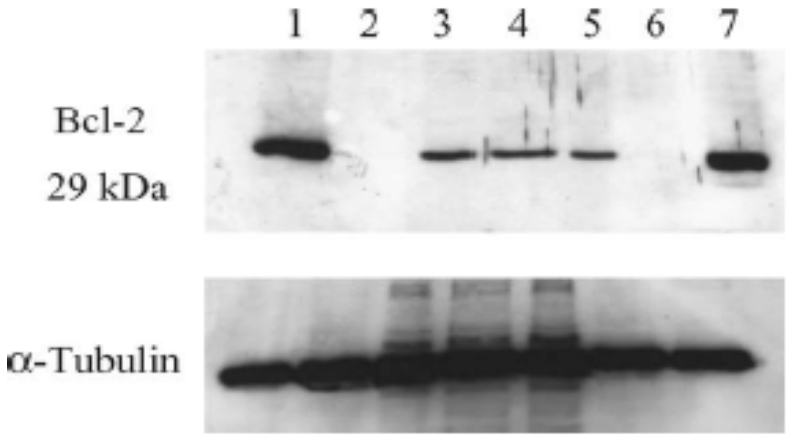

Figure 22: Western Blot analysis of Bcl-2 expression (top picture) and of tubulin-expression (lower picture). Shown are (by lanes) bcl-2 transfected and overexpressing human ovarian tumor BG-1 cells (positive control, lanes 1,7), 2 and 6 vector control BG-1 cells (negative control, lanes 2,6), lane 3 TK6 cells (lane 3), WTK1 cells (lane 4) and NH32 cells (lane 5). Each lane contains about 50 µg protein. Tubulin expression is shown in the lower panel as a control for equal loading of protein.

Due to the Bcl-2 over expression, it was possible to apply transient transfection with bcl2 antisense oligonucleotide to influence the apoptotic response in three cell lines. Transient transfection reduced Bcl-2 expression to a non-detectable amount in Western Blot analysis after 24 hour transfection (**Figure 23**).

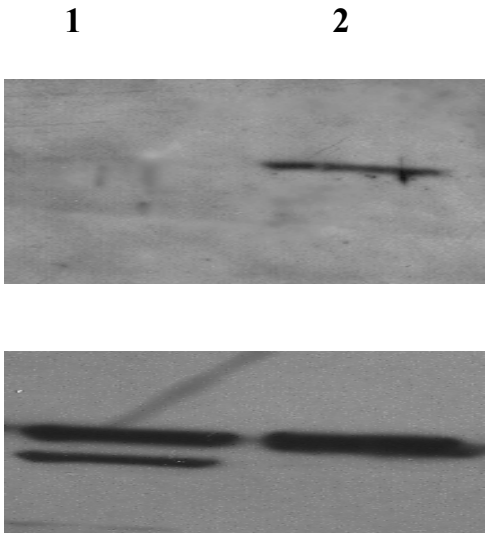

Figure 23: Suppression of Bcl-2 expression 24 hours after transient transfection with antisense bcl-2 oligo (lane 1) and recovery after 48 hours (lane 2). Tubulin expression is shown in the lower panel as a control for equal loading of protein.

Expression recovered within 48 hours after initiating treatment. Under these conditions, analysis of apoptosis with Annexin V labelling was not possible, because the cationic lipid-lipofectin treatment, which is necessary for transfection, interferes with the membrane integrity and yields non-apoptotic cells positive for Annexin V staining, i.e. after lipofectin treatment, 95% of all cells stained positively for PI and 40% for Annexin V in a control population. Therefore, microscopic evaluation of the apoptotic and micronuclei frequencies was applied after staining with bisbenzimide 33258. Micronucleus induction by etoposide was elevated in TK6 cells after treatment with bcl-2 antisense oligo but not in WTK1 and NH32 cells. Scrambled bcl2 antisense oligo was used as control (**Figure 24**).

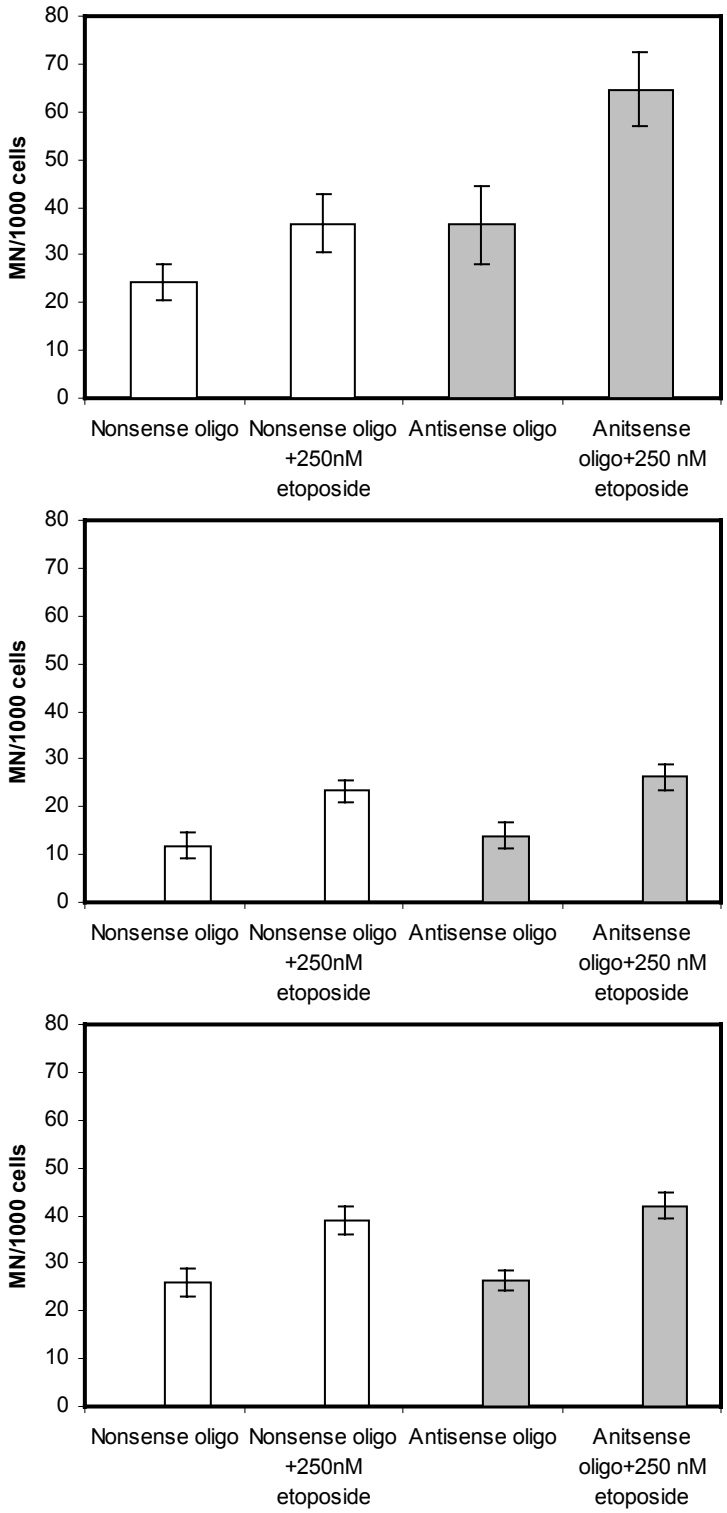

Figure 24: Micronuclei frequencies after treatment with 250 nM etoposide and transient transfection with bcl-2 antisense oligo in TK6 (wild type p53, upper panel) and WTK1 cells (mutated p53, middlle panel) and NH32 (knock out p53, lower panel) grey bars. Scrambled oligo (nonsense) was used as control, white bars. Data represent average from three independent experiments ± SD.

Etoposide-induced apoptosis was elevated by bcl-2 antisense addition in TK6 and WTK1 cell, but not in NH32 cell line (**Figure 25 a-c**). In TK6 cells, spontaneous apoptosis was also elevated after the addition of the oligonucleotide.

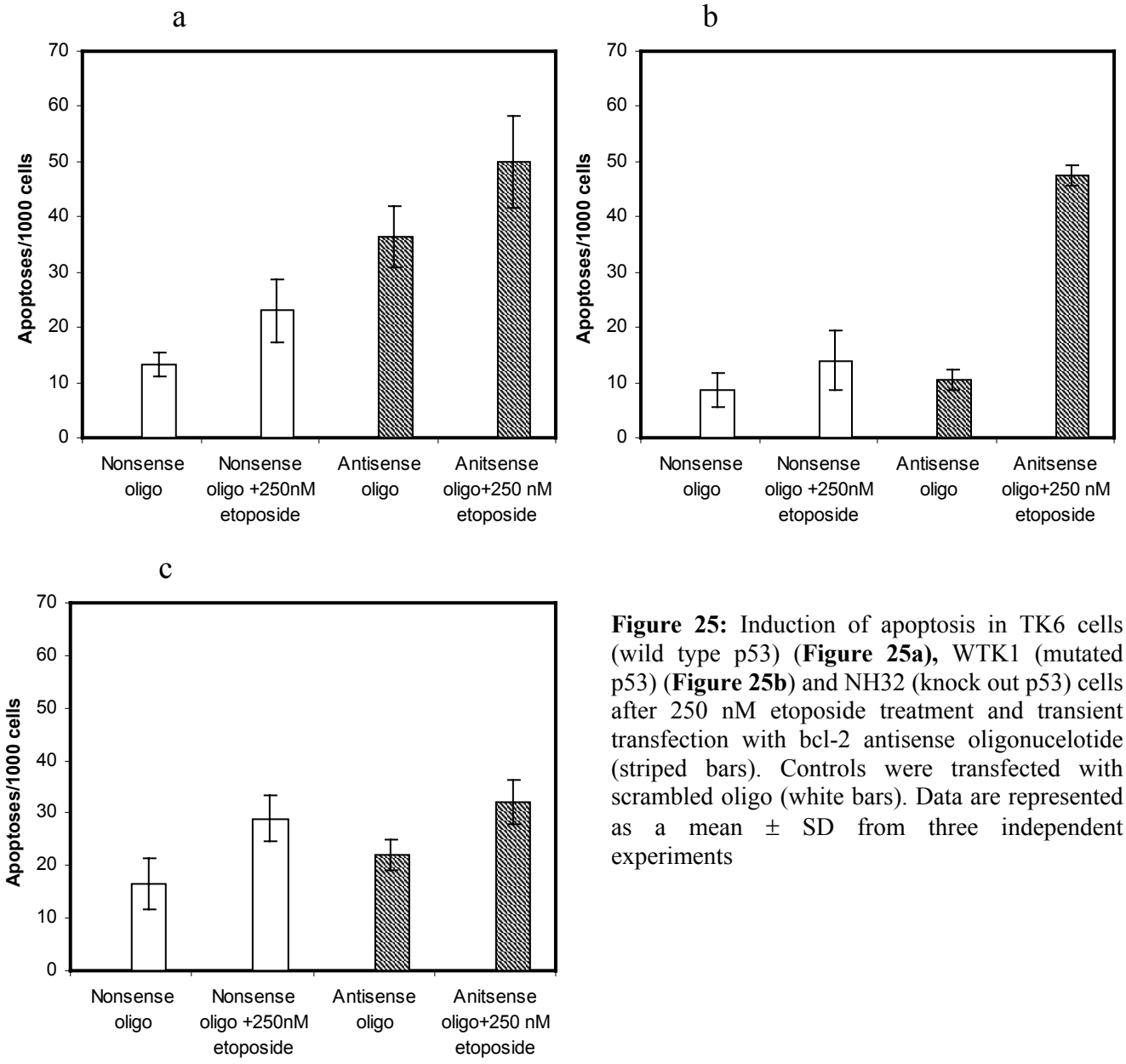

Figure 25: Induction of apoptosis in TK6 cells (wild type p53) (**Figure 25a),** WTK1 (mutated p53) (**Figure 25b**) and NH32 (knock out p53) cells after 250 nM etoposide treatment and transient transfection with bcl-2 antisense oligonucelotide (striped bars). Controls were transfected with scrambled oligo (white bars). Data are represented as a mean ± SD from three independent experiments

3.4. Modulation of Bcl-2 expression in the hormone responsive human ovarian cell line BG-1

Opposite to previous approaches to modulate the apoptotic response, a strategy of apoptosis suppression was now applied downstream of p53 on the mitochondrial level. The parental human ovarian cell line BG-1 was found appropriate for the intended manipulation since it has no detectable Bcl-2 expression. The anti-apoptotic bcl-2 gene was stably introduced in BG-1 human ovarian cancer cells to test for possible changes in cellular sensitivity to genotoxic stress. Hereby two cell lines were established: BG-1 pcDNA3 (vector control) and BG-1 pcDNA3 bcl-2. The over expression of Bcl-2 was confirmed by Western blot analysis (**Figures 22 and 26**).

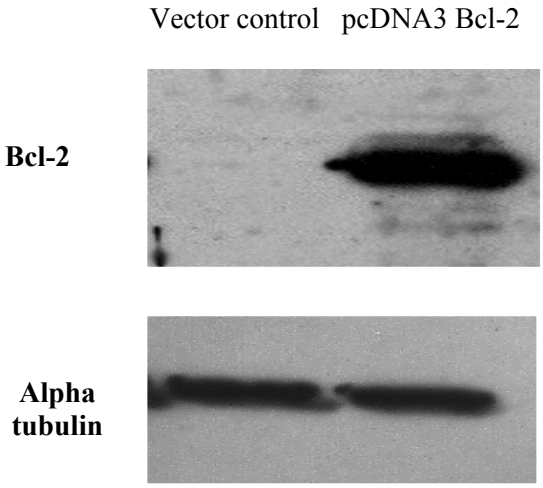

Figure 26: Western-Blot analysis of Bcl-2 expression in control (left lane) and stably transfected BG-1 cells (right lane). Control cells were transfected with pcDNA3 vector control. The lower panel shows alpha-tubulin detection as reference for equal loading of protein amount

First, the induction of chromosomal breaks after suppression of apoptosis with bcl-2 transfection was investigated. As a measure of genotoxicity, frequencies of micronuclei were determined after applying 1, 2 and 4 μM etoposide. We found a decrease in the number of micronuclei in the bcl-2 transfected cells at 1 μM etoposide in contrast to the vector control cells (**Figures 27a,b**). In addition, in both cell lines a saturation in micronuclei induction was reached at 2 μM and 4 μM etoposide treatment. Cells transfected with the vector control displayed a dose dependant apoptosis induction (**Figure 28a**). The apoptotic response was suppressed in bcl-2 transfected cells at 1 and 2 μM etoposide but not at 4 μM etoposide (**Figure 28b**).

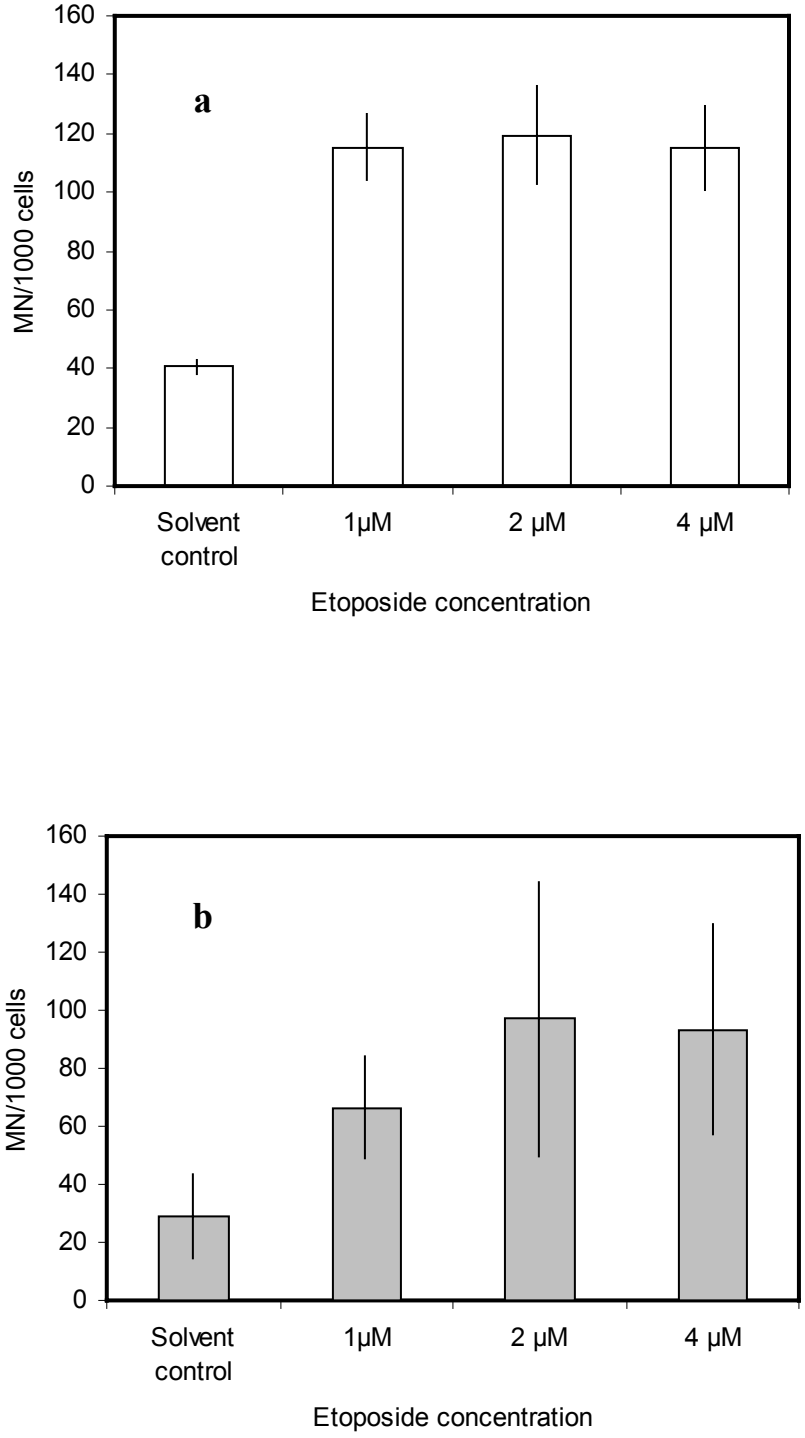

Figure 27: Micronuclei induction in BG1 (vector control) (**Figure 27a**) and BG-1 pcDNA bcl-2 (lower panel) (**Figure 27b**) after a 24 hour treatment with etoposide. Data are presented as mean ± SD from, three independent experiments

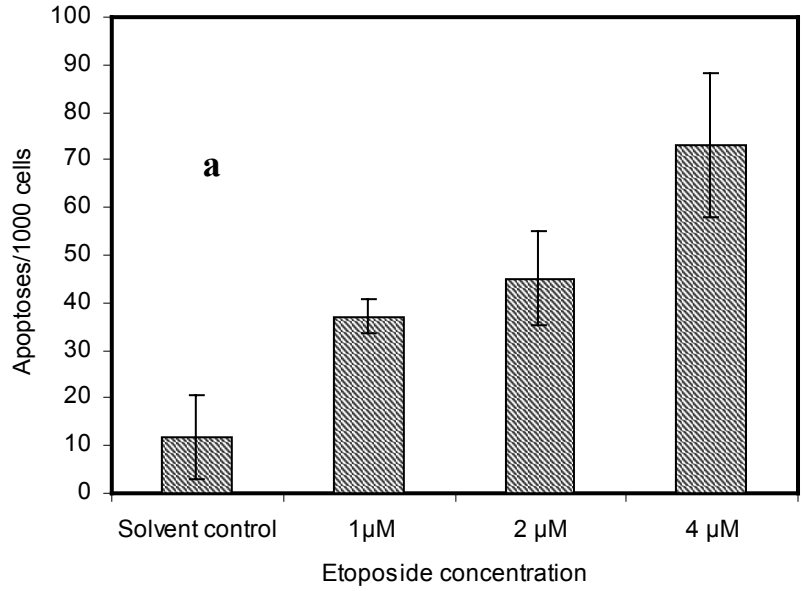

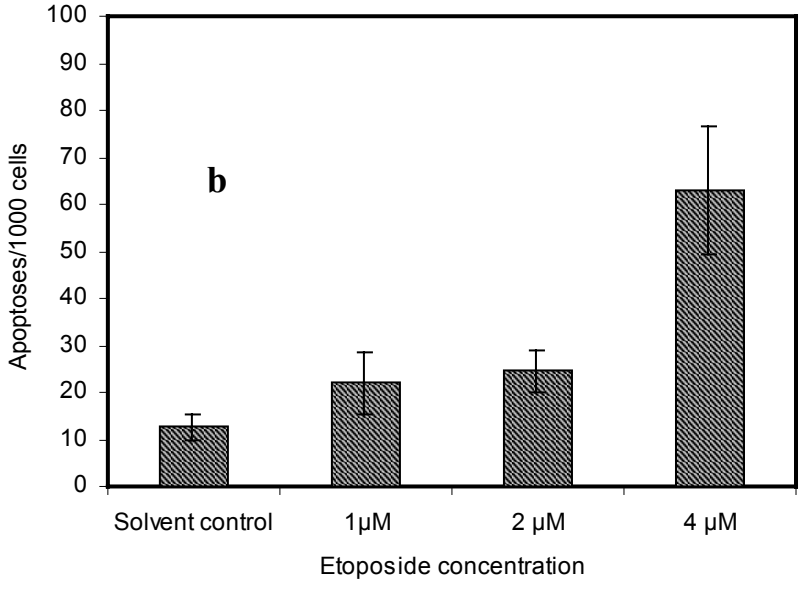

Figure 28: Apoptosis induction in BG1 vector control (**Figure 28a**) and BG1 cells transfected with bcl-2 gene (**Figure 28b**). Data are presented as a mean ± SD, from three independent experiments

Western Blot analysis (**Figure 29**) and previously flow cytometric findings (**Figure 30**) showed that p53 expression was elevated in transfected cells after etoposide treatment.

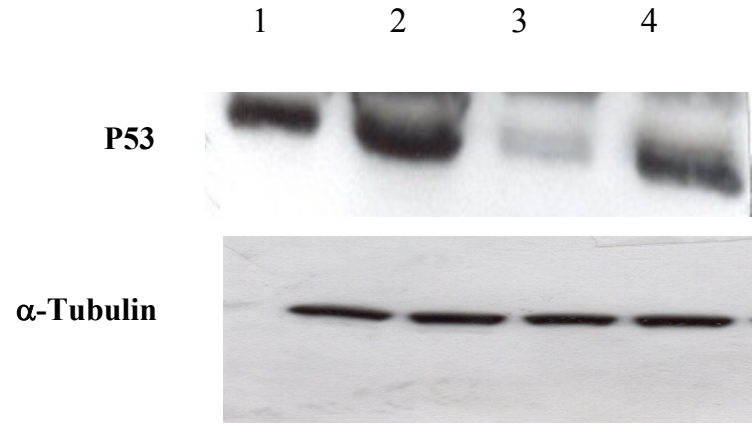

Figure 29: Western Blot analysis of p53 expression (by lanes): 1) nontreated vector control; 2) 1 µM etoposide vector control; 3) nontreated bcl-2 transfected; 4) 1 µM etoposide bcl-2 transfected

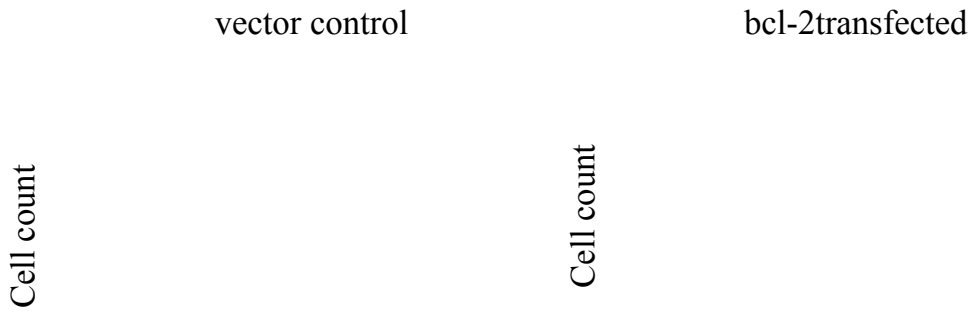

Figure 30: Flow cytometric analysis of p53 induction in BG1 vector control (left) and BG1 bcl-2 transfected cells (right) after 24 hours treatment with 1 µM etoposide. The induction was detected as shift to higher fluorescence intensity of the p53 protein within single cells compared to intensity in the control sample. In both plots the blue line shows untreated sample-controls; the red line etoposide treated cells. The data represent one out of three successful experiments.

3.4.1. Influence of estradiol on micronucleus induction by etoposide

A cconcentration of 1 µM etoposide was chosen for these experiments since higher concentrations yielded a saturation in the obtainable micronuclei formation. As control, a set of samples under the same growing and etoposide treatment conditions but not stimulated with estradiol, was used. Micronuclei (MN) frequencies were slightly lowered in bcl-2 transfected cells compared to the vector control cell line (**Figure 31 a,b**). Estradiol-stimulated increased cell proliferation enhanced the MN frequencies in vector control cell while in bcl-2 transfected cells induction remained the same (**Figure 32 a,b**).

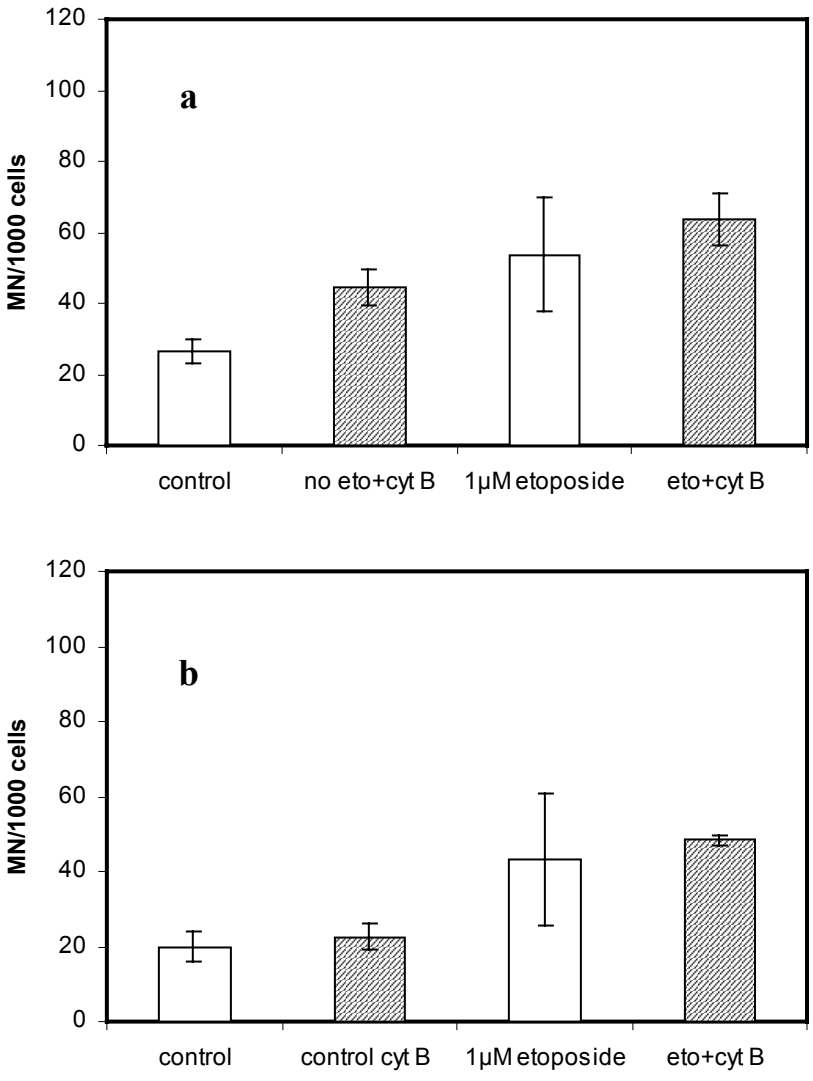

Figure 31: Induction of micronuclei in BG-1 vector control (**a**) and bcl-2 transfected cells (**b**) in absence of estradiol. Striped bars represent the addition of cytochalasin B. Data are presented as a mean ± SD from three independent experiments

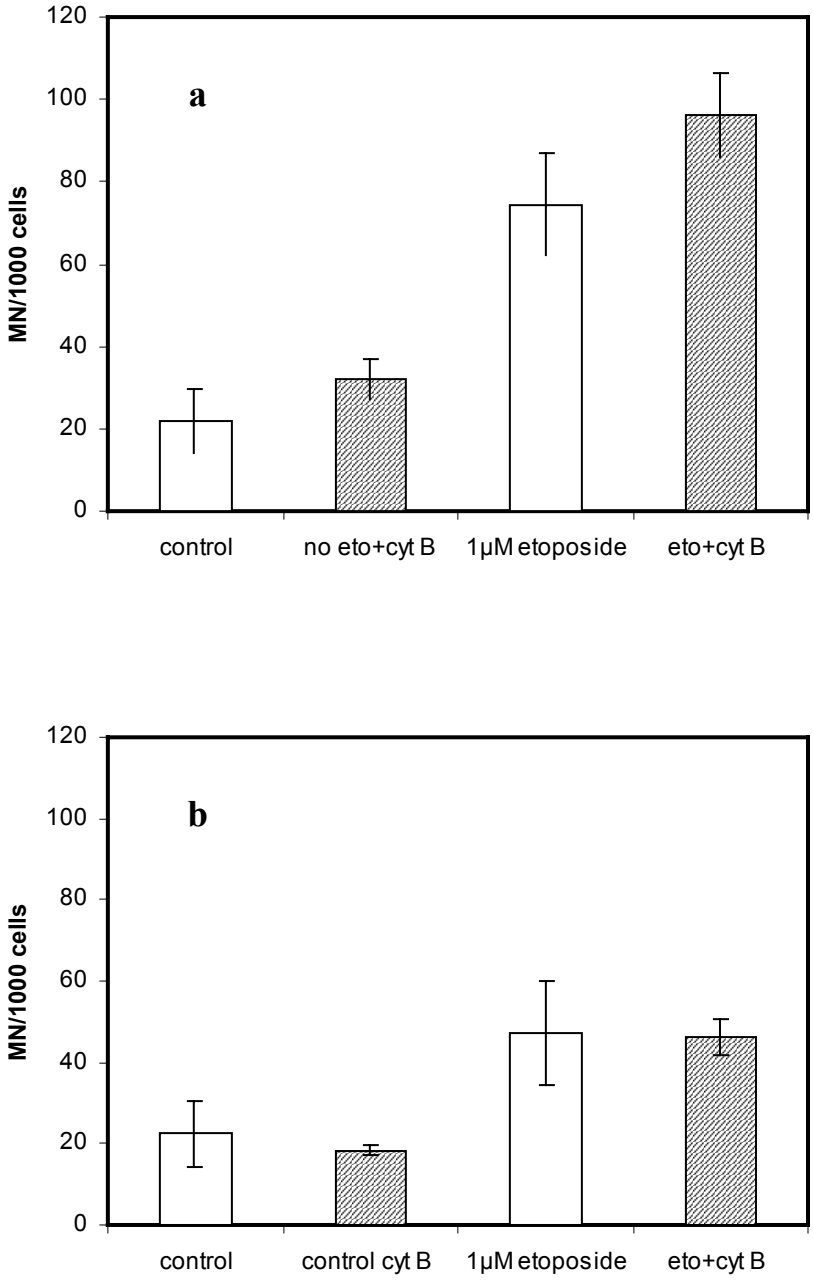

Figure 32: Micronuclei induction after estradiol treatment in BG1 vector control (**a**) and bcl-2 transfected cells (**b**). Striped bars represent the addition of cytochalasin B. Data are represented as a mean ± SD from three independent experiments

In the absence of estradiol, apoptosis in vector control cells was induced by 1 µM etoposide, but bcl-2 transfected cells failed to trigger programmed cell death (**Figure 33 a,b**). Apoptosis frequency was reduced by estradiol stimulation in both cell types (**Figure 33 c,d**). The frequencies of binucleates cells were similar for vector control and bcl-2 transfected cells (**Figure34a**), and increased after stimulation of proliferation with estradiol (**Figure 34b**); the increase was more pronounced in the vector control than in the bcl-2 transfected cells.

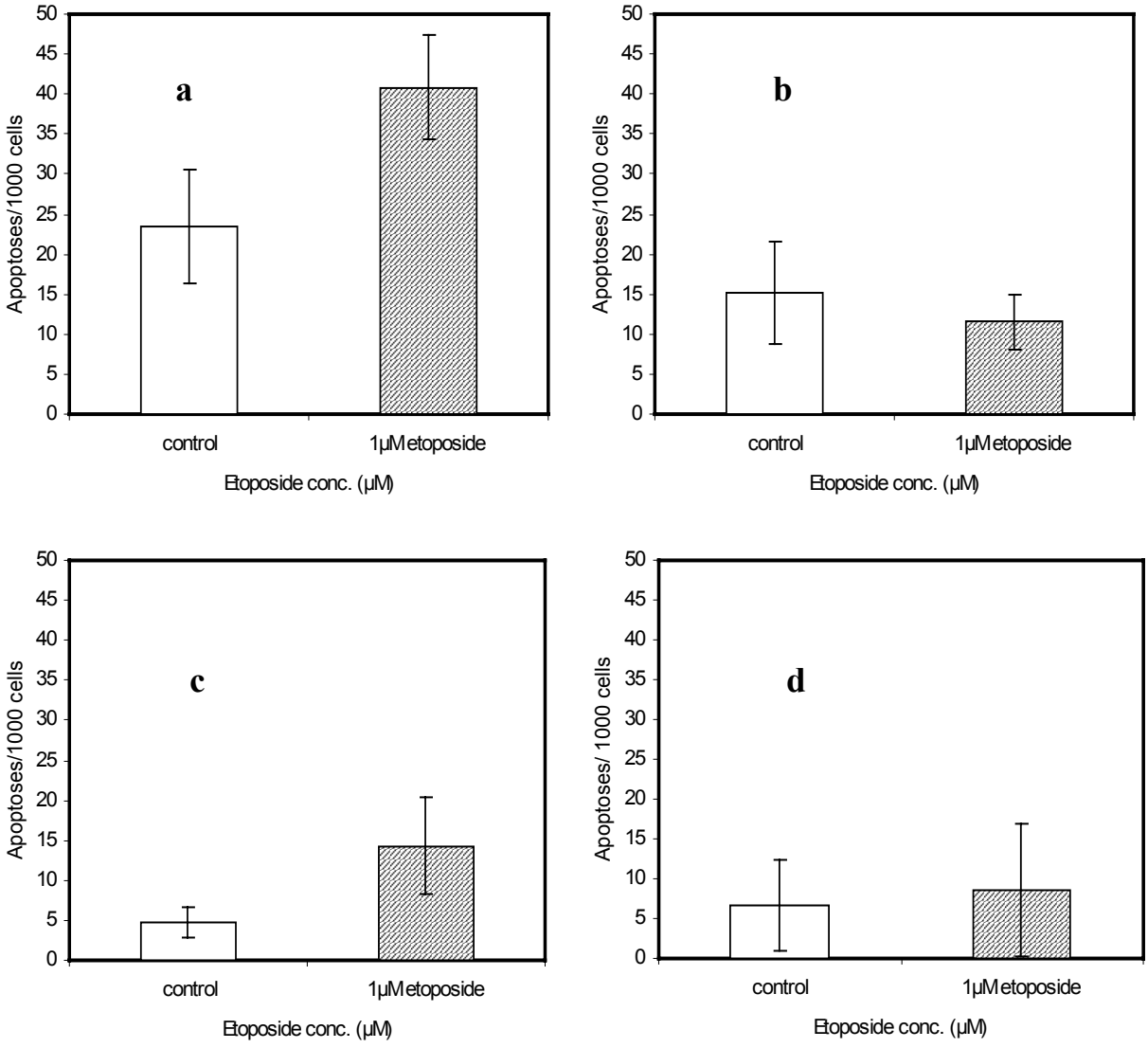

Figure 33: Apoptosis induction without estradiol treatment in BG1 vector control (**a**) and BG1 bcl-2 transfected (**b**) and with estradiol treatment in the vector control (**c**) and bcl-2 transfected cells (**d**); striped bars represent the treatment with etoposide. Data are presented as mean ± SD from three independent experiments.

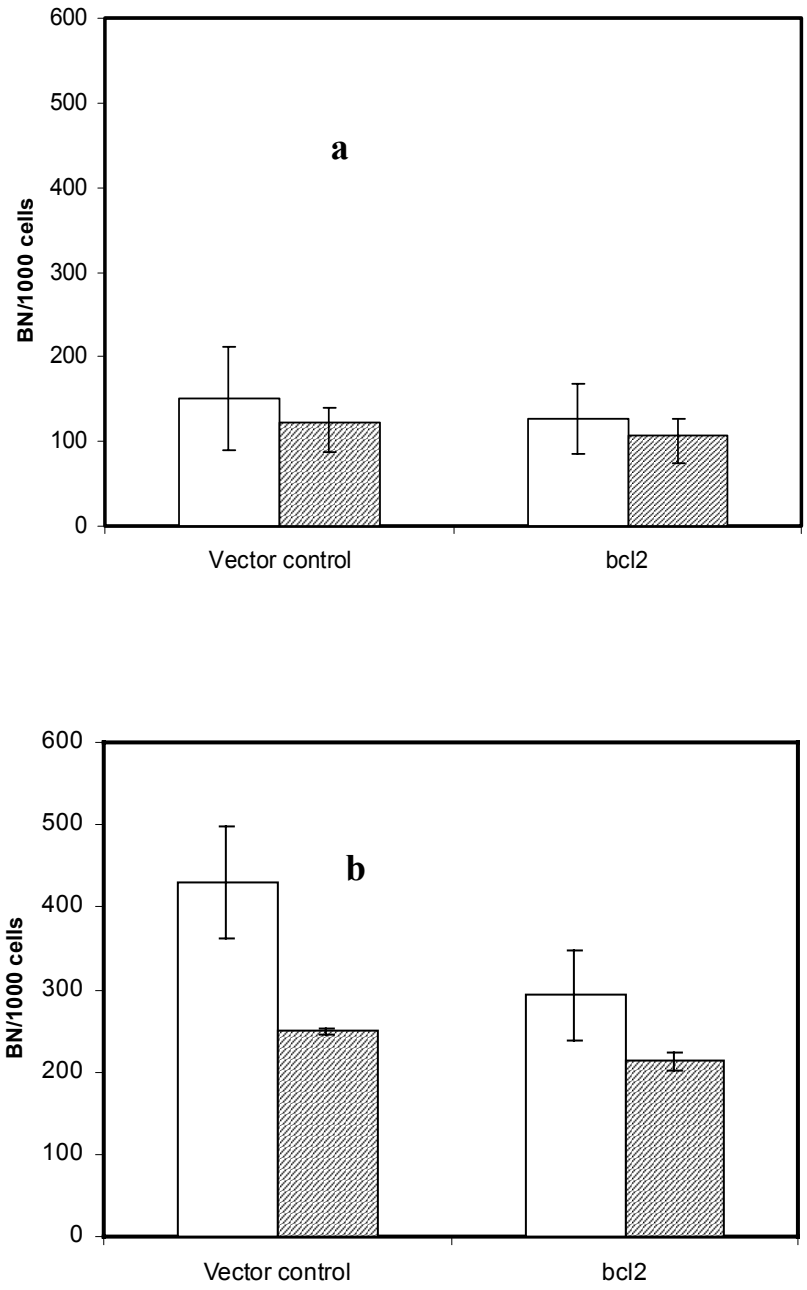

Figure 34: Frequencies of binucleates in BG1 cells without estradiol (**a**) and after estradiol treatment (**b**). Striped bars represent treatment with 1 µM etoposide; white bars represent control samples. Data are presented as mean ± SD from two independent experiments

4. Discussion

The understanding of the interactive nature of p53 seems to be a key point in the cellular response to genotoxic stress. In normally proliferating cells, p53 is a protein with very short half-life due to its down regulation by MDM2. Genotoxic stress dramatically increases P53 stability. Stabilized P53 protein regulates the maintenance of the genomic integrity through surveillance of DNA damage at multiple checkpoints and by contributing to its repair. Depending on the severity of the DNA insult, p53 activity may lead to the initiation of adequate cellular responses such as cell cycle arrest, apoptosis, necrosis or alternative kinds of cell death. The correlation between appearance of apoptosis and DNA damage is assumed as reciprocal. Therefore, micronucleus formation would be expected to have an inverse correlation with apoptosis. If micronucleus formation and apoptosis should not be interrelated like the two sides of a coin, there must be another possible end-stage for genetically damaged cells. Under suppression of apoptosis, cells that are now unable to enter apoptosis but harbor damaged genomic DNA may become necrotic instead of entering mitosis. This could occur within the experimental observation time or after a prolonged period of cell cycle arrest. Under conditions of elevated apoptosis, cells that now enter apoptosis might not have formed a micronucleus otherwise. They may harbor other forms of DNA damage not leading to micronucleus formation. Furthermore, micronucleus formation and apoptosis may sometimes not occur as opposite events, but may overlap or share common first steps. Alternatively, micronucleus formation may also be related to the process of necrosis. In the present work such aspects are explored with the main emphasis on modulating the apoptotic response which may influence the amount of surviving cells harboring DNA damage. Here were used three ways to influence apoptosis: temporary suppression of P53 protein function by pifithrin (PFT-α), transient suppression of the anti-apoptotic gene bcl-2 by bcl-2 antisense oligonucleotide and stable introduction of the bcl-2 gene.

4.1. Likelihood of a positive correlation between apoptotic response and micronuclei in human B lymphoblastoid cell lines

Human B-lymphoblastoid cancer cell lines displayed a different sensitivity to etoposide. The induction of genomic damage by etoposide as measured in the micronucleus test was higher in WTK1 cells harboring a mutated p53 gene than in the two other cell lines TK6 and NH32. The induction of apoptosis was higher in TK6 cells than in the two other cell lines in flow cytometric analysis, although microscopic analysis revealed similar apoptotic response in all cell lines. A discrepancy between the two analysis could be due to the confinement of the microscopic analysis to late stages of apoptosis (apoptotic bodies). These findings are in agreement with published results from the analysis of chromosomal aberrations and apoptosis in WTK1 and TK6 cells (Bassi et al., 2002) and correspond to the idea that the cell is less stringently prevented from mitosis despite the presence of DNA-damage and less stringently guided into apoptosis when it harbors a knockout or mutated p53 gene. Generally, a stabilized functional P53 primarily induces cell cycle arrest in G1, and/or in G2 phase but not in S phase. Abnormal p53 function or lack of expression decreases the transcriptional activity of the genes involved in G1 checkpoints and cell cycle regulation, such as $p21^{WAF}$. Cells with weak $p21^{WAF}$ expression display a different response to DNA damaging agents compared to cells with higher $p21^{WAF}$ induction leading to G1 arrest. Indeed, different cell cycle distribution patterns were obtained here depending on the p53 states and the resulting $p21^{WAF}$ induction. Cells with functional P53 showed clear $p21^{WAF}$ induction whereas a weak $p21^{WAF}$ induction was found in WTK1 cells with mutated p53 followed by a 'rapid' dose-dependant accumulation of cells in G2 phase. It appears that the p53 mutation in WTK1 cells impacts their ability to regulate the cell cycle during genotoxic stress. Some reports show (Gottifredi et al., 2003) that in some human cell lines with abnormal p53 function S phase arrest is accompanied by $p21^{WAF}$ reduction. In normal or cancer cells, DNA replication and repair is intensive in S phase and the genome is highly susceptible to genotoxic stress at that time. WTK1 cells exhibited an increase in S phase cells at higher etoposide concentrations whereas a dose dependent decrease was found in TK6 and NH32 cells. In other words, abnormal P53 function can be a reason for less stringent cell cycle control.

Nevertheless, the cells might retain an ability to launch apoptosis regardless to the disturbance of the cell cycle. It appears that depending on p53 states and severity of DNA

damage, the cell may switch from G0/G1 repair to apoptotic response in G2 phase (Gudkov et al., 2003). In TK6 cells (wild type p53) the strongest apoptotic response and G2 accumulation was observed. G1 arrest was reached at 5µM etoposide in TK6 cells. WTK1 cells with mutated p53 displayed rapid accumulation in G2 phase up to 5 µM etoposide concentration. In NH32 cells a rapid G2 accumulation was exhibited even at the lowest tested concentration. Therefore, the capability of the cells to perform assessment of the DNA damage severity was correlated with the p53 states. Moreover, the type of aberration may decide whether a part of the cells go into apoptosis or whether further proliferation if possible. Etoposide-induced micronuclei may contain chromosomal aberrations which can be lethal and irreparable. This might make them an initiator of apoptosis. We addressed the question whether apoptosis occurred within the same cell cycle or phase in which DNA damage was initiated. Alternatively, cells could commit suicide several divisions after induction of the initial DNA damage (Halicka et al., 1997, Shinomiya et al. 2001). A relatively novel concept considers apoptosis–DNA damage relation as belonging to the following three types. The first type of apoptotic death is **homo-phase apoptosis** n which the cells trigger apoptosis during the same cell cycle phase in which they were affected (**Figure 34;** Halicka et al., 1997, Shinomiya et al. 2001).

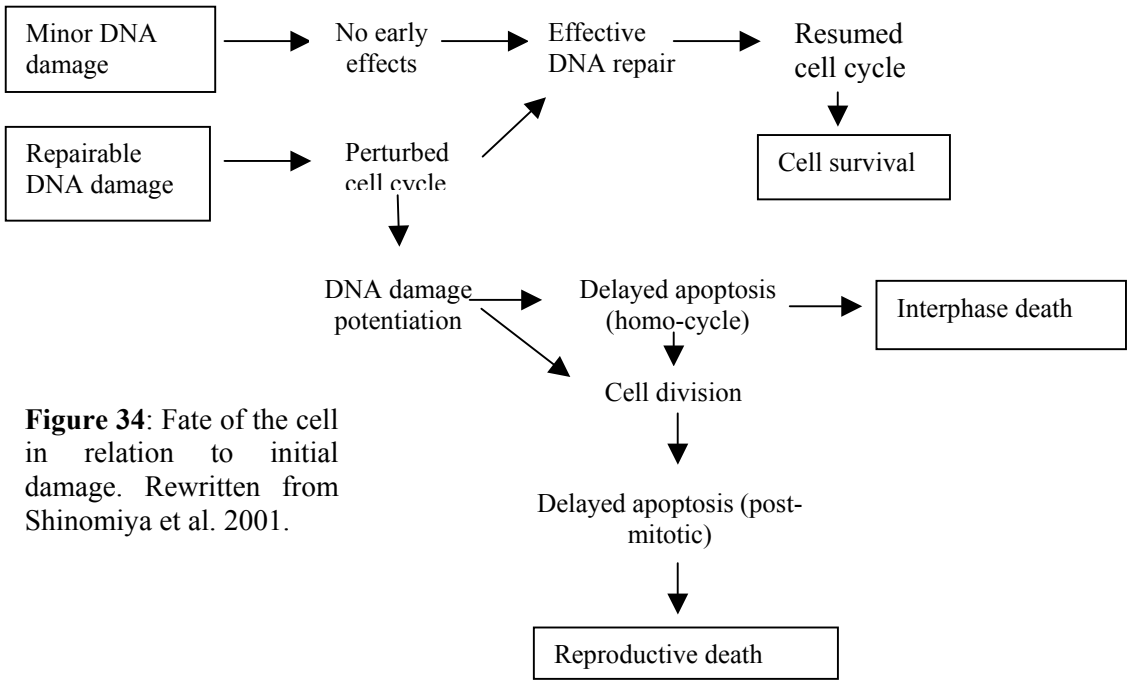

Figure 34: Fate of the cell in relation to initial damage. Rewritten from Shinomiya et al. 2001.

The second type is **post-mitotic apoptosis**, in which cells undergo apoptosis during the cell cycle subsequent to that in which the cells were initially affected. The third type is

homo-cycle apoptosis in which cells undergo apoptosis during the same cell cycle in which DNA damage was initiated, i.e., prior to or during the first mitosis after damage occurrence (Shinomiya, 2001).

The important parameter in each of the types is the number of required mitotic divisions. Here, synchronous apoptotic response and micronuclei induction was detectable after the cells had gone through one division. This corresponds to the proposed **homo-cycle apoptosis model**. According to more classical definitions, homo-cycle apoptosis corresponds to interphase death characterized by cell condensation, shrinkage and internucleosomal breakage of chromatin, all of which are also apoptotic hallmarks (Yamada et al., 1988). **Homo-cycle apoptosis** is time-correlated with micronuclei occurrence in lymphoblastoid cells. There are contradictory reports that indicate either positive or negative correlation between apoptosis and DNA damage. In some of the reports this correlation was recognized and considered as commencement of tipical DNA laddering where 'changes in nuclear chromatin precede internucleosomal fragmentation' (Abend et al 1999, Shimizu et al. 1990, Withoff et al. 1996). In addition, it was suggested that in parallel with DNA fragmentation, chromatin condensation takes place resulting in 'nuclear bodies located on the still intact nuclear membrane'. Since the membrane is still intact, it is reasonable to consider it as early apoptotic event. In a report by Abend et al., 2000, a positive correlation between apoptosis and DNA damage as measured in the form of micronuclei was found in L929, HL-60 or COLO –320 cells but not in human epithelial–like liver cells and human keratinocytes. These reports were related to reproductive cell death induced by irradiation while DNA fragmentation and homo-cycle apoptosis are mostly related to anti-cancer drugs treatment. Therefore, depending on the genotoxic stimuli and cell type rapid apoptotic response may occur during the same cell cycle or after few divisions since DNA damage was initiated (delayed apoptosis or reproductive death).

4.2. Suppression of apoptosis by PFT-α influences the cellular response to genotoxic stress

Generally, genotoxic stress induces mostly p53-dependent cell cycle arrest mechanisms. Many reports emphasize the bivalent p53 function in which activated p53 directs a cell to cycle arrest rather than to apoptosis. Such an ability to switch from one to another cellular response very likely comprises a highly active set of mechanisms. In the context of DNA insult, the role of p53 might influence the occurrence of micronuclei. Here it was investigated whether influencing the p53-dependent apoptotic response after genotoxic insult changes the amount of genomic damage, i.e. number of damaged cells, resulting from the genotoxic insult. It is generally assumed that aberrant apoptotic response leads to elevated genomic damage, since damaged cells cannot be deleted anymore. Pifithrin-α treatment provided a useful tool to influence possible molecular mechanisms which determine the balance between apoptosis and amount of DNA damage. PFT-α is a selective drug which induces a temporary block of wt p53 presumably harboured in healthy cells. Originally, PFT-α was designed to suppress p53 in healthy cells and thus keep them from entering apoptosis that might be induced during chemotherapy. Therefore the side effects of chemotherapy would be reduced. Since 70% of all cancers harbor mutated p53, such tumor cells would be insensitive to PFT-α and would still be deleted by chemotherapeutic agent. However, a recent report by Bassi et al., 2002 demonstrated that PFT-α treatment increased the number of chromosomal aberrations induced in human lymphoblastoid cells exposed to etoposide, leading the authors to the warning that more investigations are necessary to ensure the protective effects of PFT-α.

When we applied PFT for suppression of p53-mediated apoptosis we found a reduced apoptotic response in the wild-type p53 cells TK6, but not such a significant reduction in p53-mutated (WTK1) or no reduction in knockout (NH32) cells. This is in agreement with observations by Bassi et al. (2002) who found reduced apoptotic response in TK6, but not in WTK1 cells (they did not investigate NH32 cells). When we quantified the genomic damage after this combined etoposide and PFT treatment, we expected a rise in genomic damage in TK6 cells due to their inability to enter p53-mediated apoptosis. However, PFT was ‘protective’ and reduced etoposide-induced genotoxicity in TK6 cells. A smaller reduction was found in WTK1 cells with abnormal p53 function after PFT-α -

etoposide co-treatment. NH32 knocked-out p53 cells displayed insensitivity to PFT-α. At first glance this seems to contradict findings by Bassi et al., 2002, who found an inverse relationship between the changes of the apoptotic frequencies by addition of PFT and induction of chromosomal aberrations by etoposide in TK6 cells. However, if one looks at their results in more detail, the subgroup of chromosomal aberrations listed as "breaks" did not increase upon addition of PFT. Considering that micronuclei represent a subgroup of all possible types of chromosomal alterations and that their formation depends on the induction of DNA strand breaks, the group of chromosomal aberrations listed as "breaks" may correspond to micronucleus formation. This may mean that we are really in agreement with the observations of Bassi et al. 2002. At first glance this is consistent to the idea that PFT-a plays a protective role. However, the 'protective' effect of PFT-α must be carefully analysed particularly in the case of double-strand breaks such as micronuclei. Recent studies have shown that double-strand breaks (DSBs) in mammalian chromosomes can be repaired by a variety of pathways: homologous recombination with the highest repair fidelity, precise ligation-higher accuracy and nonhomologous end-joining recombination with the lowest fidelity. In most of the reports the role of p53 is seen in the precise ligation in cases when non-homologous recombination is suppressed. It was reported that treatment with PFT-α reduced recovery of precise ligation 5-10-fold while the activity of non-homologous end-joining recombination remained intact (Lin et al., 2003). More specifically, the favoured nonhomologous end-joining recombination may alter sequences by introducing small deletions, insertions or inversions. Although cells were rescued from apoptotic death, they may become genetically modified due to inaccurate relegations or induced point mutations. Therefore, such error-tending repair may pose a cell at risk for DNA damage accumulation (Willers et al., 2002).

Little is known about the molecular mechanisms which involve p53 in DSB repair. There are speculations whether accurate DSB repair is dependent on the non-specific DNA binding activity of p53, mediated through the C-terminal (Tang et al., 1999). This is consistent to the idea that PFT-α affects the C-terminus of p53 favouring low-fidelity repair which may result in lowered micronuclei levels. In addition, the C-terminal contains the cdk2/cdc2 sites but also a sequence which targets p53 for the transport to the cell nucleus. Genotoxic stress enhances nuclear export of the stabilised p53. On the other

hand, high p53 activity may result in G1 arrest via the suppression of the Cyclin E/Cdk2 kinase. PFT-α resulted in diminished G0/G1 phase and accumulation in G2/M phase in human B lymphoblastoid cells harbouring wild type and mutated p53. In support of this, Komarov et al., 1999 suggested that PFT-α decreases accumulation of nuclear p53 by blocking the import or export (or both) of p53.

On the other hand, $p21^{WAF}$ expression was not affected in TK6 and WTK1 cell lines, but p21-mediated G1 arrest failed to be observed. These findings are consistent with Komarov et al., 1999, where p21 nuclear-cytoplasmic ratio was not altered after PFT-α treatment. Since p21 is able to promote both G1 and G2 arrest, as found in HT1080 fibrosarcoma cells (Roninson et al., 2001), such an effect might be expected as a proof of a retained ability to control the cell cycle. Besides, p21 activity is regulated in p53-dependant and p53-independent fashion (Roninson et al., 2001). Bassi et al. (2002) reported that their flow cytometry experiments did not show an influence of PFT-α (same concentration as here) on the cell cycle distribution.

We also saw no changes after addition of PFT-α alone but found that PFT-α addition along with etoposide impairs cell cycle distribution by diminishing G0/G1 checkpoint and facilitating cells to accumulate in G2/M phase. It could be that N-terminus is affected and than the interaction between p53 and Chk1/Chk2 kinase is temporarily disabled by PFT-α resulting in S phase checkpoint failure. In TK6 and WTK1 cells S-phase was reduced after co-treatment and therefore DNA repair and synthesis might be incomplete. This effect was pronounced in cells with wild-type p53 but a smaller effect was found in cells harbouring a point mutation in the central core domain of p53. Moreover, we found that WTK1 cell displayed certain level of apoptosis decrease after PFT-α-etoposide co-treatment, which was smaller than in TK6 cells. Such an effect may also be linked to the suppression of a preserved proline rich region that is sited in the N-terminus (Cadwell et al., 2001). In addition, the N-terminus is a site which is recognizable for dsDNA dependent protein kinase- enzyme that may be activated in cells that have suffered DNA damage. Thus, the observed effects may be interpreted as a consequence of the N-terminus binding suppression of activity by PFT-α.

WTK1 cells over express a mutant form of p53 in which methionine is substituted with isoleucine at codon 237. This codon corresponds to the central protein- sequence specific DNA binding core. In Komarov et al., 1999 it was suggested that PFT-α does not alter the sequence specific DNA binding.

Thus, it appears that PFT-α acts as inhibitor of C and N domains in p53 protein indicating a possible functional overlap of regulatory mechanisms. In p53 deficient NH32 cells such effects could not be observed and any kind of treatment was followed by rapid accumulation of cells in G2/M phases. Thus, the temporary suppression of p53-dependent apoptosis appears to occur separately from p53 deficiency since functions such as repair, cell cycle control may be maintained to a certain extend in the presence of mutated p53. Overall, a temporary inhibition of p53 function by PFT-α could be a promising approach during chemotherapy to reduce the apoptosis in normal cells. However, side effects cannot be avoided. Particularly, this refers to the accumulation of mutations and failure of some components of the repair system, rendering genetically modified cells. It appears that PFT-α stimulates cell proliferation since a decreased percentage of cells in S-phase was apparent in TK6 and WTK1 cells and it seems to facilitate G2/M accumulation. Thus, the altered proliferation pattern caused by PFT-α may favour a more inaccurate repair system to take place since the vast majority of homologous recombination based repair systems take place in late S-phase and around the G2-checkpoint. This leads to the conclusion that cell survival does not imply preserved genomic stability.

Rescuing a tissue from necrosis in clinical cancer treatment is considered as protective effect of an applied drug since possible inflammation is avoided due to a passive leakage of the cellular content. PFT seemed to ‘protect’ all three cell types from necrosis to some extend. Since two of the cell lines do not harbor a wild type p53 gene, this effect must be mediated by some other, p53-independent activity of PFT. In fact, Kaji et al. (2003) observed p53-dependent and –independent effects on DNA-damage signal pathways in JB6 cells. Schafer et al. (2003) reported that PFT in vivo in rats was able to inhibit hepatocellular necrosis in addition to apoptosis. Although molecular targets have not been identified, the observed effects after PFT treatment are in accordance to some observations in the published literature. Thus, the controversy related to the mechanism

of PFT-α action may be extended to a discussion about the cellular capacity to retain alternative deletion mechanisms besides apoptosis and necrosis.

In other words, the repair of DNA damage might end up unsuccessfully but a cell retains the capacity to choose between few alternatives: irreversible growth arrest or mitotic catastrophe. Recent reports shed a new light on the 'bipolar' nature of functional p53 protein in cancer cells. In Gudkov et al., 2003 it was reported that cells with haematopoietic origin could respond to irradiation in other ways than apoptosis. However, there are many cell systems in which apoptosis and growth arrest may both occur. Mechanistically, the stronger and longer p53 activity may lead a cell predominantly to launch apoptosis, then growth arrest. Nevertheless, p53-responsive genes available for modulation very likely predetermine the cellular response. Depending on the cell system different p53-responsive genes can be accessible in active chromatin, which provides a specific pattern of transactivation and transrepression outcome. However, if attempts to launch apoptosis failed, the part of the cells depends on the efficiency of DNA repair and severity of DNA insult. The grade of damage and time for repair influences the efficiency of repair system. For instance, the time of maximum radioresistance, or clonogenic potential, is different from one cell line to another. Generally, S phase is the most resistant since the replication machinery is coupled with repair mechanisms. However, an affected S phase may cause engagement of inaccurate repair. When mitosis is concerned, this seems to be a highly sensitive phase which makes cells susceptible to damaging agents due to torsional stresses and DNA breaks may easily occur. Such DNA damage is difficult to be repaired before chromosome segregation in anaphase.

However, unsuccessful repair and apoptosis failure are main causes of abnormal cellular proliferation. Essentially, a lack of proper checkpoint control indicates cellular inability to arrest proliferation in order to allow adequate time for repair, so the cell enters uncontrolled premature mitosis and undergoes mitotic catastrophe. Morphologically, mitotic catastrophe is a form of cell death with improper chromosome segregation and cell division that makes cell large, nonviable with several micronuclei (Roninson et al., 2001). In contrast to this form, apoptosis is characterized by shrunk cytoplasm and condensed chromatin. Mitotic catastrophe can be an end point in human lymphoblastoid

cells after PFT-α and etoposide co-treatment. According to findings by Bassi et al., 2002, TK6 and WTK1 cells displayed an increase in frequencies of 'abnormal cells' (containing dicentrics and rings) but not in the frequencies of apoptotic cells and chromosomal breaks. However, premature mitosis is certainly not the only mechanism that may substitute a lack of apoptosis. For instance, prolonged G1/S arrest can be a cause of abnormal cell proliferation according to some reports (Stearns, 2001). Alternatively, inhibition of some G2 checkpoint genes such as p53 or p21 may promote mitotic catastrophe (Chang et al, 1999; Bunz et al., 1998; Chan et al., 1999). According to Roninson et al., 2002, this form of abnormal cell is rather potentiated than prevented by G1 and G2 checkpoints mediators, such as p21 which leads to abnormal centrosome duplication.

In spite of the starting hypothesis, a positive correlation was found between apoptotic response and micronuclei occurrence. Moreover, synchronous suppression of apoptosis and micronuclei that was achieved after PFT-α and etoposide co-treatment confirmed the assumptions that homo-cycle apoptosis is the type of apoptosis which occured. Temporary p53 inhibition has indicated a possible functional interrelation between micronuclei formation and mechanism of apoptosis launch hinting towards strong causality at least in human B lymphoblastoid cell lines.

4.3. Influence on apoptosis and DNA damage by modulation of Bcl-2 expression

Due to genotoxic or oxidative stress, the mitochondria may undergo bioenergetic crisis accompanied by ATP depletion and Ca^{+2} deregulation processes. Mitochondrial membrane dysfunction may cause a launch of both caspase-dependent and caspase-independent apoptotic mechanisms. The mechanism of the mitochondrial membrane disruption and release of apoptotic promoters is still little known. The Bcl2/Bax complex resides in the mitochondrial membrane and induces either its opening or closing by conformational changes of permeability transition pores (PTP). The leakage of apoptosis promoters depends on the relative ratio of Bcl2/Bax heterodimer components (Reed et al. 1998). The pro apoptotic Bax antagonizes anti apoptotic Bcl-2 activity and promotes apoptosis by a release of cytochrome c into the cytosol where it forms a ternary complex

with Apaf-1 and caspase 9. It is known that p53 indirectly influences mitochondrial integrity by up regulation of Bax protein, the pro apoptotic member of the Bcl-2 family. In the case of overwhelming Bcl-2 expression, mitochondrial permeability transition pores are stabilized and therefore the release of cytochrome c into the cytosol is prevented. Thus, promotion of apoptosis would be abolished.

Over expressed anti-apoptotic protein Bcl-2 was detected in human lymphoblastoid cells. This finding enabled us to use a second strategy to alter the apoptotic response to genotoxic stress in these cell lines, the use of bcl-2 antisense-oligonucleotide for suppression of Bcl-2 expression. When the antisense strategy was applied by transient transfection, we found more cells able to enter apoptosis in TK6 and WTK1 cells, but not in NH32 cells, indicating that the pathway of apoptosis enabled by Bcl-2 suppression may depend on the presence of either wild-type or mutated p53. In addition, the expectation was, that the extend of the genomic damage induced by etoposide would be decreased by enabling more damaged cells to go into apoptosis since Bcl-2 expression is diminished. However, micronucleus frequencies remained unchanged (WTK1, NH32) or were elevated (TK6). A possible explanation might be that micronucleus formation represents an amount of cellular damage incompatible with the process of starting apoptosis – cells would instead become necrotic. Alternatively, induced micronuclei frequencies in p53 wild-type cells may indicate altered sensitivity that caused high apoptotic response. In contrast to TK6 cells, in WTK1 cells even a small amount of DNA damage interfered with strong apoptotic response after Bcl-2 expression was diminished. Hypothetically, the critical threshold level of DNA damage to trigger apoptotic mechanisms could be lowered. The idea of altered sensitivity to DNA damage would be in accordance with the primary idea of a reciprocal apoptosis-micronuclei pattern by which numerically low but severe damage may increasingly delete cells by launching apoptosis.

In addition to Bcl-2 suppression, we have stably introduced the bcl-2 gene into BG-1 human ovarian cancer cells. Since BG-1 cells are estrogen-receptor-positive, it is also possible to monitor apoptotic response and micronuclei formation after proliferation was induced by estradiol treatment. In general, estrogens at physiological concentrations are considered non-genotoxic agents which induce proliferation by binding to a receptor. On

the other hand, facilitated proliferation may disturb the synchronicity of the DNA repair system and cell cycle checkpoints. It has been shown that induced proliferation may cause increasing accumulation of DNA damage throughout subsequent divisions (Fischer et al, 2001). Knowledge about the capacity of the cell to trigger programmed cell death under high proliferation rate is very small. According to recent reports, depending on cell type estradiol can be either an apoptotic promoter or suppressor (Chen et al., 1998; Razandi et al., 2000). Here, we explored possible alterations on the amount of DNA damage and apoptotic response after proliferation was induced with estradiol.

First, both cell types (vector control and bcl-2 transfected) were subjected to a range of etoposide concentrations for 24 hours. According to our expectations, the apoptotic response was minimized in cells overexpressing Bcl-2 protein. Micronuclei induction was weaker in bcl-2 transfected cells than in the vector control at 1 μM etoposide concentration. In both cell lines a saturation of micronucleus induction was rapidly reached at doses higher than 1μM etoposide. A remarkable elevation of p53 expression in Bcl-2 over expressing cells was found. According to Marchenko et al. 2000, 32D cells that were stably transfected with anti-apoptotic Bcl-2 show cellular over expression but not mitochondrial accumulation of p53. This indicates a direct or indirect signaling link between p53 and key apoptosis regulators at the mitochondrial level. These findings partially correlate with our results obtained in experiments with the human ovarian cancer cell line BG1,

Application of 1 nM estradiol stimulated proliferation. Under forced proliferation conditions amount of DNA damage was not altered. Reduced apoptotic response in both cell lines was obtained. Particularly, in the vector control cell line, apoptosis was reduced compared to estradiol non-treated cells. Bcl-2 transfected cells also showed an elevated proliferation rate after estradiol stimulation but almost 50% lower proliferation than the vector control cell line. This was also the case after induced genotoxic stress with 1 μM etoposide. In a report by Evan et al., 1998 it was observed that elevated expression of Bcl-2 suppresses apoptosis, but cells have difficulty entering the cell cycle. Intracellular mechanisms by which Bcl-2 may regulate resistance to apoptosis and cell cycle progression are not clear. It was proposed that Bcl-2 arrests cellular transition from G1 to S phase through multiple phosphorylation of this protein (Deng et al., 2004), which is

also necessary for anti-apoptotic function. This indicates a tight link between favoring survival and retarding cell cycle. In a report by Deng et al., 2003, the authors suggested a link between arrested G1→S transition and decrease of reactive oxygen species realized through Bcl-2's antioxidant property. In addition, it was proposed that cells might better resist apoptotic stress in G0/G1 phase than during DNA replication

Overall, the central result of this investigation is that we did not find an expected inverse correlation between induction of apoptosis and genomic damage after treatment with etoposide when we used micronucleus formation as biological endpoint for genomic damage. The relationship between micronucleus formation and apoptosis is far from clear. A correlation has been found by Decordier et al. (2002), who hypothesize that apoptosis might contribute to the elimination of micronucleus containing cells. Abend et al. (1999) stated that mouse L929 cell may form micronuclei after irradiation by an active process comparable with the early stages of apoptosis, involving this process in the re-organization of a damaged genome. On the other side, Meintieres et al. (2003) found enhanced micronucleus formation in cells over expressing the anti-apoptotic protein Bcl-2, and hypothesize that the cells evaluated as micronuclei containing are really apoptotic cells unable to undergo the normal apoptotic process. The type of interrelationship between micronucleus formation and apoptosis may thus depend on additional factors/mutations within a cell.

On the other hand, the role of apoptosis is sometimes paradoxical even in tumor development. Usually a loss of ability for apoptosis is considered to enhance formation of the malignant phenotype and to reduce sensitivity for treatment. However, expression of Bcl-2 can also be associated with a favourable prognosis and loss of p53 with unfavourable prognosis (Gurova et al., 2003), possibly because apoptosis can act as an accelerator of tumor progression in certain cases. There are reports that show similar growth characteristics in tumors that either express Bcl-2 or lack p53. The reason can be that, both loss of p53 or expression of Bcl-2 prevents apoptosis, but only loss of p53 makes cells genetically unstable promoting uncontrolled proliferation. Interestingly, in Gudkov et al. 2003 it was proposed that Bcl-2 positive tumors may maintain p53 wild-type because they provide no selective advantages for the p53-deficient variants. Generally, the role of p53 in tumor treatment is not as simple as thought since its impact

can be either positive or negative depending on its functionality and cellular context of the specific tumor. It is relevant to follow up these questions further, since the treatment of human cancer requires knowledge about the consequences of alterations in the apoptotic process by medical intervention in the tumor as well as in the surrounding healthy tissue.

5. Summary

The apoptotic response occurring after exogenously induced genomic damage may preserve the overall homeostasis in an organism by deleting affected cells. Failure in the apoptotic response plays an important role in both tumorigenesis and drug resistance in tumor treatment. The purpose of this study was to investigate the balance between the formations of genomic damage was measured by micronucleus induction and the induction of apoptosis upon genotoxic stress.

Micronuclei represent a subset of all chromosomal aberrations and the micronucleus test has gained fast acceptance as a routine test in gentoxicity screening. The hypothesis was that micronuclei induction correlates inversely with apoptosis occurrence. According to this idea, failure to trigger apoptosis may lead to accumulation of DNA damage.

Three cell lines containing wild-type p53, mutated p53 and knock out p53 showed induction of apoptosis after treatment with etoposide. Elevated micronuclei frequencies upon treatment with the genotoxic and apoptotic toposimerase inhibitor II etoposide were more pronounced in cells with mutated p53 than in cells with wild type or knocked out p53.

Three approaches were applied to alter molecular mechanisms that determine the interrelationship between apoptotic response and induced DNA damage. The first approach was to temporarily inhibit apoptosis by adding pifithrin-α (PFT-α), a p53 blocker. Using this compound we investigated the impact of different p53 states (wild-type, mutated and knockout) on DNA repair, the cell cycle and apoptosis. The second approach consisted of a transient introduction of bcl-2 antisense oligonucleotide to reduce the expression of Bcl-2 protein. A stable transfection of the bcl-2 gene represented the third approach. This was performed with a hormone-responsive cell line which enabled the investigation of the influence of hormonally induced cell proliferation.

PFT-α was originally designed to selectively block apoptosis in cells with wild-type p53 during tumor chemotherapy. This would theoretically minimize possible side effects to healthy tissue. Presumably cancer cells which harbor mutated or knock out p53 are

insensitive to PFT-α treatment and would still be deleted by chemotherapy. PFT-α application reduced micronuclei frequencies during the co-treatment with 125 nM etoposide in wild-type p53 cells. A smaller reduction was found in p53 mutated cells, and no reduction in p53 null cells. The apoptotic response was decreased in cells harbouring wild-type p53, a weaker reduction was observed in p53 mutated cells, and p53 null cells showed no alteration. These findings contradicted our hypothesis because apoptosis suppression did not lead to increased micronucleus frequencies.

All three cell lines with different p53 state constitutively expressed anti-apoptotic Bcl-2 protein. Therefore, apoptosis was enhanced by transient transfection with bcl-2 antisense-oligonucleotide in these cells. When apoptosis was increased upon treatment with etoposide, micronucleus formation remained unchanged or was also increased, again contradicting the hypothesis.

Stable introduction of the bcl-2 gene into human ovarian cancer cells represented the third approach for modulating of apoptosis. The used cancer cell line is hormone responsive and therefore suitable for the investigation of a potential impact of estradiol-enhanced proliferation on DNA damage and apoptosis. There was noclear change in micronucleus formation in bcl-2 transfected cells with or without genotoxic treatment compared to the vector control cells, despite the achieved decrease in apoptosis. Again, this contradicts the hypothesis. On the other hand, micronuclei induction was elevated in vector control cells after estradiol-stimulated proliferation while the frequency of apoptotic cells was decreased in both cell lines after estradiol treatment. This seems to be in agreement with hypothesis. However, this decrease may have been due to enhanced proliferation of healthy cells, diluting out the apoptotic cells.

Using the three approaches to test the hypothesis, a correlation between micronucleus induction and apoptosis was found. Possible reasons for this correlation are the following:

1.) The experimental data suggested simultaneous appearance of apoptotic and micronuclei containing cells during the same cell cycle. However, a time-correlation between apoptosis and micronuclei does not imply their causal

relationship on the level of molecular mechanisms. PFT-α seemed to have a 'protective' effect since the induction of DNA damage was prevented and cells were rescued from apoptotic death. However, other reports revealed that PFT-α treatment turns normal cells into genetically modified cells. This modification may not be detectable as micronuclei. It may be a consequence of p53-independent low accuracy DNA-repair mechanisms employed by the cell upon suppression of p53 activity.

2.) Another explanation can be based in the lowered frequency of necrotic cells after PFT-α treatment that was observed in these studies. Possibly cells which are kept from entering apoptosis become necrotic and do not form micronuclei.

3.) The number of micronucleated cells can be independent of the modulation of apoptosis, because additional apoptotic cells may be derived from cells harbouring other forms of genomic damage.

4.) Finally, micronucleus formation and apoptosis may share common mechanisms on a molecular level.

Apoptosis modulation in cancer treatment must be considered in the particular cellular context and with great care because the intended increase in apoptosis may be accompanied by increased genetic damage in the tumor as well as in healthy tissue.

5. Zusammenfassung

Apoptotische Ereignisse als Reaktion auf exogen induzierten gentoxischen Schaden erhält die Homeostase von Organismen durch die Entfernung betroffener Zellen. Fehler in der apoptotischen Reaktion spielen sowohl für die Tumorentstehung als auch für die Chemotherapie-Resistenz eine wichtige Rolle. Der Zweck dieser Studie war es, die Balance von Genom-Schaden, gemessen durch Mikrokern-Bildung, und der Induktion von Apoptose als Reaktion auf gentoxischen Stress zu untersuchen.

Mikrokerne erscheinen als Folge unterschiedlicher Chromosomenaberrationen. Der Mikrokern-Test hat schnell an Akzeptanz gewonnen und wird inzwischen als Routine-Test für Gentoxizitätsprüfung eingesetzt. Die Hypothese war, dass die Mikrokern-Bildung umgekehrt mit dem Auftreten von Apoptose korreliert ist.

In drei humanen Zelllinien mit wildtyp p53, mutiertem p53 und knock-out p53 konnten durch Behandlung mit dem gentoxischen Topoisomerase-II-Hemmer Etoposid Apoptosen induziert werden. Die dabei beobachtete Erhöhung der Mikrokern-Häufigkeit war in Zellen mit mutiertem p53 stärker ausgeprägt als in Zellen mit wildtyp p53 oder knock-out p53.

Drei Vorgehensweisen wurden angewandt, um die molekularen Mechanismen zu verändern, welche die Wechselbeziehung zwischen apoptotischen Ereignissen und induziertem DNA-Schaden bestimmen. Im ersten Ansatz wurde die Apoptose vorübergehend durch Pifithrin (PFT-α), einen p53-Blocker, verhindert. So wurde der Einfluss verschiedener p53-Zustände (Wildtyp, mutiert und knock-out) auf DNA-Reparatur, den Zellzyklus und Apoptose untersucht. Der zweite Ansatz bestand aus einer vorübergehenden Transfektion mit bcl-2 Antisense Oligonukleotiden zur Reduktion der Bcl-2-Expression. Der dritte Weg war eine stabile Transfektion des bcl-2-Gens in eine estrogenrezeptorhaltigen Zelllinie. Dies ermöglichte den Einfluss von β-Estradiol-induzierter Zellproliferation zu untersuchen.

PFT-α wurde ursprünglich entwickelt, um während einer Chemotherapie in wildtyp p53-Zellen selektiv Apoptose zu blockieren. Dies sollte theoretisch mögliche

Nebenwirkungen auf gesundes Gewebe minimieren. Tumorzellen, die knock-out oder mutierten Status von p53 besitzen wären vermutlich unempfindlich gegenüber einer PFT-α Behandlung und würden weiterhin durch die Chemotherapie eliminiert. In Zellen mit Wildtyp p53 reduzierte die PFT-α-Anwendung die Mikrokern-Häufigkeit bei gleichzeitiger Behandlung mit 125 nM Etoposid. Eine kleinere Reduktion wurde in p53-mutierten Zellen gefunden und keine Reduktion in p53 knock-out Zellen. Die Apoptose-Häufigkeit war in Zellen mit Wildtyp p53 reduziert, eine geringere Reduktion wurde in Zellen mit mutiertem p53 beobachtet und p53 knock-out Zellen zeigten keine Veränderung. Diese Befunde widersprachen der eingangs genannten Hypothese, da eine Unterdrückung der Apoptose nicht zu einer vermehrten Mikrokern-Bildung führte.

Alle drei verwendeten Zelllinien mit unterschiedlichem p53 Status exprimieren konstitutiv das anti-apoptotische Protein Bcl-2. Daher wurde die Apoptose verstärkt durch vorübergehende Transfektion mit bcl-2 Antisense-Oligonucleotiden. Während die Apoptose-Häufigkeit nach der Behandlung mit Etoposid erhöht war, blieb die Mikrokern-Bildung unverändert oder war ebenso erhöht, was wiederum der Hypothese widersprach.

Die stabile Transfektion des bcl-2-Gens in humane Ovarkarzinom-Zellen entsprach dem dritten Ansatz die Apoptose zu modulieren. Die benutzte Zelllinie besitztEstrogenrezeptoren und ist deshalb geeignet, einen potenziellen Einfluss von β-Estradiol-verstärkter Proliferation auf den DNA-Schaden und Apoptose zu untersuchen. Es zeigten sich keine klaren Änderungen in der Mikrokern-Bildung in bcl-2 transfizierten Zellen, verglichen mit der Vektor-Kontrolle, mit oder ohne gentoxischer Behandlung, trotz der erreichten Reduktion der Apoptosen. Erneut widersprach dies der Hypothese. Andererseits war die Mikrokern-Bildung in den Vektor-Kontroll-Zellen erhöht nach β-Estradiol-stimulierter-Proliferation. Die Apoptose-Frequenz war in beiden Zelllinien nach β-Estradiol Behandlung reduziert. Dies schien in Übereinstimmung mit der Hypothese. Diese Herabsetzung könnte jedoch auf verstärkte Proliferation der gesunden Zellen zurückzuführen sein, was die apoptotischen Zellen verdünnen würde.

Durch diese drei Ansätze, die formulierte Hypothese zu testen, wurde eine Korrelation zwischen Mikrokern-Bildung und Apoptosen gefunden. Mögliche Gründe für diese Korrelation sind die folgenden:

1.) Die experimentellen Daten lassen die Vermutung zu, dass apoptotische und Mikrokern-enthaltende Zellen simultan, während eines Zellzykluses auftraten. Dennoch sagt diese zeitliche Korrelation zwischen Apoptose und Mikrokern-Bildung nichts über einen kausalen Zusammenhang auf der molekularen Mechanismen-Ebene aus. PFT-α scheint ein schützender Effekt zuzukommen, sichtbar durch Verhinderung von DNA-Schadensinduktion und Schutz vor programmiertem Zelltod. Andere Berichte jedoch zeigten, dass PFT-α Behandlung normale Zellen in genetisch modifizierte abändert. Diese Modifikationen wären gegebenenfalls nicht als Mikrokerne fassbar. Dies ist möglicherweise eine Konsequenz von p53-unabhängiger weniger genauen DNA-Reparatur-Mechanismen, welche von der Zelle nach Suppression von p53-Aktivität benutzt werden.
2.) Eine andere Erklärung stützt sich auf die verminderte Häufigkeit nekrotischer Zellen, die nach der Behandlung mit PFT-α beobachtet wurde. Es ist denkbar, dass Zellen deren, programmierter Zelltod verhindert wurde, nekrotisch wurden und keine Mikrokerne ausbildeten.
3.) Die Zahl der Mikrokern-tragenden-Zellen kann unabhängig von apoptotischen Ereignissen sein, weil zusätzliche apoptotische Zellen auch auf andere Arten von Genomschaden zurückzuführen sein könnten.
4.) Letztlich lässt sich annehmen, dass Mikrokern-Bildung und Apoptose gemeinsame molekulare Mechanismen oder Anfangsschritte teilen könnten.

Die Beeinflussung der Apoptose in der Krebstherapie muss den jeweiligen zellulären Kontext sorgfältig in Betracht ziehen, da der gewünschte Anstieg an apoptotischen Zellen Hand in Hand gehen kann mit erhöhtem Genomschaden sowohl im Tumor als auch im gesundem Gewebe.

6. Literature

1. Abend M., Kehe K., Riedel M., Van Beuningen D. Correlation of micronucleus and apoptosis assays with reproductive cell death can be improved by considering other modes of death. Int. J. Radiat. Biol., 2000, vol.76, no.2, 249-259.

2. Abend M., Frombeck S., Van Beuningen D., 1999. Indications for an active process underlying spontaneous and radiation-induced micronucleation in L929 cells. Int. J. Radiat. Biol. 75(12), 1567-1578.

3. Bassi L., Carloni M., Fonti E., Palma de la Pena N., Meschini R., Palitti F. Pifithrin-α, an inhibitor of p53, enhances the genetic instability induced by etoposide (VP16) in human lymphoblasoid cell treated in vitro. Mutation Research, 2002, vol. 499, 163-176.

4. Boos G., Stopper H. Genotoxicity of several clinically used topoisomerase II inhibitors. Toxicology Letters, 2000, vol. 116, 7-16.

5. Bunz F., Dutriaux A., Lengauer C., Waldman T., Zhou S., Brown J. P. Requirement for p53 and p21 tu sustain G2 arrest after DNA damage. Science, 1998, No. 282, 1497-1501.

6. Cadwell C., Zambetti P. G. The effects of wild-type p53 tumor suppressor and mutant p53 gain-of-function on cell growth. Gene, 2001, No.227, 15-30.

7. Cao-Garcia I., Cao-Garcia M., Caballero M. J., Criado L. M., Klatt P., Flores M. J., Weill C. J., Blasco A. M., Serrano M. `Super p53' mice exhibit enhanced DNA damage response, are tumor resistant and age normally. The EMBO Journal, 2002, Vol. 21 No. 22, 6225-6235.

8. Chan T. A., Hermeking H., Lengauer C., Kinzler K. W., Volgestein B. 14-3—3 Sigma is required to prevent apoptotic catastrophe after DNA damage. Nature, 1999, No. 401, 16-620.

9. Chan J., Gokhale M., Schofield B. Inhibition of TGF-β-induced apoptosis by ethinyl estradiol in cultured, precision cut rat liver slices and hepatocytes. Carcinogenesis, 2000, No. 21, 1205-1211.

10. Chang B. D., Xuan Y., Broude E. V., Zhu H., Schott B., Fang J., Role of p53 and $p21^{WAF}$ in senescence-like terminal proliferation arrest induced in human tumor cells by chemotherapeutic drugs. Oncogene, 1999, No. 18, 4808-4818.

11. Decordier I., Dillen L., Cundari E., Kirsch-Volders M., 2002. Elimination of micronucleated cells by apoptosis after treatment with inhibitors of microtubules. Mutagen. 17(4), 337-344.

12. Decordier I., Dillen L., Cundari E., Kirsch-Volders M., 2002. Elimination of micronucleated cells by apoptosis after treatment with inhibitors of microtubules. Mutagen. 17(4), 337-344.

13. Deng X., Gao F., Flagg, May S. Mono- and multisite phosphorylation enhances Bcl2's antiapoptotic function and inhibition of cell cycle entry functions. PNAS, 2004, vol.101, no. 1, 153-158.

14. Deng X., Gao F., May S. Bcl-2 retards G1/S cell cycle transition by regulating intracellular ROS. Blood, 2003, vol. 102, num. 9, 3179-3185.

15. Duggan J. B., Cotter E. F., Kelly D. J., Hamilton W. P., Williamson E. K. Antisense Bcl-2 oligonucleotide uptake in human cell carcinoma. European Urology, 2001, vol. 40, 685-695.

16. Evan G., Littlewood T. A matter of Life and Cell death. Science, 1998, Vol. 281, 1317-1321.

17. Fenech M. Chromosomal biomarkers of genomic instability relevant to cancer. Drug Discovery Today, 2002, vol.7, No. 22, 1128-1137.

18. Fenech M., Crott W., J. Micronuclei, nucleoplasmic bridges and nuclear buds induced in folic acid deficient human lymphocytes-evidence for breakage-fusion- bridge cycles in the cytokinesis-block micronucleus assay. Mutation Research, 2002, vol. 504, 131-136.

19. Fischer H. W., Keiwan A., Schmitt E., Stopper H. Increased formation of micronuclei after hormonal stimulation of cell proliferation in human breast cancer cells. Mutagenesis, 2001, vol.16, no.3, 209-212.

20. Gottifredi V., McKinney K., Poyurovsky V.M., Prives C. Decreased p21 levels are required for efficient restart of DNA synthesis after S phase block. JBC, 2003, Manuscript M310373200.

21. Gudkov A.,V., Komarova A., E. The role of p53 in determining sensitivity to radiotherapy. Nature reviews-Cancer, February 2003, vol3, 117-129.

22. Gurova K.V., Gudkov A.V., 2003. Paradoxical role of apoptosis in tumor progression. J. Cell Biochem. 88(1), 128-137.

23. Halicka H. D., Seiter K., Feldman E. J., Traganos F., Mittelman A., Ahmed T., Darzynkiewicz Z. Cell cycle specificity of apoptosis during treatment of leukaemias. Apoptosis, 1997, No.2, 25-39.

24. Hartwell L.H., Weinert T.A., 1989. Checkpoints: controls that ensure the order of cell cycle events. Science 246(4930), 629-634.

25. Hopkins-Donaldson S., Cathomas R., Simoes-Wust A.P., Kurtz S., Belyanskya L., Stahel R.A., Zangemeister-Wittke U., 2003. Induction of apoptosis and chemosensitization of mesothelioma cells by Bcl-2 and Bcl-xL antisense treatment. Int. J. Cancer 106(2), 160-166.

26. Hentze H., Latta M., Kunstle G., Dhakshinamoorthy, S., Ng P.Y., Porter, A.G., Wendel A. Topoisomerase inhibitor camptothecin sensitizes mouse hepatocytes in vitro and in vivo to TNF-mediated apoptosis. Hepatology. 2004, 39(5), 1311-20.

27. Johnstone R.W., Ruefli A.A., Lowe S.W., 2002. Apoptosis: a link between cancer genetics and chemotherapy. Cell 108(2), 153-164.

28. Kaji A., Zhang Y., Nomura M., Bode A.M., Ma W.Y., She Q.B., Dong Z., 2003. Pifithrin-alpha promotes p53-mediated apoptosis in JB6 cells. Mol Carcinog. 37(3), 138-148.

29. Kirsch-Volders M., Vanhauwaert A., Eichenlaub-Ritter U., Decordier I. Indirect mechanisms of genotoxicity. Toxicology Letters, 2003, vol.140-141, 63-74.

30. Komarov G. P., Komarova A. E., Kondratov V. R., Tselkov C. K., Coon J. S., Chernov V. M., Gudkov V. A. A Chemical Inhibitor of p53 That Protects Mice form the Side Effects of Cancer Therapy. Science, September 1999, vol. 285, 1733-1737.

31. Komarova A. E., Gudkov V. A. Chemoprotection from p53-dependant apoptosis: potential clinical applications of the p53 inhibitors. Biochemical Pharmacology, 2001, vol.62, 657-667.

32. Komarova E. A., Neznanov N., Komarov P.G., Chernov, M. V., Wang K., Gudkov A.V., p53 inhibitor pifithrin alpha can suppress heat shock and glucocorticoid signalling pathways. J. Biol. Chem. 2003, 278 (18), 15465-15468.

33. Krammer H. P. CD95's deadly mission in the immune system. Nature, vol. 407, 789-794, October, 2000.

34. Kuang-Yu J., Gewirtz M. A. Suppression of gene expression by targeted disruption of messenger RNA: available options and current strategies. Stem Cells, 2000, vol. 18, 307-319.

35. Lin Y., Waldman C., B., Waldman S., A. Suppression of high-fidelity double-strand break repair in mammalian chromosomes by pifithrin-α, a chemical inhibitor of p53. DNA repair, 2003, vol.2, 1-11.

36. Liu Y., Kulesz-Martin M. P53 protein in the hub of cellular DNA damage response pathways through sequence-specific and non-sequence-specific DNA bindindg. Carciongenesis, 2001, No.22, 851-860.

37. Livingstone L.R., White A., Sprouse J., Livanos E., Jacks, T,. Telsty T.D., 1992. Altered cell cycle arrest and gene amplification potential accompany loss of wild-type p53. Cell 70(6), 923-935.

38. Marchenko D. N., Zaika A., Moll M. U. Death signal-induced localization of p53 protein to mitochondria. The Journal of Biological Chemistry, May 2000, vol 275, No.21, 16202-16212.

39. Meintieres S., Biola A., Pallardym M., Marzin D., 2003. Using CTLL-2 and CTLL-2 bcl2 cells to avoid interference by apoptosis in the in vitro micronucleus test. Environ. Mol. Mutagen. 41(1), 14-27.

40. Miller B., Potter-Locher F., Seelbach A., Stopper H., Utesch D., Madle S. Evaluation of the in vitro micronucleus test as an alternative to the in vitro chromosomal aberration assay: position of the GUM Working group on the in vitro micronucleus test. Mutat. Res. 410 (1), 81-116.

41. Negulescu O., Bognar I., Lei J., Devarajan P., Silbiger S., Neugarten J. Estradiol reverses TGF-β-induced mesangial cell apoptosis by case kinase 2-dependant mechanism. Kidney International, 2002, vol. 62, 1989-1998.

42. Navakauskiene R., Treigyte G., Gineitis A., Magnusson K.E. Identification of apoptotic tyrosine-phosphorylated proteins after etoposide or retinoic acid treatment. Proteomics. 2004 Apr;4(4):1029-41.

43. Paterson B.M., Roberts B. E., Kuff E. L. Structural gene identification and mapping by DNA-mRNA hybrid arrested cell-free translation. Proc Natl Acad Sci USA 1977, vol.74, 4370-4374.

44. Pietenpol J.A., Stewart Z.A., 2002. Cell cycle checkpoint signalling: cell cycle arrest versus apoptosis. Toxicol. 181-182, 475-481.

45. Proietti De Santis, L., Balajee, A.S., Lorenti Garcia, C., Pepe, G., Worboys, A.M., Palitti, F., 2003. Inhibition of p53, p21 and Bax by pifithrin-alpha does not affect UV induced apoptotic response in CS-B cells. DNA Repair 2(8), 891-900.

46. Razandi M., Pedram A., Levin E. R. Plasma membrane estrogen receptors signal to antiapoptosis in breast cancer. Molecular Endocrinology, 2000, No. 9, 1434-1447.

47. Reed C. J., Jurgensmeier M.J., Matsuyama S. Bcl-2 family proteins and mitochondria. Biochimica et Biophysica Acta, vol. 1366, 127-137, 1998.

48. Rincheval V., Renaud F., Lemaire C., Godefrov N., Trotot P., Boulo V., Mignotte B., Vayssiere L. J. Bcl-2 can promote p53-dependant senescence versus apoptosis without affecting the G1/S transition. Biochemical and Biophysical Research Communications, 2002, vol.298, 282-288.

49. Roninson B. I., Broude V. E., Chang B. D. If not apoptosis, then what? Treatment-induced senescence and mitotic catastrophe in tumor cells. Drug Resistance Updates, 2001, 4, 303-313.

50. Samorapoompichit P., Steiner M., Lucas T., Wachtler F., Schedled A., Sperr W.R., Valent P., 2003. Induction of apoptosis in the human mast cell leukemia cell line HMC-1 by various antineoplastic drugs. Leuk. Lymphoma 44(3), 509-515.

51. Schafer T., Scheuer C., Roemer K., Menger M.D., Vollmar B. Inhibition of p53 protects liver tissue against endotoxin-induced apoptotic and necrotic cell death. FASEB J. 17(6), 660-667.

52. Schwartz J.L., Jordan R., Evans H.H., Lenarczyk M., Liber H., 2003. The TP53 dependence of radiation-induced chromosome instability in human lymphoblastoid cells. Radiat. Res. 159(6), 730-736.

53. Schwartz J.L., Jordan R., Murnane P.J., Liber H., Evans H. H. TP53-dependent chromosome instabilty is associated with transient reductions in telomere length in immortal telomerase-positive cell lines. Genes, Chromosomes and Cancer, 2001, No. 30, 236-244.

54. Shimizu N. Selective elimination of acentric double minutes from cancer cells into primary human lyphocyte DNA in vivo. Mutation research, 2000, vol.448, 81-90.

55. Shimizu T., Kubota M., Tanizawa A., Sano H., Kasai Y., Hashimoto H., Akiyama Y., Mikawa H. Inhibition of both etoposide-induced DNA fragmentation and activation of poly (ADP-ribose) synthesis by zic ion. Biochemical and Biophysical Research Communications, 1990, 169, 1172-1177.

56. Shinomiya N. New concepts in radiation-induced apoptosis. ‘premitotic apoptosis’ and ‘postmitotoic apoptosis’. J.Cell.Mol.Med,. 2001, Vol.5, No.3, 240-253.

57. Stearns T. Centrosome duplication. A centriolar pas de deux. Cell, 2001 No.105, 417-420.

58. Stopper H., Müller S.O. Micronuclei as a biological endpoint for genotoxicity: a minireview. Toxicol. Vitro, 1997, vol.11, 661-667.

59. Tang W., Willers H., Powell S.N. P53 directly enhances rejoining of DNA double-strand breaks with cohesive ends in gamma-irradiated mouse fibroblasts. Cancer Research, 1999, No.385, 21-29.

60. Vairo G., Soos J. T., Upton M. T., Zalvide J., DeCaprio A. J., Ewen E. M., Ko A., Adams M. J. Bcl-2 retards cell cycle entry through p27 (Kip1), pRB relative P130, and altered E2F regulation. Mol. Cell. Bio., 2000, vol.20, 4745-4753.

61. Vukicevic V., Kampfinger K., Stopper H. Influence of altered apoptosis in human lymphoblastoid cell lines on micronucleus frequency. Toxicology Letters, 2003.

62. Willers H., Xia F., Powell N. S. recombinational DNA repair in cancner and normal cells: the challenge of functional analysis. Journal of Biomedicine and Biotechnology, 2002, 2:2, 86-93.

63. Withoff S., de Jong S., de Vries E.G., Mulder N. H. human DNA topoisomerase II: biochemistry and role in chemotherapy resistance (review). Anticancer research, 1996, 16, 1867-1880.

64. Yamada T., Ohyama H. Radiation-induced interphase death of rat thymocytes in internally programmed (apoptosis). Int. J. Radiat. Biol. 1988, No.53, 65-75.

65. Yin, Y., Tainsky, M.A., Bischoff, F.Z., Strong, L.C., Wahl, G.M., 1992. Wild-type p53 restores cell cycle control and inhibits gene amplification in cells with mutant p53 alleles. Cell 70(6), 937-948.

66. Zhang Y., Lei X.Y.. Effect of bcl-2 antisense oligodeoxynucleotides on drug sensitivity of leukemic cells. Hematol. J., 2003, 4(3), 187-197.

67. Zörnig M., Hueber OA., Baum W., Evan G. Apoptosis regulators and their role in tumorigenesis. Biochimica et Biophysica Acta, 2001, vol. 1551, 1-37.

Table of contents

Table of contents

Declaration

Hereby, I declare that enclosed PhD thesis ‘Mechanisms of Apoptosis Modulation and their Contribution to Genomic Instability in Tumor Cells’ is entirely authentic and results were obtained by own and independent research. I have not used any other sources and supporting material than stated in the thesis. I also declare that this PhD thesis has not previously been submitted within another exam process in this or another form.

I have not received or attempted to receive any other academic degree than those submitted with this request.

Würzburg, 2004

CURRICULUM VITAE

PERSONAL DATA

Vladimir Vukicevic

Born: 23.1. 1969. Prokuplje, Republic of Serbia, Yugoslavia (Serbia and Montenegro)

ADDRESS

Institute of Toxicology and Pharmacology
Versbacherstr. 9
97076 Wuerzburg
Germany

Phone: 0931 20148760
0931 20148756

Email: v_vukicevic@yahoo.com

BASIC EDUCATION

1976-1984 Elementary School, Prokuplje, Yugoslavia

1984-1988 Gymnasium, Prokuplje, Yugoslavia

UNIVERSITY STUDIES

1989-1997 University of Belgrade, Faculty of Biology, department of Molecular biology and Physiology, Group of Biomedicine. Obtained title ‘ Master of Science (MSc) in Molecular biology and Physiology’.

POSTGRADUATE STUDIES

November 2000-August 2004 PhD student at Institute of Toxicology and Pharmacology, Würzburg University.

The parts of this work was published in scientific journals and presented at scientific meetings, as listed:

List of publications

Vukicevic V., Kampfinger K. and Stopper H. **Influence of altered apoptosis in human lymphoblastoid cell lines on micronucleus frequency.** Toxicology Letters 147 (2004) 187-195.

S.K. Abraham, V. Vukicevic, and H. Stopper. **Coffee mediated protective effects against directly acting genotoxins and gamma-radiation in mouse lymphoma cells.** Cell Biology and Toxicology, Accepted in March 18, 2004 (In press).

H. Stopper, K. Hempel, A. Heidland, S. Vershenya, V. Vukicevic, J. Grawe. **Reticulocyte-Micronuclei: new tool in human biomonitoring?** Submitted to Toxicology Letters

Grawe J, Biko J, Lorenz R, Reiners Chr, Stopper H, Vershenya S, Vukicevic V, Hempel K. **Evaluation of the reticulocyte micronucleus assay in patients treated with radioiodine for thyroid cancer**, Submitted to Mutation Research

Vukicevic, V., Stopper, H. **Estrogenic stimulation and transfection with anti-apoptotic protein influence genomic stability in human ovarian BG-1 cells** (in preparation).

Scientific meetings and congress participation

Deutsche Gesellschaft für experimentelle und klinische Pharmakologie und Toxikologie, 43rd Spring Meeting 2002, Mainz Germany

7. Tagung des DNA-Reparatur-Netzwerks, Karlsruhe 2002, Germany

Deutsche Gesellschaft für experimentelle und klinische Pharmakologie und Toxikologie, 44rd Spring Meeting 2003, Mainz Germany

12th International AEK Cancer Congress of the German Cancer Society, Würzburg 2003

Deutsche Gesellschaft für experimentelle und klinische Pharmakologie und Toxikologie, 45th Spring Meeting 2004, Mainz Germany

Acknowledgments

The Graduate College 639 ‘Tumor Instability’ of the Deutsche Forschungsgemeinschaft (DFG) supported this work.

Special gratitude to Prof. Dr. rer. nat. Helga Stopper (‘Doktormutter’) for exciting and constructive guidance through research. Also, many thanks for being supportive, inspiring enthusiasm and new scientific approaches.

Thanks to Dr. rer. nat. Annette Bitsch for great support and friendship.

I thank Prof. Manfred Schartl (Institute of Physiological Chemistry, University of Würzburg) for reviewing this work.

We thank H. Liber for NH32 cells, M. Kessler for expert technical assistance and S. Müller and the US National Institute for Environmental Health Sciences for providing BG-1 cells.

All present and previous associates from laboratory and the Institute of Toxicology and Pharmacology: Andreas Brink, Maria Scheurich, Kay Schwabe, Elmar Schmitt, Uschi Fröhlig, Elisabeth Rub-Spiegel, Elisabeth Stein, Carolin Joa, were ‘responsible’ for team-work and a good mood.